Leptopilina Parasitoid Wasps, Ion Channels, and Dendritic Morphology in *Drosophila* Nociception Paradigms

by

Jessica Leigh Robertson

Department of Cell Biology
Duke University

Date:_____

Approved:

_____
W. Daniel Tracey, Supervisor

_____
Fan Wang

_____
Scott Soderling

_____
Wolfgang Liedtke

Dissertation submitted in partial fulfillment of
the requirements for the degree of Doctor
of Philosophy in the Department of
Cell Biology in the Graduate School
of Duke University

2013

ABSTRACT

Leptopilina Parasitoid Wasps, Ion Channels, and Dendritic Morphology in *Drosophila* Nociception Paradigms

by

Jessica Leigh Robertson

Department of Cell Biology
Duke University

Date:_____

Approved:

_____
W. Daniel Tracey, Supervisor

_____
Fan Wang

_____
Scott Soderling

_____
Wolfgang Liedtke

An abstract of a dissertation submitted in partial fulfillment of the requirements for the degree of Doctor of Philosophy in the Department of Cell Biology in the Graduate School of Duke University

2013

Abstract

Almost everyone will experience pain at some point in their lives. While pain is generally adaptive, and alerts the body to potential tissue damage, chronic pain is a disruptive disease with a huge psychological and economic cost. Of all the senses, the molecular basis of pain is perhaps the least understood. Without an understanding of the genes involved in pain, it is difficult to develop new drugs to treat pain. Current pain drugs are often ineffective at treating pain, especially chronic pain, and can cause many side effects. In this dissertation, I have further developed the *Drosophila* nociception paradigm.

First, I investigated the responses of *Drosophila melanogaster* larvae to a naturally occurring noxious stimulus, the parasitoid wasp. These wasps use a sharp ovipositor to lay their eggs inside of the larvae. The eggs hatch, and the wasp larva then eats the *Drosophila* larva from the inside, resulting in the death of the *Drosophila*. In response, *Drosophila* larvae have evolved multiple mechanosensory behaviors to fight attacks from wasps. The type of defensive behavior depends on the somatotopic location of the attack along the larval body wall, as well as the degree of penetration of the larval cuticle by the wasp ovipositor. I found that the class IV neurons, which are the larval nociceptors, and the *pickpocket* gene, are important for mediating nocifensive responses to parasitoid wasp attacks.

While parasitoid wasps are the most ecologically relevant noxious stimulus for *Drosophila* larvae, the behavioral assays are time consuming and very low throughput. Thus, I utilized a thermal nociception assay in a genetic screen to discover new ion channels involved in the detection of noxious heat. In this assay larvae are touched lightly with a hot probe. In collaboration with Kia Walcott, I completed a forward genetic screen that knocked down 90% of the ion channels in the *Drosophila* genome. We found fourteen ion channel genes that are important for larval nociception.

The dendritic morphology of the nociceptor neurons is well studied, but the role of ion channels in governing the dendritic morphology had yet to be explored. We therefore screened the fourteen genes that we found to have a role in thermal nociception for a role in dendrite morphogenesis. Knockdown of six of the genes caused dendritic defects. These required genes represented a wide variety of transporters and channels, including potassium channels, TRP channels, and ligand gated channels. I also generated a genetic null mutant fly for *coyotemint*, an ABC transporter.

Lastly, I investigated the role of the calcium gated potassium channel, *SK*, in thermal nociception. Previous work in the lab had demonstrated that larvae null for *SK* exhibited a hypersensitive phenotype to a noxious thermal stimulus. I determined that one isoform of *SK*, *SK-M*, rescues this phenotype, and is necessary for thermal nociception. Additionally, I built an apparatus that allowed for the confocal imaging of genetically encoding calcium indicators while a larva undergoes a thermal ramp. This

set-up allowed us to explore the role of *SK* in the physiology of the class IV neurons. We found the larvae null for *SK* exhibit increased levels of calcium during a thermal ramp.

In conclusion, my work has explored both the ethology of nociception in *Drosophila* larvae, as well as engaged in the search for new genes involved in nociception.

Contents

List of Tables

List of Figures

Acknowledgements

There are so many people that I would like to thank for their help during my PhD. I would never have been able to complete this journey by myself. First I would like to thank my advisor, Dan Tracey. He provided invaluable support and scientific advice. Dan had interesting ideas and hypotheses when I got stuck, and was always enthusiastic about my latest finding. I would also like to thank my past mentors, especially Paul Heideman, for continuing to mentor and advise me. My committee members, Fan Wang, Scott Soderling and Wolfgang Liedtke were extremely helpful, and have wonderful ideas. I would also like to thank my co-workers. This work would not have been possible without my teammates Asako Tsubouchi and Kia Walcott. It was a joy to work with both of you. I would also like to thank the rest of my lab mates, current and former, Lixian Zhong, Jay Caldwell, Stephanie Mauthner, Qi Xiao, Melissa Christiansen, Richard Hwang, Meghan Pantalia, Ken Honjo and Andrew Bellemer. Lastly, I would like to thank Shirley Morton for keeping the lab running smoothly.

My family and friends were a source of inspiration and encouragement during my PhD. Brianna Wilson, Elizabeth Bryant, Joshua Specht and Matthew Oreska cheered me on from afar. Nearby, I had the best possible support system. I would like to thank Katie Kretovich, Lauren Lilley Lohmer, Meghan Morrissey, Melissa Keenan, and Audrey Bone for editing, providing advice, and generally just being there for me. My

extended family, including my in-laws, Jim, Susan and Max Yedor, were consistently supportive of my work. My Grammie urged me to always look on the bright side of any situation. My parents, Bob and Janet Robertson, were always there for me with words of advice and encouragement.

I definitely would not have been able to complete my PhD without the support of my dog, Mendel, and my husband, Justin Yedor. Justin was my rock during graduate school. He was with me to celebrate my successes, and helped push me through my failures. Thank you so much.

1. Introduction

Pain is experienced by all people, but is poorly understood. In the United States alone, 116 million people are living with chronic pain [1]. Current medications to treat chronic pain have many side-effects, including the possibility of dependency, and are often ineffective in relieving the symptoms of patients. Individuals living with pain are at a significantly higher risk for depression [2], self-medication [2] and suicide [3]. In addition to the emotional and physical distress caused by pain, pain is also a drain on the economy. Those that live with pain are often unable to work, leading to 61.2 billion dollars in lost productivity in the United States alone [4]. With the goal of determining how painful stimuli are transduced, we have characterized novel ion channels in *Drosophila melanogaster*, and have further investigated the role of ion channels in governing dendritic morphology. Greater understanding of the role of ion channels may lead to new drug targets for more effective pain treatment.

1.1 Nociception

Pain is defined as the "sensory and emotional experience associated with actual or potential tissue damage" (International Association for the Study of Pain). Painful stimuli are detected through the nociceptors, which innervate the skin surface and viscera and have elaborately branched neurites. Nociceptors are responsible for detecting noxious thermal, chemical and mechanical stimuli. Although pain is a

debilitating disease, the molecular mechanisms underlying the perception of pain remain poorly understood.

Since pain, by definition, involves emotional processing, the true study of pain is limited to animals with the cortical capacity to experience emotions. However, animals from *C. elegans* to mammals have nociceptive processing. Nociception is the detection and neural processing of a noxious stimulus. Nociception is an evolutionarily conserved neuronal ability, with even evolutionarily ancient multicellular organisms possessing nociceptive processing capabilities [5]. Nociception is likely well conserved because animals face a variety of noxious stimuli in their environment and benefit from having appropriate behavioral responses which allow them to survive. For example, nociceptive processing is necessary to respond to a variety of naturally occurring stimuli, including noxious temperatures, attacks from conspecifics, and attacks from predators. Following an injury nociception is beneficial in preventing further injury to damaged tissue, which speeds the healing process.

Defensive behaviors in response to a noxious stimulus are called nocifensive behaviors. There are many types of nocifensive behaviors, including paw withdraw from a noxious stimuli in mice, limping on an injured limb in humans, and tail thrashing in zebrafish [6, 7]. Nocifensive behavior may also serve to protect animals from attacks by predators [8]. The parasitoid wasps are a common predator of insects, and lay eggs

either inside of, or on top, of their prey. When the wasp progeny hatch, they begin to eat the host prey. A successful attack by a parasitoid wasp is often lethal for the prey, so insects have developed nocifensive behaviors to respond to attacks by parasitoid wasps [8].

1.1.1 Paradigms for the discovery of novel genes in nociception

Several paradigms have been used to discover new genes related to nociception. To date, the most widely used organisms for nociceptive gene discovery are humans and mice. In humans, some genes related to pain have been discovered by using families that show extreme sensitivity or insensitivity to pain. These studies have been successful in discovering several ion channelopathies [9, 10]. However, these genetically linked pain sensitivities are extremely rare in comparison to the total number of people who experience chronic pain.

In addition to studying families with a genetic susceptibility to pain, other studies have concentrated on finding genetic variables for sensitivity to pain using genome wide association studies (GWAS) [11, 12]. For example, one study identified a single nucleotide polymorphism (SNP) associated with decreased pain following back surgery [13]. However, the interpretation of GWAS results is difficult. First, the data tend to be noisy, and it can be difficult to identify regions of the genome that might be associated with the pain phenotype. Additionally, once the regions of interests are

discovered, it can be difficult to determine the effect of the SNP unless it falls within a protein coding region of a gene. If the variable region is upstream from a gene, the effect of the SNP could be to increase transcription of a neighboring gene, or to decrease it. Perhaps the SNP doesn't affect a neighboring gene at all, but is in an enhancer site for a gene far downstream. Additionally, if novel genes are discovered, it can be difficult to determine the site of action for the gene. For example, is the gene functioning in the periphery, or in the central nervous system?

Mice are a more genetically tractable system in which to look for novel regulators of pain. Isogenic lines of mice have been specially bred to have extreme sensitivity or insensitivity to pain [14, 15]. This allows the researcher to determine how the genome of the strains differ, and target those differing genes for further investigation. Although selective breeding allows for more control over the genetics of the mice, both the mice and human studies rely on natural variation in pain genes. It is possible that many genes involved in nociception may be under strong selective pressure such that they show little genetic variation, making their discovery through these methods difficult if not impossible.

1.1.2 *Drosophila* as a model for nociceptive gene discovery

Drosophila melanogaster has recently been developed as a paradigm for nociception research [8, 16-18]. *Drosophila* is an excellent model for gene discovery, since

forward genetics can be used to screen for novel genes involved in nociception, independent of natural population variation [13, 16]. The powerful GAL4 UAS genetic system allows for the expression of genetic tools in specific tissues. GAL4 is a yeast transcription factor which binds to the UAS enhancer sequence, causing the element under the control of the UAS enhancer to be expressed wherever the GAL4 is expressed.

The RNA interference (RNAi) tools developed by the Vienna Drosophila Research Center (VDRC) and the Transgenic RNAi Project (TRiP) are especially useful in screening for novel nociceptive genes. *UAS-RNAi* transgenic flies have been developed for the vast majority of genes in the *Drosophila* genome [19]. This allows for the *in vivo* knockdown of genes in a tissue specific manner [19]. The *UAS-RNAi* construct is a large inverted repeat of 300-400 nucleotides, which generates a hairpin. This hairpin is then cleaved by the enzyme *Dicer-2* resulting in the formation of small interfering RNA (siRNA). These siRNA interact with the RNA-induced silencing complex and bind to the mRNA of the gene of interest, causing degradation of the mRNA [20]. Since RNAi can be expressed in a tissue specific manner, this approach allows for targeted knockdown of even essential genes.

In addition to the advantages of RNAi, there are also many tools for creating mutants, tagged proteins, and determining expression patterns in *Drosophila*. *Drosophila* also has a very short lifecycle, increasing the pace of experiments and the generation of

novel genetic mutants. Since nociception is so well conserved, this makes *Drosophila* an ideal system for identifying novel genes involved in nociception.

1.1.3 Nociception paradigms in *Drosophila*

Nociception paradigms have been developed for both adult and larval *Drosophila* [8, 13, 16, 21-23]. Nociception in adult flies has been tested by determining a preference index on hot plates, a two choice assay with a thermal challenge, responses to a laser focused on the abdomen, and jumping responses to a hot plate [13, 21-23]. The first two assays allow for the testing of large groups of flies at once, which is beneficial for large-scale genetic screens. However, a difficulty in working with adult flies is that the identity of the nociceptor neurons is unknown. *Drosophila* larvae are a simpler system for doing nociception behavioral analysis.

Drosophila larvae are a useful model for pain research, since they respond to noxious thermal and mechanical stimuli through stereotyped rotation around the long body axis, called nocifensive escape locomotion (NEL) [8, 16]. This response is easily distinguishable from normal peristaltic locomotion. The perception of noxious stimuli, as well as NEL, is thought to be advantageous for *Drosophila* larvae. In the wild, *Drosophila* larvae are attacked by several species of parasitoid wasps that use a sharp ovipositor to lay their eggs inside of *Drosophila* larvae [24-26]. Attacks by parasitoid wasps can trigger NEL, which is hypothesized to deter the wasp [8]. Additionally, the

nociceptor neurons are well described, and genetic tools are available for tissue specific targeting of the nociceptors [8]. Larval NEL is thus an evolutionarily relevant, easily quantifiable behavior in response to a noxious stimulus.

1.2 Ion channels

The nociceptor neurons are responsible for detecting and transmitting information about noxious, potentially tissue damaging stimuli to the central nervous system. To do this, they transduce the noxious stimuli into an electrical signal. Noxious stimuli are detected by ion channels which by opening or closing allow ions to flow through the channel, resulting in a change in electrical potential of the cell membrane. If the nociceptor becomes sufficiently depolarized, the signal is conducted down the axon in the form of an action potential. This electrical communication allows for central nervous system processing of peripheral stimuli. Ion channels are also important for the regulation of the electrical properties of the neuron. Since ion channels are thought to be responsible for both the detection and transmission of the noxious signal, ion channels have been targeted in the study of nociception [9, 10, 16-18, 27-43].

Ion channels are evolutionarily conserved molecules, and are present in bacteria and archae [44, 45]. Ion channel function can also be evolutionarily conserved across phyla. For example, the electrophilic detection properties of the TRPA channel are predicted to date back approximately 500 million years, to the divergence of the

vertebrates from invertebrates [46]. Since both ion channels and nociception are so well conserved, *Drosophila* can be used to study the role of ion channels in nociception.

1.2.1 Ion channels in *Drosophila* nociception

Recent studies have found ion channels to be an underlying cause of several pain disorders in humans [10, 47, 48]. A mutation in the ion channel TRPA1 was found to cause Familial Episodic Pain Syndrome (FEPS) in humans [48]. FEPS results in extreme pain, typically following fatigue, cold, and/or hunger. Additionally, SNPs in the $\alpha 2\delta 3$ calcium channel subunit are important in pain sensitivity and in pain perception during recovery from back surgery [49]. Of the three ion channels known to have naturally occurring mutations or polymorphisms that affect pain perception in humans, all of them have homologues that are also known to affect nociception in *Drosophila* [16, 17, 47, 49, 50].

Five ion channel subunits, *painless*, *dTRPA1*, *pickpocket*, *straightjacket*, and *piezo* have been found to be important for nociception in *Drosophila* larvae [16, 17, 49]. Of these five ion channels, all of them have human homologues. These genes represent four different classes of ion channels, transient receptor potential (TRP) channels, degenerin epithelial sodium channels (DEG/ENaC), calcium channels, and piezo channels, indicating that multiple types of channels may play a role in nociception.

The large family of TRP channels are known to function in mediating a wide range of sensory modalities, including taste, hearing, thermosensation, hygrosensation and nociception [42, 51-62]. TRP channels are cation channels, have four subunits, and can be either homomeric or heteromeric [63]. *painless* is a TRPA channel that was found to be important in both thermal and mechanical nociception responses in *Drosophila* [16]. In *Drosophila* larvae, *painless* is expressed in the chordotonal and multidendritic neurons [16]. In adult flies, *painless* was found to be important in mediating thermal nociception [22], as well as chemical nociception to allyl isothiocyanate (AITC, the active compound in wasabi) and benzy isothiocyanate (BITC) [64].

TRPA1, a member of the TRPA family, is important for nociception in both *Drosophila* and humans [47, 48]. A gain of function mutation in *TRPA1* causes Familial Episodic Pain Syndrome (FEPS), which was recently discovered in a Columbian family and causes debilitating pain [48]. In *Drosophila* larvae, a specific isoform of *dTRPA1* is responsible for mediating thermal nociception [50]. Other isoforoms of *dTRPA1* have been hypothesized to be responsible for thermal allodynia and hyperalgesia, although this needs further investigation. *dTRPA1* is also necessary for mechanical nociception in larvae, and is involved in chemical nociception in adult flies [46, 50].

pickpocket (*ppk*) is a Deg/ENaC channel that is important for mechanical nociception, but not thermal nociception [17]. Deg/ENaC channels are sodium-selective,

and the crystal structure revealed that they form trimers [65-68]. *ppk* is expressed strongly in the class IV neurons, and weakly in the class III neurons [8]. *ppk* does not have a direct orthologue in humans; however, mammalian acid-sensing ion channels (ASICs) are in the DEG/ENaC family. There is controversy as to the exact function of ASICs in mammalian nociception. In one study, ASIC3 null mice showed decreased sensitivity to a noxious pinch [69]. In other studies, ASIC3 null mice, as well as mice with disrupted ASIC1A, ASIC2, and ASIC3 showed increased sensitivity to a noxious mechanical stimuli [70, 71]. ASICs are also targets of snake venom proteins that trigger pain [27].

In adult flies, a screen for thermal nociception mutants found that *straightjacket* was necessary for thermal nociception [49]. *straightjacket* is a subunit of a voltage gated calcium channel, and is in the $\alpha 2\delta$ family of genes [49]. In humans, minor SNPs in the intron of the mammalian homologue of *straightjacket*, *α2δ3*, were associated with decreased pain sensitivity in healthy volunteers, as well as decreased pain following back surgery [49]. These studies shows that screens for genes involved in nociception in flies can be applied across the evolutionary tree, potentially all the way to humans.

piezo was recently discovered to be necessary for mechanical nociception in *Drosophila* larvae [72]. The *piezo* gene is well conserved throughout the eukaryotic animal kingdom [73]. The *piezo* protein is very large and has between 24 and 36

transmembrane domains [73], and forms a homo-multimeric structure, most likely a tetramer [74]. Larvae null for the *piezo* gene fail to respond to a noxious mechanical stimulus, but show normal responses to noxious heat and a gentle touch [72]. Genetic epistasis studies found that *painless* and *piezo* likely function in the same pathway, while *pickpocket* and *piezo* are in parallel pathways [72]. Heterologous expression of *piezo* results in mechanically sensitive currents [74]. Interestingly, the pore domain for this channel has not yet been identified.

1.3 Drosophila nociceptor characterization and structure

In mammals, the aδ and c fibers are the nociceptors, and detect noxious mechanical and thermal stimuli. The nociceptor neurons are structurally different than many other neurons, since the unenclosed sensory endings of the neurite projects to the skin surface. The cell bodies of the nociceptors reside in the dorsal root ganglion (DRG), and they synapse onto neurons in the dorsal horn of the spinal cord. The aδ fibers are lightly myelinated, and contribute to the fast perception of pain immediately after the injury. The c fibers are unmyelinated and contribute to the slow component of pain felt after injury, often perceived as a burning sensation [75].

There are two types of sensory neurons in *Drosophila*, the ciliated type I neurons and the non-ciliated type II neurons [76]. The type II neurons, also known as

multidendritic (md) neurons have branched dendrites that are non-ciliated. The md neurons are categorized into four morphological subclasses based on dendritic structure, with the class I neurons having the least complicated branching structure to the class IV neurons having the most complicated branching structure [77]. In addition to having different structures, the md neurons also project to different areas in the central nervous system [78]. The class I neurons are the only md neurons to project to the dorsal neuropil, while class II-IV project to the ventral neuropil, indicating that the class I neurons likely have a different functional role than the class II-IV neurons [78].

The md neurons were first implicated in nociception when *painless*, a gene that is expressed in the md neurons, was discovered to be important in mechanical and thermal nociception [16]. In order to identify the nociceptors, our lab used the GAL4 UAS system to systematically silence the different classes of md neurons and determine the effect on nocifensive behaviors. Silencing the class I and II neurons diminishes NEL to both noxious thermal and mechanical nociception; however, the class I neurons are known proprioceptors [79, 80]. Therefore, silencing of these neurons disrupts coordination, making it unlikely that these neurons are the nociceptors. Silencing of the class II and III neurons mildly affected the NEL response to mechanical stimulation, but had little to no effect on thermal nociception. However, silencing of the class IV neurons severely impaired NEL responses to noxious thermal and mechanical

stimulation [8]. This indicates that the class IV neurons are necessary for nociceptive behaviors in *Drosophila* larvae.

In addition, optogenetic activation of class IV neurons triggers NEL. Channelrhodopsin2 is a light-activated cation channel that is not endogenously expressed in *Drosophila* [81]. By expressing this channel in *Drosophila* neurons using the GAL4 UAS system and feeding the larvae all-trans retinal, a cofactor of Channelrhodopsin2, it is possible to activate specific classes of neurons using blue light [82]. Expression of Channelrhodopsin2 in the class IV neurons results in NEL in response to blue light, while NEL is not observed with optogenetic activation of other md neuron classes. Thus, the class IV neurons are necessary and sufficient for nociception, and are the larval nociceptors.

1.3.1 Class IV dendritic morphology

The class IV neurons have an elaborately branched dendritic arbor [77, 83-89], and completely tile the larval body wall [77, 84]. There are three bilaterally symmetrical pairs of class IV neurons in each abdominal segment. These are located in the dorsal, lateral and ventral clusters of sensory neurons [77] (Fig. 1). Similar to nociceptors in vertebrates, the class IV neurons have "naked" dendrites buried in the epidermis [90]. Although the development of the class IV neurons has been well characterized [86], the regulation of the morphology through ion channels has not been characterized.

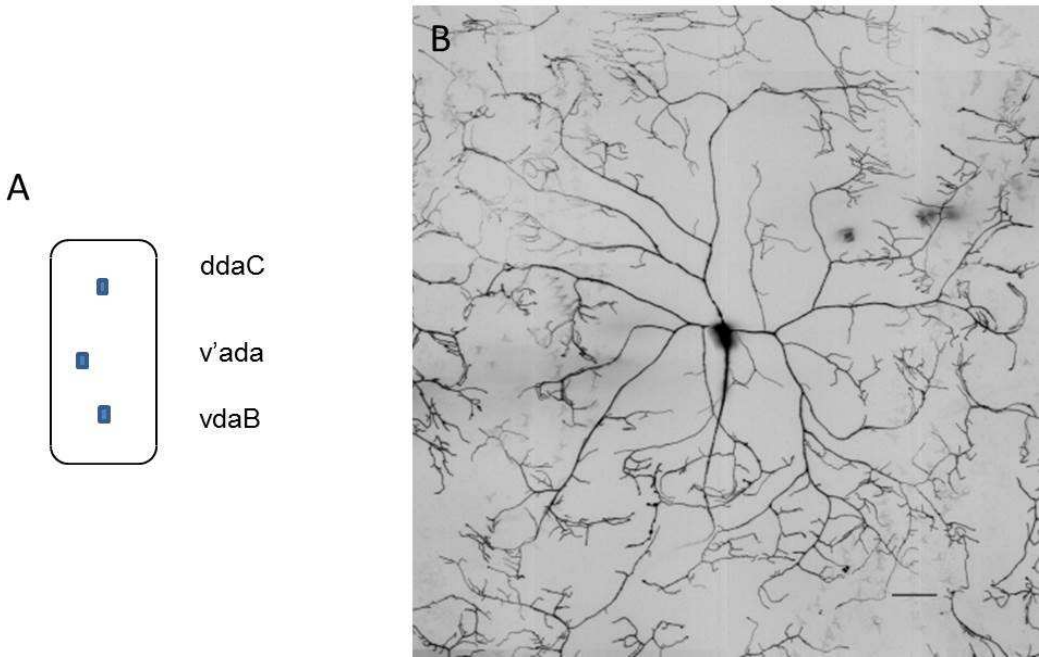

Figure 1: Class IV multidendritic neurons.

Figure 1: Class IV multidendritic neurons. **A.** There are three class IV neurons in every larval hemisegment, and they tile the larval body wall. **B.** Shown is a representative photomicrograph of ddaC. Scale bars are 50 μm.

The class IV neurons have been developed as a model for the study of dendritic branching, and several regulators of nociceptor morphology have been discovered (reviewed in [86]). These include transcription factors, cytoskeletal elements, and cell adhesion molecules [91-100]. Differential regulation of the expression levels of transcription factors can influence the formation of the complex dendritic structure of the class IV neurons [92]. *collier* and *cut* are both important transcription factors required for the specification of the class IV neurons [91, 92]. *cut* expression is absent in the class I neurons, low in the class II neurons, high in the class III neurons and intermediate in the class IV neurons [92]. Without *cut*, the class IV neuron branching is severely reduced [92]. The class IV morphology is also regulated by *collier* [91]. Expression of *collier* is high in the class IV neurons, and absent in the other md neurons. *collier* counteracts the formation of actin rich protrusions regulated by *cut* [91]. Therefore the formation of the class IV dendritic field is dependent on a delicate balance of transcription factors.

Spastin and *katanin p60-like1* (*Kat60-L1*) are both microtubule severing proteins that play a role in dendrite morphogenesis [91, 93]. Deletion of these genes reduces the coverage and complexity of the class IV neurons [91, 93] . Interestingly, deletion of *Kat60-L1* also affects thermal and mechanical nociception, indicating that there is a relationship between dendritic structure and function [93].

1.3.2 Regulation of dendrite morphogenesis through ion channels

Ion channels have a well-established role in regulating synaptic morphology (reviewed in [101]). However, the nociceptors are unique in that they have no presynaptic partners, but rather terminate directly in the epidermis. Additionally, very few studies have been done on changes to the morphology of the mammalian nociceptors. Most of these studies have concentrated on the effects of capsaicin on mammalian nociceptor morphology. Capsaicin is a potent agonist of the TRPV1 channel, which is highly enriched in mammalian nociceptors [28, 33]. In neonatal rats, systemic treatment with capsaicin causes selective degeneration of the small unmyelinated fibers and insensitivity to noxious heat and mechanical stimulation which persists in to adulthood [102-104]. Capsaicin treatment in humans (either through an intradermal injection or topical application) causes a reduction in sensitivity to noxious thermal and mechanical stimuli, as well as degeneration of the epidermal nerve fibers [105-107].

There are several potential mechanisms for the degeneration of the epidermal nerve fibers in response to capsaicin. In dissociated rat DRG cells, application of capsaicin can cause apoptosis in the presence of extracellular calcium, indicating that the cell death signal is likely due to the influx of calcium through TRPV1 [108]. The intracellular increase in calcium can activate calcium proteases such as calpain, which

cause the breakdown of a wide variety of cellular proteins [108]. Blocking calcium proteases decreases the amount of cell death caused by capsaicin [108]. These studies show that in the case of TRPV1, activation of the channel by capsaicin causes changes in dendrite morphology due to the toxic rise of intracellular calcium.

1.4 Conclusion

Drosophila melanogaster is an ideal model organism for studying nociception. The nociception behavioral paradigm and the morphology of the nociceptors are well established, allowing for easy observation [8, 16, 77]. Additionally, *Drosophila* has been utilized in the past to determine how ion channels affect nociception [16-18, 72]. However, there are many unanswered questions. For example, what role do ion channels play in detecting an ecologically relevant stimulus, such as the parasitoid wasp? Which ion channels are regulating the transduction step of nociception, and which are regulating action potential transmission? Can ion channels regulate the elaborate morphology of the dendritic field? In this dissertation, I will attempt to answer these questions.

2. A genetically tractable model for studying predator-prey interactions

2.1 Introduction

The evolutionary arms race produces an ever-changing range of predatory behaviors and defensive prey responses. Indeed, predator-prey interactions are an important evolutionary force. While predator and prey behaviors have been characterized on a macro-scale, essentially nothing is known about the genetic basis of these behaviors, many of which are innate and encoded by the genome of both the predator and the prey. Parasitoid wasps are a common predator of *Drosophila* larvae, and can infect up to 70% of larvae in the wild [109]. These wasps inject eggs into the body of *Drosophila* larvae [110], which after hatching, proceed to eat the *Drosophila* larva from the inside [111]. The predatory adaptations that parasitoid wasps use to find and infect *Drosophila* larvae, including search strategies, ovipositor properties, and immunosuppressive mechanisms, are well described [25, 26, 112-121]. However, little is known about the behavioral responses of the *Drosophila* larvae to parasitoid attack [8, 26, 122]. Given the powerful genetic tools available to *Drosophila* researchers, this system represents an opportunity for the study of predator-prey interactions in unprecedented detail.

Previous studies have shown that *Drosophila* larvae show nocifensive escape locomotion (NEL), a corkscrew-like rolling along the anterior/posterior axis, in response

to noxious thermal and mechanical stimulation [8, 16, 23, 123, 124]. A single class of neuron, the multi-dendritic class IV neuron, is both necessary and sufficient for NEL [8], and thus are functionally defined nociceptors in *Drosophila* larvae. Within each larval hemi-segment, there are three different class IV neurons, localized to the dorsal, lateral, and ventral region (named ddaC, v'ada, and vdaB, respectively) [77]. The class IV neurons possess elaborately branched dendritic arbors [77, 83-89] which tile the larval body wall [77, 84]. Similar to nociceptors in vertebrates, the class IV neurons possess naked dendrites. In *Drosophila*, these dendrites are attached to the epidermal basal lamina and are partially ensheathed by overlying epidermal cells [90, 125, 126].

In a previous study it was shown that like optogenetic activation of Class IV neurons, attacks by parasitoid wasps also triggers NEL [8]. This led to the proposal that larval NEL may have evolved as an adaptation to protect against parasitoid wasps. Here, we explore this idea further. First, we describe the full range of behaviors shown by larvae in response to wasp attacks. We find that the location of the attack, as well as the penetration of the larval cuticle, determine which type of response the larvae exhibit. Next, we explore the role of the class IV neurons in mediating the behavioral response to the wasp attack, and find that the class IV neurons are necessary for NEL following the wasp attack. We further show that *pickpocket*, a DEG/ENaC channel necessary for mechanical nociception [17], is also necessary for NEL in response to wasp attacks.

Finally, we measure the mortality of larvae that produce nocifensive responses and our results suggest that nocifensive behavior leads to escape from 50% of wasp attacks. Our study establishes a new paradigm for observing and genetically manipulating predator – prey interactions.

2.2 Materials and methods

2.2.1 Fly and wasp strains and husbandry

The following fly strains were used: Canton S, w[1118], *w;Df(2L)ppk1Aid/In(2)LR Bc*, *w;Df(2L)ppkMirB/In(2)LR Bc*, *w;pickpocket1.9-GAL4, UAS-mCD8::GFP, w;hs-flp;<tub-GAL80>*, *w;pickpocket1.9-GAL4, UAS-dTRPA1-A; UAS-mCD8::GFP/K87 Tb*, *w;UAS-TNT (E), w;UAS-IMP TNT(V)*. Flies were maintained on standard cornmeal molasses medium at room temperature. *Leptopilina boulardi-17* were kept in fly vials at room temperature and fed by placing several drops of a 50% honey solution on the vial plug. Wasp strains were maintained by first allowing Canton S flies to lay eggs for 1-3 days on standard molasses cornmeal medium. After removing the flies, male and female wasps were added to the vial and allowed to parasitize the fly larvae for 1-3 days. The infected vials were kept at room temperature until the wasps emerged, 3-4 weeks later. Once the wasps began to eclose, in order to minimize potential contact with larvae, vials were emptied of wasps once per day. Mated naïve wasps aged 3-12 days were used for all experiments.

2.2.2 Wild type behavioral assays

Approximately 40 female and 20 male Canton S flies were allowed to lay eggs for 3-3.5 hours on agar apple juice plates with a small amount of yeast paste. Behavioral assays were conducted 72.5 -76 hours post egg lay. 50 larvae were placed on a 30 mm petri dish containing 1% agar and a small amount of conditioned yeast paste from the agar apple juice plate. This yeast contained the larval kairomones which are necessary to activate the wasp oviposition behavior [113]. 2-3 wasps were placed in the petri dish with the larvae and allowed to acclimate. Video recording through the stereomicroscope began when a wasp began ovipositing.

2.2.3 Class IV silencing and *ppk* null behavioral assays

For the class IV silencing experiment, 40-50 virgin females (genotype *w;ppk-GAL4*) were crossed with 20 males (genotype *w;UAS-TNT*, or *w;UAS-IMP TNT*). For the *ppk* null experiments, the nulls were generated by crossing 40 virgin females of genotype *w;Df(2L)ppk1Aid/In(2)LR Bc* with 20 males of genotype *w;Df(2L)ppk1Mirb/In(2)LR Bc* [127]. For the heterozygous controls, 40 virgin females of genotype *w;Df(2L)ppk1Aid/In(2)LR Bc* or *w;Df(2L)ppk1Mirb/In(2)LR Bc* were crossed to w[1118] males. The mutant chromosomes were followed by absence of the dominant visible *Black Cells (Bc)* marker. Flies were allowed to lay eggs for 3-3.5 hours on agar apple juice

plates with a small amount of yeast paste. Behavioral assays were then performed as described above, with the exception of using a 3% agar plate, and 40 larvae.

2.2.4 Behavioral analysis

After an acclimation period, wasp behavior was monitored for 10 minutes from the first clear attack. Larval behavior was monitored during the attack. Any larva for which the behavior during the attack could not be clearly visualized was excluded from the study, including any larva that was burrowed during the attack. Any trial with less than 5 wasp attacks during the 10 minute period was excluded from the study. Lastly, if the larva was completely motionless the attack was excluded. In some instances (20% of attacks), multiple attacks occurred on the same larva, and any time the wasp changed its position along the larval body wall was counted as a new attack. NEL was scored if the larvae performed a complete 360° around the anterior/posterior axis. Partial rotations and/or the repeated back and forth movement of the anterior or posterior were scored as writhing. Turning was scored if either the anterior or posterior moved to one side. Peristaltic locomotion was scored when a peristaltic wave of locomotion propelled the larvae in either the forward or reverse direction. Behavioral assays were carried out on several different days, and the results were pooled, after which we performed the Fisher's Exact Test. For Figure 2C and 4C only the first response to each attack was utilized for analysis. In the class IV silencing and *ppk* null experiments, behavioral

analysis was performed with coded samples that blinded the experimenter to the genotype of the larvae. For Figure 2B, the percentage of primary behaviors was calculated by dividing the number of behavioral occurrences within a category by the total number of primary behaviors. For the secondary behaviors, the percentage was calculated by dividing the total number of times the behavior was seen as a secondary behavior by the total number of secondary behaviors.

2.2.5 Cuticle penetration assay

Approximately 40 virgin *w;pickpocket1.9-GAL4, UAS-mCD8::GFP* females were crossed with 20 CS males and allowed to lay eggs for 3-3.5 hours on agar apple juice plates with a small amount of yeast paste. Approximately 70 hours after egg lay, larvae were placed on a 1% agar plate with a small amount of yeast paste and 2-3 wasps. When one of the wasps began injecting, the other wasps were removed to ensure that all attacks could be observed. After observing the attack the larvae were removed from the plate to an eppendorf tube, which had an air hole poked through the top, and yeast paste for the larva to eat. The location of the injection and the behavioral response were noted on the tube. The next day, larvae were anesthetized with ether and imaged using a 40X oil immersion lens on a Zeiss LSM 5 live confocal microscope. The diameter of the melanotic spot was measured at the widest point using the Zeiss confocal software package.

2.2.6 Larval mortality assay

The same behavioral protocol was followed as outlined in the cuticle damage assay. Larvae were removed from the arena following the attack and pooled (according to the behavior shown (motion, turning, writhing or NEL)) into fly food vials containing yeast paste. The flies that eclosed from each group were counted and mortality was determined by subtracting the number of flies that eclosed from the total number of pupal casings in the vial.

2.2.7 Single cell activation assay

50 virgin females of the genotype *w;hs-flp;<tub-GAL80>* were crossed to 10-20 males of the genotype *w;pickpocket1.9-GAL4, UAS-dTRPA1-A; UAS-mCD8::GFP/K87 Tb* for the negative controls and experimental group. For the positive controls, 50 virgin CS flies were crossed to 10-20 males of the genotype *w;pickpocket1.9-GAL4, UAS-dTRPA1-A; UAS-mCD8::GFP/K87 Tb.* The flies were allowed to lay eggs on apple juice plates for 2-2.5 hours. Three hours after egg lay, embryos were heat shocked in a hot water bath at either 35 or 37°C for 30 minutes. Two temperatures were used in order to increase the variability in the number of neurons expressing GAL4. Negative controls were not heat shocked. Four days later, larvae were placed one at a time in a 50 μl water droplet on a hot plate set to 32.5°C, which heated the water droplet to a temperature of 31.7°C as measured by a fine thermocouple probe (IT-23, Physitemp). The larval behavior was

observed for 10 seconds. After the behavioral assay, larvae were placed in PBS and a small cut was made to segment A8 so that the intestinal tract could be removed with forceps. Larvae were mounted between coverslips in PBS and the class IV neurons expressing mCD8::GFP were counted and identified on a Zeiss LSM 5 Live microscope using a 20X objective. For the no heat shock controls, larvae were also visualized after the behavioral experiment to rule out leaky expression of the heat shock FLPase in the parental gametes. Larvae in which all of the class IV neurons were expressing mCD8::GFP (which occurs due to leaky heat shock FLPase expression) were excluded from the analysis.

2.3 Results

2.3.1 *Drosophila* larvae show multiple stereotyped behaviors in response to attacks by *Leptopilina boulardi*

To better understand this system we observed the defensive behaviors performed by *Drosophila* larvae in response to attacks by parasitoid wasps. The larval prey (40-50) were first placed in small agar containing petri dishes that were lightly coated with conditioned yeast paste (see Materials and Methods). The latter provided important chemosensory cues to stimulate egg-laying by the wasps [114]. Next, 2-3 mated *Leptopilina boulardi* wasps (a well characterized, specialist parasitoid of *Drosophila melanogaster* [24, 25]) were placed in the petri dish with the larvae, and all wasps were observed until one of the wasps began attacking. We then followed the actively

attacking wasp for a period of 10 minutes while videorecording the interactions between the wasp and the larvae. Interestingly, prior to contact with the wasps, larvae appeared to be unable to sense their presence. Larvae did not alter their course of locomotion despite the nearby presence of the wasps and they would often crawl right up to them, even bumping directly into their legs. However, once physical contact with the wasp was made, larvae did show responses that resembled previously described mechanosensory behaviors [8, 16, 72, 128, 129].

Several distinct types of larval responses were seen. Larvae displayed peristaltic locomotion in either the forward or the reverse direction (Fig. 2A) and/or rapid turning responses (Fig. 2A). The persistaltic locomotion responses and the turning responses are also seen in so-called "gentle touch assays" in which larvae are stroked with an eyelash by an investigator [128, 129]. In addition, as described in a previous study, we also observed nociceptive-related behaviors, including writhing (turning of either the anterior or posterior back and forth) (Fig. 2A) and NEL (Fig. 2A) [8, 16, 23, 123, 124]. Thus, stimulation of the larvae by the wasp ovipositor causes a variety of mechanosensory behaviors that include both gentle touch-like and nociceptive behaviors.

In over half of attacks, larvae responded by showing a combination of these different behaviors. To test whether these behaviors occurred in a specifically ordered

sequence, we created an ethogram describing the frequency and order with which each behavior occurred and broke the behaviors down into either primary, secondary, or tertiary responses (Fig. 2B). The most commonly observed primary response was peristaltic locomotion, which occurred in 40% of attacks (Fig. 2B). Turning, writhing, and NEL each occurred at approximately equal frequency, and were the primary response in about 20% of the attacks (Fig. 2B).

As with the primary response, peristaltic locomotion was the most frequent secondary response, and was observed after turning, writhing, or NEL (Fig. 2B). Peristaltic locomotion was equally likely to occur as a primary (40%) or secondary behavior (45%). Writhing was also equally likely to occur as a primary (19%) or secondary (12%) behavior. Turning behavior tended to occur more as a secondary response (36%) than a primary response (19%, $p<.05$, Fishers Exact Test with Holm-Bonferroni correction). Lastly, NEL occurred most frequently as a primary response (22%), and more rarely as a secondary response (8%, $p<.05$, Fishers Exact Test with Holm-Bonferroni correction).

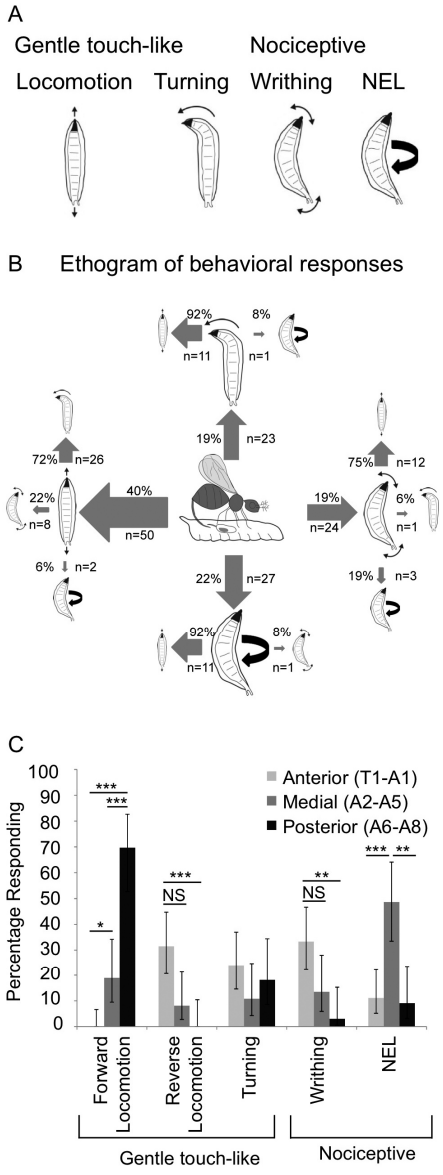

Figure 2: Behavioral responses of *Drosophila melanogaster* larvae to attack by LB.

Figure 2: Behavioral responses of *Drosophila melanogaster* larvae to attack by LB.

A. Classification of behavioral responses to attacks by parasitoid wasps. The cartoons depict peristaltic locomotion, turning, writhing and NEL ((NEL) also see supplemental videos). **B.** Ethogram of behaviors shown by third instar larvae (based on observations of 124 attacks). The size of the arrow is weighted according to the observed frequency of the behavior. Primary behaviors are indicated by large cartoons, and secondary behaviors are indicated by the smaller cartoons. Tertiary behaviors are not shown. **C.** Attack position along the larval body wall influences behavioral response. Fisher's Exact Test with Holm-Bonferroni correction. Data are presented as percentages ± 95% confidence intervals. P< .05 =*, P<.01=**, P< .005 =***. N=54(Anterior), N=37(Medial), N=33(Posterior).

We noticed that some of the variation in the larval behavioral responses appeared related to the location of the wasp attack along the larval body. As shown in Figure 2C, this observation was supported by further analysis. Wasps attacked the anterior segments (T1-A1) 54 times, the medial segments (A2-A5) 37 times and the posterior segments (A6-A8) 33 times. Forward locomotion occurred most frequently when the wasp attacked in the posterior region, and reverse locomotion or writhing happened most frequently when the wasp attacked in the anterior region (Fig. 2C). Interestingly, NEL was much more likely to occur when the attack was in the medial segments (Fig. 2C).

Note that the frequency of forward locomotion as a response was likely to be overestimated. This is because many of the larvae (30%) that were scored as showing forward locomotion were already engaging in forward locomotion at the moment when they were first attacked. Thus, in these attacks we were unable to discern whether the forward locomotion that we observed was an actual response to the attack, or if the larvae had simply continued their previous behavioral pattern.

2.3.2 Attacks with nocifensive responses show greater penetration of the larval cuticle

Our above observation of wasp attacks and larval behavior did not provide information on whether or not the wasps successfully penetrated the larval cuticle in a particular attack. Thus, the observation of larval behaviors does not provide any specific

information on the degree to which a particular behavior might provide a selective advantage to the larvae. Nevertheless, because successful epidermal penetration by the wasps triggers a melanization cascade in the larvae, and this leaves a "melanotic spot" that is visible under a microscope [130], we were able to directly test whether specific attacks resulted in penetration. To achieve this, we observed larvae being attacked by wasps, recorded the larval behavioral response, and later searched for the presence or absence of a melanotic spot while simultaneously observing the nociceptor dendrites under a confocal microscope. These analyses revealed that successful cuticle penetration occurred in only 44% of all wasp attacks. Cuticle penetration was relatively rare in the attacks that resulted in non-nociceptive behaviors, occurring only 24% of the time (Fig. 3A). Larvae that showed writhing behavior had an intermediate frequency of cuticle penetration (56%) (Fig. 3A). Interestingly, larvae that performed nocifensive escape locomotion following attacks showed the highest frequency of cuticle penetration (71%) (Fig. 3A). The cuticle penetration of larvae that showed nocifensive responses was primarily confined to the medial body segments (at least 70% of the time) further confirming the importance of somatotopy in determining the behavioral responses of larvae.

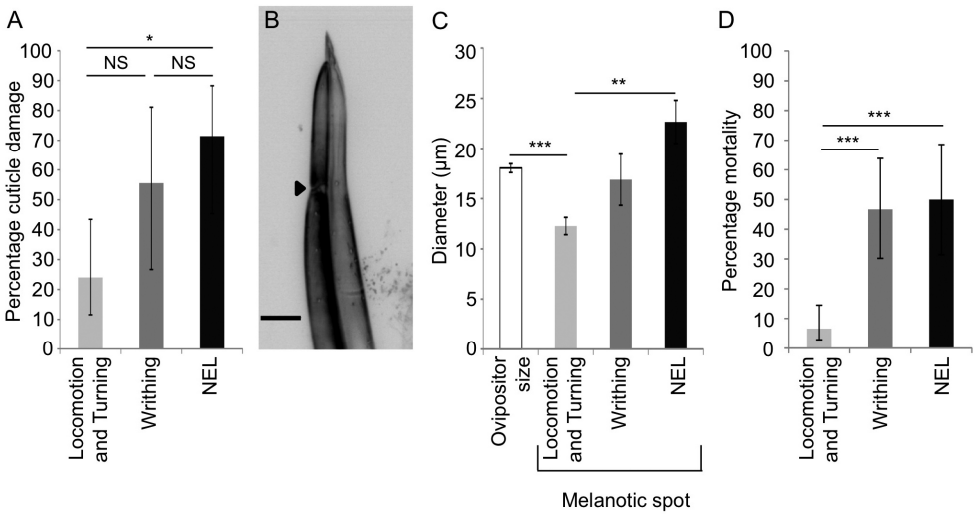

Figure 3: Cuticle penetration and mortality is more frequent in attacks with nociceptive behaviors.

Figure 3: Cuticle penetration and mortality is more frequent in attacks with nociceptive behaviors. Cuticle penetration and mortality is more frequent in attacks with nociceptive behaviors. **A.** Larvae that showed NEL showed frequent penetration of the cuticle (N=14, 71% (+17/-26)). Gentle touch-like behaviors (turning and locomotion) rarely showed penetration to the cuticle (N=25, 24% (+19/-13)). Writhing behaviors were associated with an intermediate level of penetration (N=9, 56%, (+26/-29)). Fisher's Exact Test with Holm-Bonferroni correction. Data are presented as percentages ±95% confidence intervals. **B.** Representative photomicrograph of a wasp ovipositor (scale bar=20 μm). The arrowhead indicates the location of the ovipositor clip. **C.** The melanotic spot was similar to the diameter of the ovipositor clip (N=12, 18μm, ± .4) when attacks triggered either writhing (N=5, 17μm, ±2.6) or NEL (N=9, 23μm, ±2.2). The size of the melanotic spot was smaller than the diameter of the ovipositor clip when larvae that showed non-nociceptive behaviors (N=6, 12μm, ±.9). T-test with Bonferonni-Holm correction. Error bars denote standard error of the mean. **D.** Mortality was high in larvae that displayed writhing (N=30, 47%,+(17/-16)) or NEL (N=24, 50%, (+19/-19)) relative to larvae that displayed locomotion and turning (N=76, 7%, (+8/-4)) . Fisher's Exact Test with Holm-Bonferroni correction. Data are presented as percentages ±95% confidence intervals. P<.05=*, P<.01=**, P< .005 =***.

The wasp ovipositor possesses a specialized structure that resembles the barb of a fish hook. It is believed that this structure, termed the clip, prevents removal of the ovipositor from the struggling larvae during the attack (Fig. 3B) [119, 122]. Interestingly, when the attack resulted in nociceptive related responses, the diameter of the melanotic spot was similar to the diameter of the ovipositor clip which is consistent with the idea that the ovipositor penetrated to the depth of the clip in these attacks (Fig. 3C). In contrast, in attacks that elicited gentle touch-like behaviors the diameter of the melanotic spot was significantly smaller than the wasp ovipositor clip which suggests that these attacks resulted in only partial penetration (Fig. 3C).

2.3.3 Larval mortality following different behavioral responses

The data above indicate that wasps most successfully penetrated the cuticle when attacking medially and that the penetrating attacks were the most likely to elicit nocifensive behavior. Is the NEL also an effective means of escape following cuticle penetration? If this were so, we would expect that larval mortality in attacks that elicited NEL would be lower than the penetration rate for these attacks (71%). Consistent with this hypothesis we found that the mortality of larvae that showed NEL behavior during wasp attacks was 50% (Fig. 3D, methods). Because *Drosophila melanogaster* is not capable of mounting a successful immune response to *Leptopilina boulardi,* the difference observed between the frequency of cuticle penetration and

mortality likely indicates that larvae are able to escape from wasps prior to oviposition when performing NEL.

2.3.4 Sparse activation of the class IV neurons causes NEL

Behavioral assays that trigger NEL are used for studies on the cellular and molecular mechanisms of nociception in *Drosophila* larvae [8, 16, 17, 23, 124]. We targeted the NEL response for further investigation so we could further understand this behavior in the context of an ecologically relevant stimulus. The class IV neurons are the primary nociceptors of *Drosophila* larvae and have an elaborate dendritic field which tiles the larval body wall [77, 83-87, 90]. Within each larval hemi-segment, there are three identifiable class IV neurons (ddaC, v'ada, and vdaB), which are localized to the dorsal, lateral, and ventral region, respectively [77]. Previous experiments have shown that either optogenetic or thermogenetic activation of class IV neurons is sufficient to trigger NEL [8, 18]. The neuronal activators used in these approaches have been expressed in all of the class IV neurons and it thus remains unknown whether activation of a limited number of cells is sufficient for triggering the behavioral response. The wasp system presents a useful paradigm to investigate the circuitry of the NEL response due to the small size of the wasp ovipositor (Fig. 3B and 2C) and to the ability to visualize the point of insertion after the attack. Interestingly, in our examination of melanotic spots described above, we found that the melanotic spot could be found

within a single dendritic field of either the dorsal, the lateral, or the ventral Class IV neuron (Fig. 4A).

Although the injury revealed by the melanotic spots was confined to the dendritic field of a single class IV neuron, it remained possible that the force generated by the insertion of the wasp ovipositor could be sensed by a more distributed population of neurons. Thus, we wished to determine the minimum complement of class IV neurons whose activation would be sufficient to cause NEL. To achieve this, we used an approach which allowed us to thermogenetically activate a small random subset of the class IV neurons. We first exposed animals of the genotype *w;hs-flp /pickpocket1.9-GAL4, UAS-dTRPA1-A;<tub-GAL80>/ UAS-mCD8::GFP* to a 30 minute heat shock [131]. This caused expression of GAL4 in a random subset of the class IV neurons, which in turn caused expression of the warmth activated dTRPA1-A [18, 132-135] channel and a fluorescent plasma membrane marker (mCD8::GFP). We then placed larvae in a 50 μL water droplet heated to 32°C, and observed the larval behavior for 10 seconds. Following the behavioral observations, larvae were mounted for microscopy and the class IV neurons expressing mCD8::GFP (as a proxy for GAL4 and dTRPA1-A expression) were then identified.

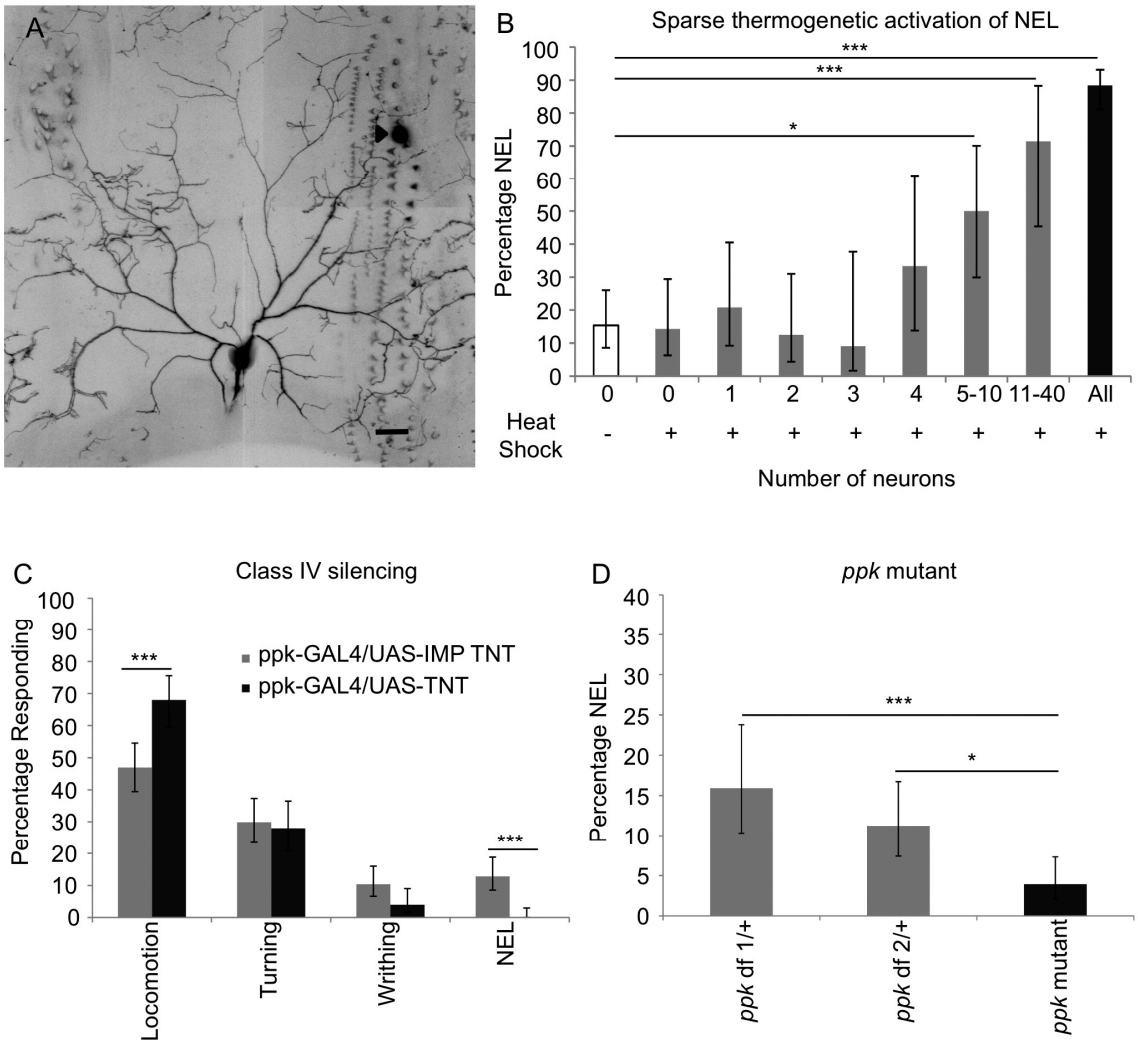

Figure 4: Role of the class IV neurons and NEL in response to wasp attack.

Figure 4: Role of the class IV neurons and NEL in response to wasp attack. A. Confocal micrograph of the dendritic field of the dorsal (ddaC) class IV neuron taken from a larva (*ppk-GAL4 UAS-mCD8::GFP*/+) that displayed NEL following wasp attack. Scale bars are 20 μm. The location of ovipositor penetration is denoted by an arrowhead. **B.** Expression of dTRPA1-A in 5-10 class IV neurons is sufficient to cause NEL. (0 neurons in the no heat shock control (N=65, 15%, (+11/-7)), 0 neurons following heat shock (N=35, 14% (+15/-8)), 1 neuron (N=24, 21%, (+20/-12)), 2 neurons (N=24, 13%, (+19/-8)), 3 neurons (N=11, 9%, (+29/-7)), 4 neurons (N=12, 33%, (+28/-20)), 5-10 neurons (N=20, 50% (+20/-20)), 11-40 neurons (N=14, 71%, (+17/-26)), positive controls (N=112, 88%, (+5/-7)). The genotype used was *w;hs-flp /pickpocket1.9-GAL4, UAS-dTRPA1-A;<tub-GAL80>/ UAS-mCD8::GFP*. For positive controls the genotype was *pickpocket1.9-GAL4, UAS-dTRPA1-A/+; UAS-mCD8::GFP*/+. **C.** Larvae with class IV neurons silenced by UAS-TNT-E (N=125) show no NEL (0%, (+3/-0)) and increased locomotion (68%, (+8/-9)) compared to larvae expressing impotent TNT in the class IV neurons (N=164, NEL 13%, (+6/-4), locomotion 47%, (+8/-7)). The genotypes are *w;ppk-GAL4/UAS-TNT*, *w;ppk-GAL4/UAS-IMP TNT*. **D.** *ppk* null larvae show significantly less NEL than controls. (*ppk Df1(w;Df(2L)ppk1Aid*/+), N=113 (16%, +8/-6)), (*ppk Df2(w;Df(2L)ppk1Mirb*/+), N=178 (11%, +5/-4)), and (*ppk* null (*w;Df(2L)ppk1Aid/Df(2L)ppk1Mirb)*N=229, 4%,+3/-2). Fisher's Exact

Test with Holm-Bonferroni correction. Data are presented as percentages ±95% confidence intervals. P< .05 =* and P< .005 =***

These experiments indicated that 5-10 GAL4 expressing neurons were needed to trigger NEL above the background level seen in control animals (without detectable expression of mCD8::GFP (Fig. 4B)). These results indicate that although the wasp ovipositor is capable of triggering NEL when penetrating a single dendritic field, expression of dTRPA1-A in a single class IV neuron was not sufficient to cause NEL in response to warm temperatures under these experimental conditions.

2.3.5 The class IV neurons and the *ppk* gene are necessary for NEL in response to wasp attacks

The class IV neurons are necessary for NEL in response to artificially applied noxious thermal or mechanical stimuli [8]. However, the wasp attack represents a qualitatively distinct stimulus, with the potential for breaking through the cuticle, epidermal cells, and possibly the dendrites of the nociceptors. Thus, we were interested in determining whether the Class IV neurons were indeed required for nocifensive responses to wasp attacks. To test this possibility, we silenced the class IV neurons through expression of tetanus toxin light chain (TNT) [136] and investigated the effects on the larval response to wasp attacks. As expected if the nociceptive neurons were specifically involved in sensing the harshest of attacks, larvae with silenced class IV neurons showed an abolishment of NEL (Fig. 4C). This indicates that the class IV neurons are responsible for mediating the NEL response to wasp attacks. We also noted that there was an apparent increase in the peristaltic locomotion response in these

animals. This may indicate that "gentle touch" pathways are still engaged during attacks that would normally have triggered nocifensive responses in an intact animal. Alternatively, larvae null for the *ppk* gene, which is expressed highly in the class IV neurons, show higher base-line levels of locomotor activity [137]. The increased response locomotion response could reflect a deficiency in *ppk* signaling.

We next tested whether known molecular transduction pathways were involved in mediating the nocifensive escape responses to wasp attacks. This was achieved through observations on the NEL responses in larvae null for the *pickpocket (ppk)* gene. *ppk* encodes a DEG/ENaC channel that shows strong expression in the class IV neurons, and is weakly expressed in the class III neurons[17]. *ppk* is necessary for mechanical nociception [17]. We used overlapping deficiencies that remove only the *ppk* gene [127]. These deficiencies are maintained separately a stocks and crossed together to create the *ppk* null larvae. As in the Class IV neuron silencing experiments, larvae null for *ppk* showed significantly decreased NEL compared to heterozygous mutant controls (Fig. 4D). This suggests that *ppk* is necessary for stimulus transduction that results in NEL in response to the naturally occurring wasp stimulus. However, since the larvae utilized in this experiment were null for the *ppk* gene in all tissues, there is a possibility that the deficit in NEL in response to wasp attacks is not necessarily due to lack of *ppk* in the class IV neurons, as the class III neurons could also be contributing.

2.4 Discussion

In this study, we have fully characterized the somatosensory behaviors shown by larvae in response to attack by *Leptopilina boulardi* wasps, and found that larvae show both non-nociceptive and nociceptive responses. The precise somatosensory response to the wasp attack depends on the somatotopic location of the attack, as well as the penetration of the cuticle by the ovipositor. Lastly, we investigated the cellular and molecular basis of the larval responses to wasp attacks, and found that both the class IV multidendritic neurons and the *ppk* gene are necessary for NEL in response to wasp attacks.

In response to wasp attacks, larvae showed a variety of somatosensory responses, including both forward and reverse locomotion, turning behavior, writhing and NEL. Forward locomotion was included as an escape behavior from wasp attacks even when a particular larva had previously been showing forward locomotion prior to the onset of the attack. In these cases, it was difficult to determine if the larvae were truly responding to the attack or if they were simply continuing their previous behavior. We included forward locomotion as it may be an important means of escape for larvae that are burrowed into a fruit in the wild. Consistent with this there were several instances where we observed a burrowed larva that was attacked in the posterior and the larval forward locomotion response was seen to pull the wasp down into the

burrow. Because the wasp ovipositor has a limited length, it is possible that this response would cause the wasp to disengage its attack prior to egg-laying.

Our data showed that larvae that engage in NEL are more likely to show cuticle penetration by the wasp ovipositor (Fig. 3A), and have larger wound sites than larvae engaging in non-nociceptive behaviors (Fig. 3B). Indeed, larvae that engaged in non-nociceptive behaviors have wound sites smaller than the diameter of the ovipositor measured at the ovipositor clip. In previous studies the ovipositor clip was proposed to function similarly to the barb on a fish hook, in other words, to prevent larvae that are struggling vigorously against an attack to escape [119, 122]. Our data are consistent with this hypothesis, and they further suggest that the most vigorous escape responses in the larvae actually occur primarily in those attacks that involve successful and deep penetration of the larval epidermis. Thus, the ovipositor clip may have evolved as an adaptation against the nocifensive responses.

We found that larvae that displayed nociceptive responses to a wasp attack have higher mortality rates (Fig. 3D). While it is tempting to speculate on the efficacy of each of the different behavioral responses as a method of escape from the wasp, these comparisons are difficult. For example, larvae show both low levels of cuticle penetration as well as little mortality in attacks that elicited gentle touch-like behaviors. One interpretation of these findings is that these behaviors are highly effective methods

of escape and they thus prevent the wasp from penetrating the cuticle. Alternatively, the forces applied by the wasps in these particular attacks may merely be insufficient for penetrating the cuticle and/or triggering nocifensive responses.

In investigating the cellular basis of the NEL, we found that although damage to a single dendritic field of the class IV neurons was sufficient to cause NEL, expression of dTRPA1 in 5-10 neurons was needed to cause NEL in response to a sub-noxious thermal stimulus. Although these results must be interpreted in the context of technical limitations of this approach (for example it is possible that the expression levels of dTRPA1-A in this experiment are too low to reliably induce activation of every neuron that expresses GFP) a more intriguing interpretation is that the penetration by the wasp might activate a small population of Class IV neurons even though the ovipositor damage is confined to the field of a single neuron. This could occur through viscoelastic coupling of the forces across several segments of the larvae, or alternatively, damage to epidermal cells may allow the damage signal to spread to many neurons at once. The latter possibility is consistent with the results of recent studies which indicate that the nociceptor dendrites are ensheathed by epidermal cells [125, 126] and with the previously described electrical coupling of epidermal cells that occurs through gap junctions [138].

Both the class IV neurons and the *ppk* gene had previously been found to be necessary for NEL in response to noxious mechanical stimulation [8, 17]. Although the wasp ovipositor is a different stimulus, since it often breaks through the larval cuticle and the attack can occur at any location along the larval body wall, we found that the class IV neurons and the *ppk* gene are also necessary for NEL in response to wasp attacks. This is a good preliminary indication that the mechanical nociception assay may be a good, higher throughput way to screen for genes that are necessary for nocifensive responses to wasp attacks. Genes identified through the mechanical nociception assay could then be tested in follow-up experiments using the wasp.

In conclusion, *Drosophila* larvae show a variety of mechanosensory behaviors in response to attacks by parasitoid wasps. These responses are strongly influenced by the somatotopic location of the attack. Attacks with nocifensive responses showed the highest frequency of cuticle penetration and penetration of a single nociceptor field was sufficient to trigger nocifensive responses. Nevertheless, expression of dTRPA1 in a population of 5-10 nociceptive neurons was needed to trigger NEL. Interestingly silencing of Class IV md-da neurons, as well as deletion of the *ppk* ion channel eliminated NEL responses to wasp attacks, which demonstrates that the neuronal and molecular pathways identified with artificial stimuli also play a role in escape from a natural deadly stimulus. Our thorough characterization of the interactions between

Drosophila larvae and parasitoid wasps open up the field of predator-prey interactions and will allow for a detailed analysis of the genomic encoding of prey escape behavior.

3. Larval behavioral responses to parasitoid wasps are species-dependent and age-dependent

3.1 Introduction

There are thousands of species of parasitoid wasps that utilize other insects as hosts to feed their offspring. Different species of parasitoids have unique strategies that they use to detect and parasitize their hosts. For example, parasitic wasps in the genus *Asobara* use vibrotaxis to locate *Drosophila* on rotting fruit, whereas *Leptopilina* localize their host through probing the substrate with their ovipositor [116]. Other species of wasps have unique ways of incapacitating their prey so that they will be successfully parasitized. The jewel wasp, which preys on cockroaches, injects the subesophogeal ganglion with a neurotoxin that renders the roach incapable of moving on its own, and proceeds to trap it in a den as a live food source for its progeny [139]. In addition to vastly different detection and attack strategies, different species of parasitoid wasps specialize in parasitizing different parts of the insect life cycle, with some parasitoids choosing to prey on the larval stages, while others prey on adults.

Leptopilina boulardi (LB) and *Leptopilina heterotoma* (LH) are two well-studied parasitoids of *Drosophila* [24]. These two species are closely related, but are in separate phylogenetic groups [140]. When attacked by parasitoid wasps, *Drosophila* attempt to mount an immune response to encapsulate the parasitoid egg with lamellocytes, which, if successful, causes a chemical reaction to kill the parasitoid egg [24]. While the

melanogaster species is capable of encapsulating the eggs of some parasitoid species, it fails to encapsulate eggs from the most virulent strains of LB and LH [25].

Although closely related, LB and LH are markedly different in virulence. LB is a *Drosophila melanogaster* specialist, and has very limited success in parasitizing other species of *Drosophila* [141, 142]. LH is a *Drosophila* generalist, and is able to infect a wider range of *Drosophila* species [141, 143]. LH is able to completely shut down the immune response to the foreign egg, and thus never becomes encapsulated and killed [141, 144, 145]. This is achieved through the injection of virus like particles (VLP) with the venom that passes through the ovipositor. VLP's have some similarity to poly-DNA viruses, but lack any genetic element [146]. LH's VLP's attack the larvae's lamellocytes, which are responsible for encapsulating the egg, causing them to lyse [145, 147, 148]. The venom of LB also contains VLP's, but the LB VLP's do not shut down the initiation of the immune response [25, 146]. Rather, LB eggs attach to the gut (as opposed to free floating as in LH) [149], which makes them more difficult to encapsulate. Additionally, the VLP's alter the shape of the lamellocytes [141, 150, 151]. In species other than *melanogaster*, LB's eggs become encapsulated and killed [141].

LH and LB attack all three instars of *Drosophila* larval development, but prefer to attack second and third instar larvae [24]. Many developmental changes take place between first and third instar. Third instar larvae are easier for the wasp to find, since

they are a bigger target, but also present more danger, since their large size could injure the wasp during the larval behavioral response to an attack [8, 122]. Larger larvae have developed immune-competence against wasp attacks, and their immune systems will attempt to attack the wasp eggs [123, 152]. In contrast, first instar larvae are much smaller than the parasitoid wasps, and even a violent behavioral response poses little danger to the wasp. However, since they are at an earlier stage of the life-cycle, the odds of them successfully pupating are lower than that of later stage larvae, indicating that it is less likely for the wasp progeny to make it to adulthood. We hypothesized that *Drosophila* larvae will show age-related changes in their behavioral responses to wasp attacks.

In this study we expand upon our previous work describing the range and genetic basis of attacks on larvae by parasitoid wasps to encompass developmental and species differences seen in response to attacks by LB and LH. Our results indicate that *Drosophila* larvae exhibit different behaviors depending on the species of wasp that is attacking, and develop new behavioral responses as they age. This study represents a major step forward in understanding how *Drosphila* larvae experience nociception due to a naturally occurring and evolutionarily relevant stimulus.

3.2 Materials and methods

3.2.1 Fly and wasp strains and husbandry

The Canton S fly strain was used for all experiments. Flies were maintained on standard molasses cornmeal medium at room temperature. *Leptopilina boulardi-17* (LB) and *Leptopilina heterotoma-14* (LH) were maintained by allowing them to parasitize Canton S larvae. Canton S flies were allowed to lay eggs for 1-3 days on standard cornmeal molasses medium, after which the wasps were allowed to parasitize the larvae for 1-3 days. After eclosion, wasps were kept in fly vials at room temperature and fed by placing several drops of a 50% honey solution on the vial plug. In order to minimize potential contact with larvae so that wasps would not gain experience in attacking larvae, wasp vials were emptied of wasps every day. For all experiments, only mated wasps between 3-11 days were used.

3.2.2 Behavioral assays

Approximately 40 female and 20 male Canton S flies were allowed to lay eggs for 3 – 3.5 hours on agar apple juice plates with a small amount of yeast paste. To investigate the behavioral responses of first instar larvae, behavioral assays were conducted 25 - 27.5 hours post egg lay. For third instar larvae, behavioral assays were conducted 72.5 - 76 hours post egg lay. 40-60 larvae were placed on a 30 mm petri dish containing 1% agar and a small amount of yeast paste from the agar apple juice plate (in

order to entice the wasp to begin attacking) [113]. Two to three wasps were placed in the petri dish with the larvae and allowed to acclimate. Video recording through the stereomicroscope was started when a wasp began consistently attacking. The data gathered on third instar LB from Chapter 2 were used for analysis in this chapter.

3.2.3 Behavioral analysis

For an in depth description of the behavioral analysis, please see the materials and methods in Chapter 2. Briefly, after an acclimation period, wasp behavior was monitored for ten minutes from the first clear attack. Larval defensive behavior was monitored during the attack, and possible paralysis was monitored for five seconds after the wasp had disengaged from the larva. Any larvae for which the behavior during the attack were unclear was excluded from the analyses. Any trials with less than five attacks during the ten minute period were also excluded. Lastly, if the larva was completely motionless for the duration of the attack it was excluded. To score paralysis following the attack, larvae were observed for five seconds after the wasp had disengaged from the attack. Larvae that did not resume forward peristalsis during those five seconds were scored as paralyzed.

3.2.4 Ovipositor imaging

Naïve female wasps were dissected in PBS, and the ovipositor was removed and mounted on a coverslip for imaging on an LSM 5 Live Confocal Microscope. We then

imaged the ovipositors at 532 nm, which causes auto-fluorescence. This allowed us to see the final details of the ovipositor clearly. Measurements of the ovipositor at the clip were taken using the LSM 5 Live software.

3.3 Results

3.3.1 Larvae show species dependent differences in behavioral responses to parasitoid wasps

Although LB and LH are in the same genus, they have different virulence for *Drosophila*. LB is a *Drosophila melanogaster* specialist, and is not very successful at infecting other species of *Drosophila*, whereas LH is a *Drosophila* generalist, capable of infecting a wide variety of *Drosophila* species [25]. Thus, we investigated whether the difference in virulence was related to different behavioral defenses employed against the two species of wasp. Indeed, we found that third instar larvae attacked by LH have significantly higher rates of peristaltic locomotion compared to larvae attacked by LB (Fig. 5A). Additionally, larvae attacked by LH exhibited significantly lower rates of nocifensive escape locomotion (NEL) (Fig. 5A).

It has been previously reported that LH venom contains a paralytic [122]. Consistent with this, a large fraction of third instar larvae were paralyzed following an attack by LH (Fig. 5B). In contrast larvae were not paralyzed following attack by LB (Fig. 5B). To measure paralysis, larvae were observed for five seconds following the wasp's disengagement. Larvae that were not capable of forward locomotion following

the attack were scored as paralyzed. Virtually no third instar larvae were paralyzed following attack by LB, whereas over a third of larvae showed evidence of paralysis following attack by LH (Fig. 5B).

In the previous chapter, I found that the location of the attack by LB along the larval body wall affected the behavioral outcome. Specifically, NEL was more likely to occur if the attack was in the medial segments. Since larvae attacked by LH showed significantly lower rates of NEL, one possibility is that LH preferentially targets the anterior and posterior for attack, avoiding the medial segments. However, LH attacked the anterior, medial and posterior equally (Fig. 6A). There were no significant differences in the anterior, medial, or posterior location of attacks along the larval body wall for LH relative to LB (Fig. 6A).

Next, I wanted to determine if the location of the attack by LH influenced the larval behavioral response. The only significant effect of location on the behavioral outcome was that attacks in the posterior were more likely to result in locomotion (Fig. 6B). Although this was the only statistically significant finding, the trends in the somatotopic regulation of the behavior were similar to that seen during attacks by LB. For example, attacks on the anterior resulted in higher rates of writhing, although after the Bonferonni correction this was not significant (Fig. 6B). Lastly, while only two attacks resulted in NEL, both of these attacks were in the medial segments (Fig. 6B).

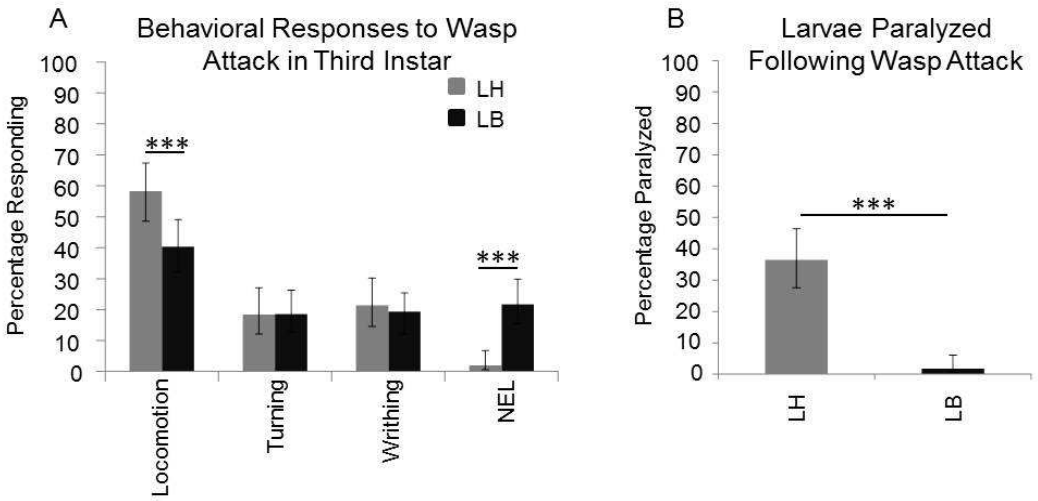

Figure 5: Third instar larvae show different behavioral responses to attacks by LB and LH.

Figure 5: Third instar larvae show different behavioral responses to attacks by LB and LH. **A.** Larvae showed significantly more peristaltic locomotion following attack by LH (N=103, 58% (+9/-9) than attack by LB (N=124, 40% (+9/-8)). Larvae attacked by LH showed significantly lower rates of NEL (2% (+5/-1)) than larvae attacked by LB (22% (+8/-6)). **B.** LH causes higher levels of immobility following attack. Larvae attacked by LH are incapable of forward locomotion 36% of the time following the attack (N= 96, 36%, (+10/-9)), whereas larvae are rarely immobile following attack by LB (N=117, 2%, (+4/-2)). Data are presented as percentages ± 95% confidence intervals. Fisher's Exact Test with Holm-Bonferroni correction.P< .05 =*, P<.01=**, P< .005 =***.

In our study on LB, we found that larger wound sites were associated with nociceptive behaviors. Another hypothesis to explain the lack of NEL in attacks by LH was that the wasp ovipositor might have been smaller, making it more difficult to detect. Therefore, I looked at the gross morphology of the wasps' ovipositor. I detected no gross structural differences between LH (Fig. 6C) and LB (Fig. 6D) using confocal microscopy. In addition measurements of the width of the ovipositor at the ovipositor clip did not reveal a difference (Fig. 6E).

3.3.2 Larvae show developmental differences in response to attacks by parasitoid wasps

Parasitoid wasps are faced with an interesting problem. Although third instar larvae are better developed and potentially more likely to make it to pupation than younger larvae, they are also much bigger, and may be capable of inflecting more harm on the wasp**.** Parasitoid wasps show a preference for infecting later instar larvae, although they will still infect and attack first instar larvae [24]. A previous study found that only third instar larvae are able to show NEL in response to noxious thermal stimulus [153]. In order to determine if larval behavior to attack by parasitoid wasps changed with development, we observed attacks by LB in first and third instar larvae. First instar larvae showed significantly higher rates of locomotion following attack by LB.

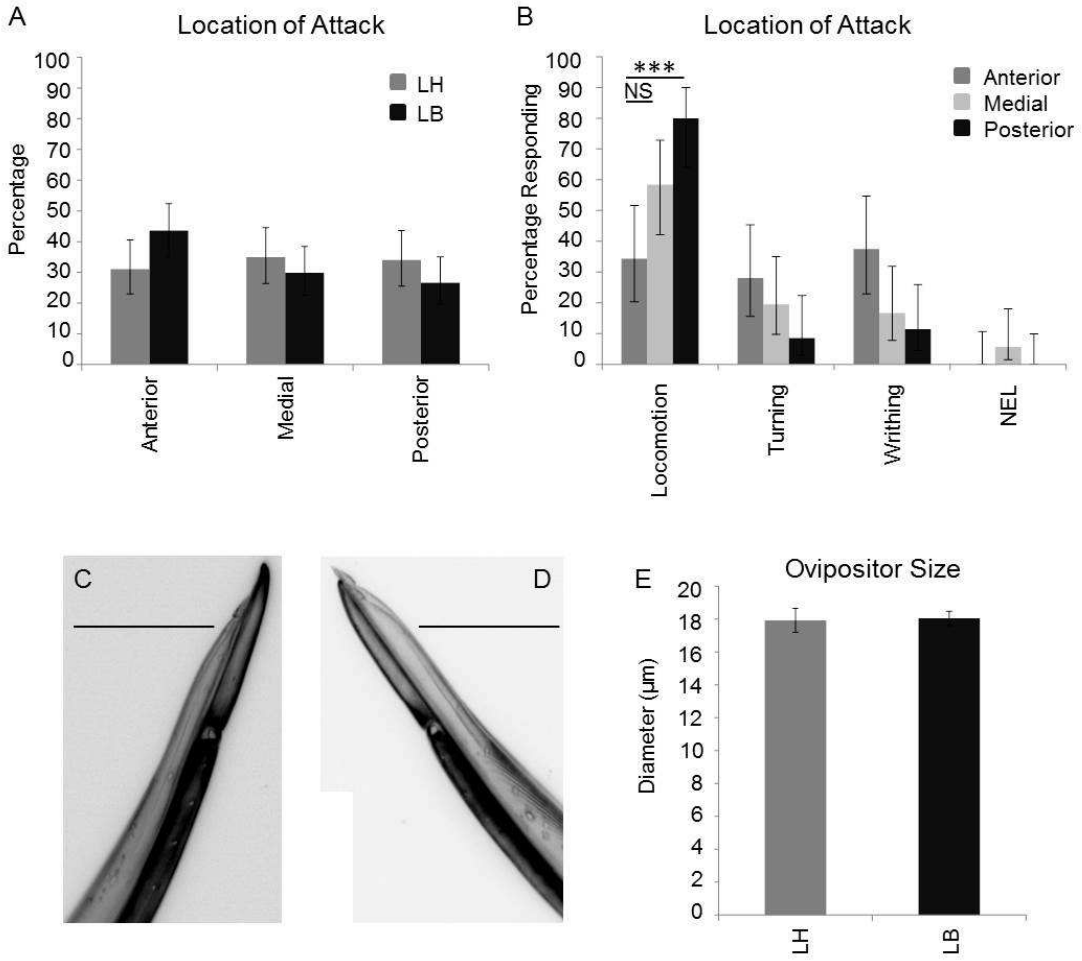

Figure 6: Comparisons in attack localization and ovipositor morphology between LH and LB.

Figure 6: Comparisons in attack localization and ovipositor morphology between LH and LB. A. LH (N=103) and LB (N=124) show no significant differences in the localization of attack along the larval body wall. Fisher's Exact Test (p = .1539). **B.** Larvae attacked by LH show significantly higher rates of locomotion when attacked in the posterior. The other behaviors show no statistically significant differences due to the location of the attack, but follow the same trends seen following attacks by LB. (Anterior N=32, Medial N= 36, Posterior N = 35). Data are presented as percentages ± 95% confidence intervals. Fisher's Exact Test with Holm-Bonferroni correction. **C.** Representative photomicrograph of an ovipositor from LH. Scale bar is 50 μm. **D.** Representative photomicrograph of an ovipositor from LB. Scale bar is 50 μm. **E.** There is no difference in the size of the wasp ovipositor between LH (N=11, 17.9 μm ± .7) and LB (N=12, 18.0μm, ± .4). Data presented are mean ± SEM. T-test. P< .05 =*, P<.01=**, P< .005 =***.

Additionally, first instar and third instar larvae show stark differences in NEL (Fig. 7A). This indicates that either the circuitry for NEL or the ability to sense the wasp ovipositor may not be fully developed in first instar larvae.

3.4 Discussion

In this chapter, I have shown that *Drosophila* larvae show species dependent and developmentally dependent changes in their somatosensory behavioral responses to attacks by parasitoid wasps. Only third instar larvae attacked by LB show a high percentage of NEL compared to other behaviors, while first instar larvae attacked by LB and third instar larvae attacked by LH rarely show this behavior.

I have ruled out several hypotheses to explain the differences in NEL between LB and LH. I observed no significant differences in the location of the attack along the larval body wall, or between the size of the ovipositor. Perhaps the most likely explanation is that the paralytic in LH venom may limit NEL [122]. The paralytic can only be injected when the ovipositor penetrates the cuticle, so only NEL will be affected, as we have observed (Fig. 5A). There are several ways that the paralytic may limit NEL. For instance, the paralytic could be extremely fast acting so that the larva is unable to respond with NEL. Alternatively, the wasp could return to inject a larva that had been previously paralyzed. Although immobile larvae were not included in the analysis, the effects of the paralytic could be long lasting, and larvae may be able to initiate

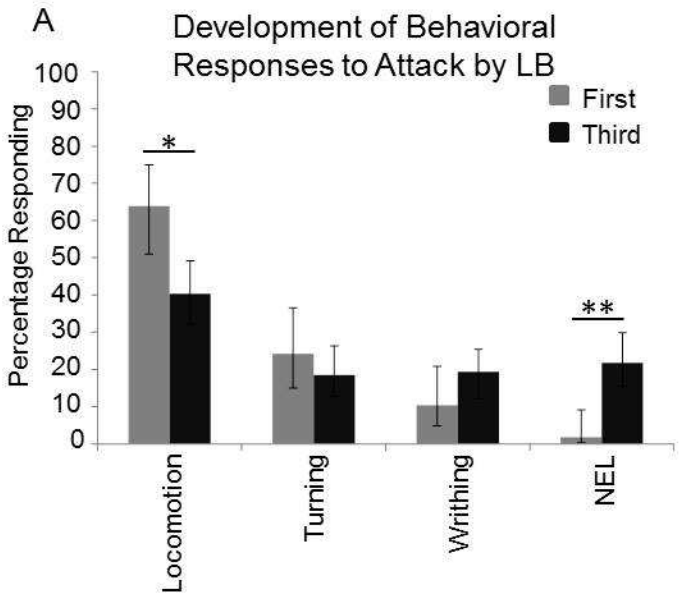

Figure 7: Larvae show developmental changes in response to attacks by LB.

Figure 7: Larvae show developmental changes in response to attacks by LB. A. First instar larvae show significantly higher rates of peristaltic locomotion (N=57, 64% (+11/-13)) than third instar larvae (N=124, 40% (+9/-8)). Additionally, first instar larvae show significantly lower rates of NEL (2% (+7/-1)) compared to third instar larvae (22% (+8/-6)). Data are presented as percentages ± 95% confidence intervals. Fisher's Exact Test with Holm-Bonferroni correction.P< .05 =*, P<.01=**, P< .005 =***.

locomotion before they are able to respond to a noxious stimulus with NEL. This hypothesis is testable, as larvae that have been paralyzed could be tested for responses to a noxious mechanical stimulus following the attack.

Although the presence of the paralytic is the most likely explanation for the differences in NEL, there are several other possible explanations. It is possible that LB attacks with a greater force than LH. This hypothesis could be evaluated through the use of high speed cameras to capture the speed at which the ovipositor hits the larval body wall. It is also possible that the higher rates of rolling triggered by LB could indicate that *Drosophila melanogaster* larvae have evolved to be able to better detect the attack of the *Drosophila melanogaster* specialist.

First instar larvae attacked by LB fail to show NEL. There are several possible explanations for this. Firstly, the tiling of the epidermis by the class IV neurons is not complete in the first instar larvae, and this may lead to a defect in detection of the ovipositor [84]. Alternatively, the downstream circuitry needed for NEL may not be sufficiently developed in first instar larvae. A previous study had found that first instar larvae fail to show NEL when touched with a hot probe, so it may be that the larvae fail to detect and process the signal [123]. This leaves first instar larvae without a strong behavioral protection against attacks by parasitoid wasps.

Our lab successfully maintains our wasp colonies by allowing the wasps to parasitize first instar larvae, but when given a choice, LB and LH only rarely parasitize first instar larvae, and prefer second and third instar larvae [24]. This could indicate that in the wild, first instar Drosophila larvae may not be targeted for attack, so a behavioral response is not selected for. A possible explanation for the wasp preference is that although there is less physical danger for the wasp in attacking a first instar larvae, a first instar larvae is potentially less likely to make it to pupation than a larvae that has already passed into second or third instar. Thus, there may be a trade-off such that parasitoids forego attacking the earliest instar larvae in favor of later instar larvae so that the larvae, and thus their progeny, survive to pupation.

In the future, it would be interesting to determine how these differences in behavior affect the survival of the larvae. For example, do the small number of larvae that roll in response to LH have higher rates of survival? Additionally, another extremely interesting area of study is the wasp venom. Depending on the site of action, it is possible that this venom could be used to silence neurons in *Drosophila*, or, in the best case scenario, be used as the basis for the development of a pain or paralytic drug. There is a long history of drug development from naturally occurring toxins, and parastoid wasps could be next on the list.

4. An *in vivo* screen for regulators of thermal nociception in *Drosophila melanogaster*

4.1 Introduction

Nociception is an evolutionarily conserved process. Humans lacking nociceptive processing face grave, sometimes lethal injuries since they cannot sense tissue-damaging stimuli [10, 30]. Ion channels are responsible for detecting noxious stimuli, as well as communicating the signal to the nervous system via action potentials. Ion channels are ancient molecules, and are present in bacteria and archae [44, 45]. Since both ion channels and nociception are well conserved, it can be advantageous to use genetically-tractable model organisms, like *Drosophila*, to screen for novel ion channels involved in nociception.

Drosophila melanogaster larvae are an excellent model for nociception research. The *Drosophila* genome has homologues of 77% of human genes associated with disease [154]. Even the temperature threshold for nociception is similar between humans and *Drosophila* – both sense pain when the nociceptive nerve endings are heated to 39° C [16, 155, 156]. Additionally, the structures of the nociceptors are similar in mammals and *Drosophila*, with both having "naked" dendrites [16, 23].

Several ion channels have already been shown to be important for thermal nociception in both humans and *Drosophila*. For example, a gain of function mutation in *TrpA1*, a member of the TRP superfamily, causes Familial Episodic Pain Syndrome

(FEPS) [9]. This syndrome causes debilitating pain when the patients are cold, hungry and/or tired. *TrpA1* has also been found to be important in thermal nociception in *Drosophila* [16, 18, 39]. A screen in adult *Drosophila* revealed that $\alpha 2\delta 3$, a calcium channel subunit, is necessary for thermal nociception [13]. They went on to discover that humans with a minor SNP variant in this gene reported less sensitivity to noxious heat, as well as reduced back pain following surgery [13]. Thus far, many of the genes found to be important in human nociception have also been found to be important in *Drosophila* nociception.

Although several ion channels have been characterized in *Drosophila* and mammals, there is reason to believe that there are other, novel ion channels involved in nociception. In this study, we used the genetic tools of *Drosophila* to investigate the function of 90% of the ion channels in the *Drosophila* genome for their role in sensitivity to a noxious thermal stimulus. Using the GAL4-UAS system, we performed tissue specific knockdown of genes solely in the sensory neurons. We targeted the sensory neurons since we are most interested in which genes play a role in detecting and processing noxious stimuli in the periphery. Drugs that target pain processing in the brain have many undesirable side effects, such as addiction. By understanding the genes involved in the detection and processing of noxious stimuli in the periphery,

drugs could be developed that target solely the peripheral pain sensors, leading to a decrease in the number of side effects.

In response to a noxious thermal stimulus, larvae show nocifensive escape locomotion (NEL), which is a stereotyped, corkscrew-like rolling behavior also exhibited in response to attacks by parasitoid wasps and a noxious mechanical stimulus [16]. NEL is distinct from normal peristaltic motion seen during larval feeding and from the behavioral response to a gentle touch [16, 128]. NEL results in increased speed, which is thought to aid in the escape from the noxious stimulus [8]. NEL is quantifiable as the time taken to respond to the thermal stimulus. Unlike the wasp attack behavioral paradigm, thermal nociception is high throughput, allowing for the testing and analysis of many genotypes in a short amount of time. Thus, the NEL response is a distinctive, easily quantifiable behavior that makes screening through large numbers of genes possible.

The multidendritic (md) neurons are a morphologically diverse group of neurons that tile the body wall of *Drosophila* larvae [77]. There are four distinct classes of md neurons [77]. The classes show different levels of dendritic field branching complexity, with class I neurons exhibiting the least complex dendritic arborization and class IV neurons the most complex [77]. The md neurons were first implicated in nociception when *painless*, a TRP channel necessary for nociception, was found to be expressed in the

md neurons [16]. Deletion of *painless* severely impairs the NEL response to noxious thermal and mechanical stimuli [16]. The class I neurons were later implicated in proprioception [79, 80], but the functions of the remaining classes were unknown. To determine which class of neuron functions as the nociceptors, the GAL4 UAS system was used to silence different classes of md neurons. Specifically silencing the class IV neurons resulted in severely impaired NEL responses to both mechanical and thermal stimuli [8]. Additionally, optogenetic activation of the class IV neurons using the Channelrhodopsin2 system [82] results in NEL behavior [8]. Thus the class IV neurons are both necessary and sufficient for triggering nociception responses in *Drosophila* larvae. In accordance with the behavioral phenotype, recordings from the class IV neurons show that they respond to temperatures above 39°C [156].

The GAL4 UAS system is a unique and extremely useful tool for driving tissue specific expression of genes in *Drosophila*. Both the GAL4 protein and the Upstream Activating Sequence (UAS) were isolated from yeast, and are not naturally present in the *Drosophila* genome. GAL4 is a transcription factor that binds to the UAS enhancer sequence [157]. The binding of GAL4 to the UAS sequence activates transcription of the gene downstream of the UAS sequence [158].

The Vienna Drosophila Research Center (VDRC) and the Transgenic RNAi Project (TRiP) collection at the Drosophila Screening Center at Harvard have designed

UAS-RNAi fly strains which target 90% of the ion channels in the *Drosophila* genome. When used in combination with the GAL4 system, it is possible to drive RNAi expression in a tissue-specific manner. Briefly, RNAi causes post-translational suppression of genes by expressing double stranded RNA (dsRNA), which is cleaved by *Dicer-2* in to short strands of RNA complimentary to the target gene, called small interfering RNA (siRNA). The siRNA are recruited to the RNA-induced silencing complex, which then binds to the target gene's RNA and destroys it [20]. Since we have GAL4 drivers for all the multidendritic neurons (*md-GAL4*) as well as the class IV neurons alone (*ppk-GAL4*), it is possible for us to silence gene expression for the vast majority of the predicted ion channels in the *Drosophila* genome in a tissue-specific manner.

Here, in collaboration with Kia Walcott and Richard Hwang, I have utilized 325 RNAi lines which target 90% of the ion channels present in the *Drosophila* genome. We have found a diverse set of genes that are required for sensitivity to a noxious thermal stimulus, including TRP channels, potassium channels, voltage gated sodium channels, and ligand gated channels. Some, but not all of these genes have a nociceptor specific role. Additionally, we investigated the requirement for these ion channels in optogenetically triggered nociception responses. In summary, we describe a novel set of ion channels responsible for nociception.

4.2 Materials and methods

4.2.1 Fly strains

The following fly strains were used: *w; md-GAL4;UAS-Dicer2/K87*, *w; ppk-GAL4;UAS-dicer2/K87*, *w; ppk-GAL4, UAS-ChR2* line C; *UAS-Dicer2/k87*, *isow*, and *yw; attp[empty]*. RNAi lines were obtained from the VDRC and TRiP collection, and are listed in Appendix A.

4.2.2 Initial screen

For the initial screen, the driver strain was *md-GAL4;UAS-dicer2/K87*. Five virgin females of this genotype were crossed to three males of the relevant *UAS-IR* line. Dicer2 was used to increase the efficiency of the knockdown. Flies were placed in vials containing standard cornmeal molasses fly food, and kept at 25°C. Five - seven days later, wandering third instar larvae were tested for sensitivity to a 46°C thermal probe, as described in [16]. For the initial screen, latency was measured by counting and recording the seconds that passed until a larva completed a full 360° roll. Initially a small sample size was tested (N=2-24, Mean=7.4). Crosses were retested if they were one standard deviation from the mean of the controls. Since the relevant control strains are different for the first and second generation VDRC lines, different cutoff points were used for these two collections.

For retesting, six *md-GAL4;UAS-dicer2/K87* females were crossed to 3 *UAS-RNAi* males. Wandering third instar larvae were tested five - seven days after the crosses were set up. For the retest, the trials were video recorded, and latency to show NEL was measured precisely using a stopwatch following the trial. The data were then analyzed using an ANOVA followed by a Dunnett's test. A larger sample size was used for this test (N=13-82, Mean=34). Lines that were significantly different ($p<.05$) were then rescreened using the nociceptor-specific driver, *ppk-GAL;UAS-dicer2*.

4.2.3 Optogenetic activation screen

Ten virgin females of the genotype *ppk-GAL4, UAS-CHR2* line C/*CyO*; *UAS-Dicer2* or *ppk-GAL4, UAS-CHR2* line C; *UAS-Dicer2/K87* were crossed to five males of the relevant *UAS-RNAi* lines. Only lines that had a significant defect in the nociceptor specific portion of the screen were tested using channelrhodopsin. The methods used are the same found in [8]. Briefly, crosses were placed in vials containing standard cornmeal molasses medium at 25°C for two days. Flies were then moved in to apple juice plates containing yeast paste that had been treated with all-trans-retinal (500 μm). The flies were allowed to lay eggs for 24 hours and three days later, larvae were transferred to petri dishes with a small amount of water and tested for NEL in response to illumination with blue light (460-500 nm, at 145,000 lux). Data were analyzed using a Fisher's Exact Test with Bonferonni Correction.

4.3 Results

4.3.1 A screen reveals novel genes involved in thermal nociception

Initially, we targeted all of the multidendritic sensory neurons for RNAi knockdown using *md-GAL4* (Fig. 8A and B). Approximately 20% of the lines from the first generation and 15% of the lines from the second generation were retested. Of the lines selected for retest, 17% of the first generation lines were significantly different than controls. The second generation VDRC collection had a higher hit rate, with 53% of the lines differing significantly from controls in the retest.

Eighteen lines targeting fourteen genes showed robust and reproducible phenotypes in the *md-GAL4* portion of the screen. These genes are predicted to encode TRP channels (*dTrpA1*, *nanchung*), DEGenerin epithelial sodium channels (DEG/ENaCs) (*shadrach, meshach*), a voltage gated sodium channel (*paralytic*), potassium channels (*Irk3, Task6, slowpoke*), ligand gated channels (*abednego*, *nAChRα-96ab*, *Ir7c*) and an ABC transporter (*coyotemint*). Additionally, *bruchpilot*, which is a coiled-coil protein that is important for establishing the appropriate density of calcium channels in the active zones of synapses, was identified [159]. These genes included several novel regulators of nociception, as well as previously identified regulators. For example *dTrpA1* had already been shown to be important in thermal nociception in *Drosophila* [18, 39], and

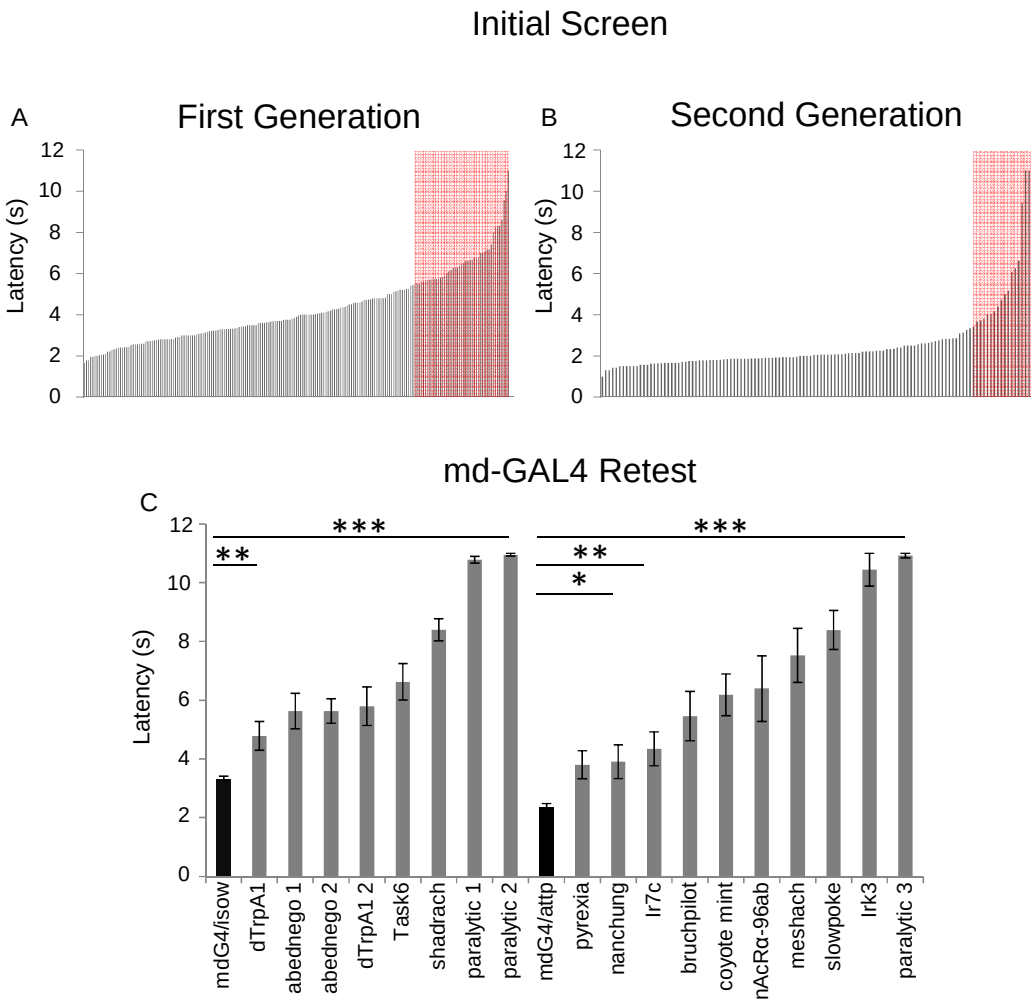

Figure 8: Screen for RNAi lines that function in the multidendritic neurons.

Figure 8: Screen for RNAi lines that function in the multidendritic neurons. A. Using the *md-GAL4*;UAS-*Dicer2* driver, 201 *UAS-IR* lines from the first generation VDRC RNAi collection were tested for sensitivity to a 46°C probe. Lines that were one standard deviation from the control values (red box) were isolated for retest. **B.** Using the *mdGAL4;UAS-dicer2* driver, 124 *UAS-IR* lines from the second generation VDRC RNAi collection were tested for sensitivity to a 46°C probe. Lines that were one standard deviation from the control values (red box) were isolated for retest. **C.** The average latency of ion channel *UAS-IR* lines when knocked down in all of the md neurons using *md-GAL4;UAS-Dicer2*. Control genotypes (black) are the driver crossed to the appropriate RNAi background strains, *isow* or *yw;attp[empty]*^{60100}. Data are presented as the mean ± SEM. One-way ANOVA followed by Dunnett's test. N=13-808. *p<0.05, **p<.001, ***p<.0001.

came out of our screen. This is a good internal control, and indicates that our screen is capable of picking up thermal nociception genes.

When using *UAS-RNAi* to knockdown genes, it is important to eliminate the possibility that the phenotype is due to non-specific effects of the *UAS-RNAi* transgene. For instance, some of the VDRC lines were created using random insertions into the genome, so that the insertion itself could be causing the defect rather than the RNAi knockdown. Additionally, there could be leaky expression of the RNAi outside of the multidendritic neurons, causing effects that are not specific to the peripheral sensory neurons. To control for these effects, I tested the *UAS-RNAi* alone, without the driver, for sensitivity to a noxious thermal stimulus. In the no-driver controls, only *pyrexia* was significantly insensitive compared to the control (Fig. 9). Since this *UAS-RNAi* line is created using a conserved docking site in the genome, also present in the controls, the most likely explanation for the insensitive phenotype is that there is leaky knockdown of *pyrexia* in other tissues.

To determine the extent to which genes that came out of the *md-GAL4* portion of the screen were functioning specifically in the nociceptors, we rescreened the lines using *ppk-GAL4*, which drives expression in the class IV neurons. Expression of *dTrpA1*, *abednego*, *shadrach*, *task6*, *Irk3*, *nAcRα-96ab*, *meshach* and *paralytic* in the class IV neurons is necessary for nociception (Fig. 10).

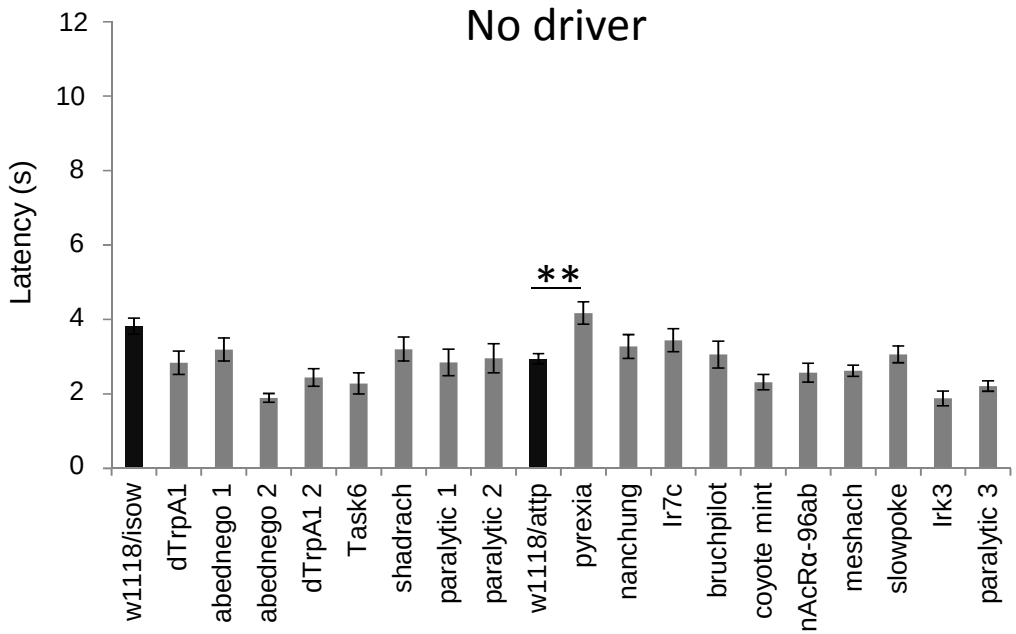

Figure 9: No driver controls for *UAS-RNAi* lines.

Figure 9: No driver controls for *UAS-RNAi* lines. To determine if the insensitive phenotype was due to non-specific effects of the RNAi line, we performed no driver controls where the RNAi line was crossed to flies of the *w[1118]* background. Control genotypes (black) were *w[1118]* crossed to the appropriate genetic background, *isow* or *yw;attp[empty]*^{60100}. One way ANOVA followed by Dunnett's test. Only lines that are significantly insensitive are starred. P<.001

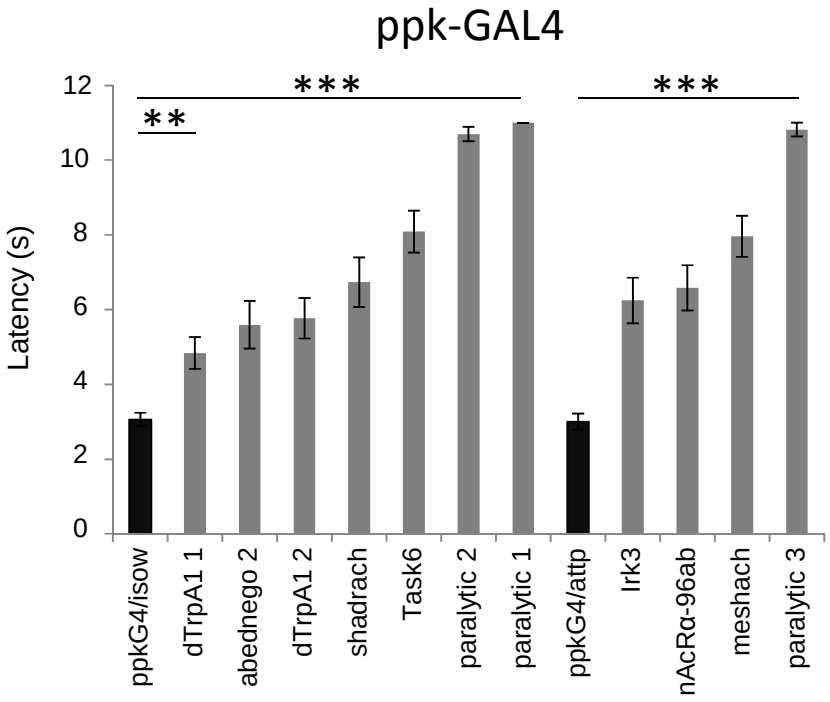

Figure 10: *UAS-RNAi* lines that function in the nociceptors.

Figure 10: *UAS-RNAi* lines that function in the nociceptors. The average latency of ion channel *UAS-RNAi* lines when knocked down in only the class IV neurons using *ppk*-Gal4;UAS-*Dicer2*. Control genotypes (black) were *ppk*-Gal4;UAS-*Dicer2* crossed to RNAi background strains, *iso w* or *yw;attp[empty]*^{60100}. Data are presented as the mean ± SEM. One-way ANOVA followed by Dunnett's test. N=31-148. **p<.001, ***p<.0001.

4.3.2 Optogenetic screen

The insensitive thermal phenotypes caused by knockdown of the above genes could be explained by a failure to transduce a noxious stimulus, or a failure to transmit that signal to the central nervous system. To test the hypothesis that some of the defects are due to a failure to properly propagate action potentials in the class IV neurons, we bypassed transduction by activating the class IV neurons directly using Channelrhodopsin2. When Channelrhodopsin2 is expressed in the class IV neurons, blue light activates the NEL behavior. The only RNAi line with severe defects in the Channelrhodopsin assay was *paralytic* (Fig. 11). However, *dTrpA1* and *shadrach* also had slight defects. This indicates that these channels are downstream of channelrhodopsin2, and could play a role in transmitting action potentials to the central nervous system.

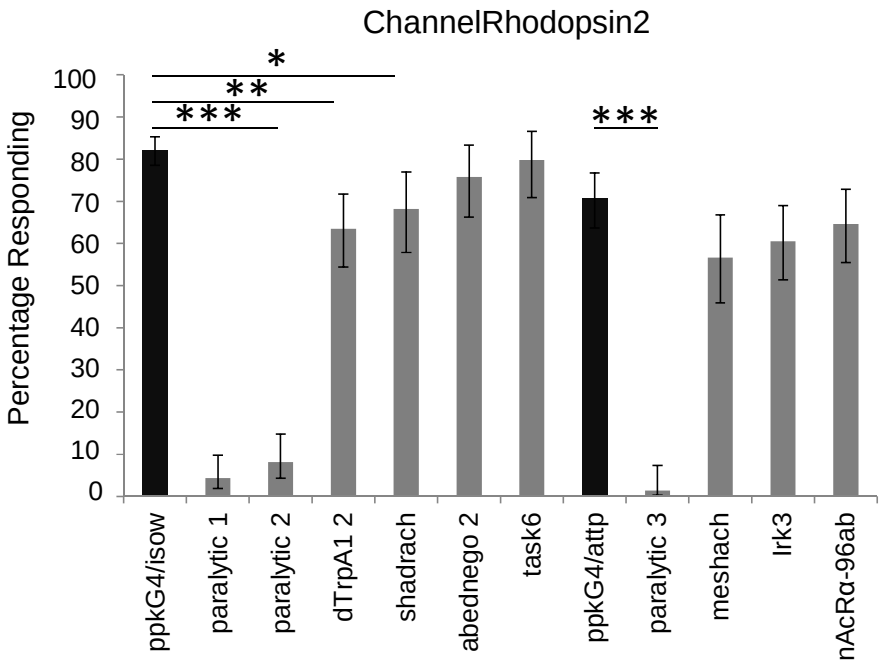

Figure 11: Optogenetic screen.

Figure 11: Optogenetic screen. The percentage NEL after exposure to blue light. To induce NEL in response to blue light, female flies of the genotype *ppk-Gal4,UAS-ChR2* line C;*UAS-Dicer2* were crossed to a *UAS-RNAi* line. For the controls, females of the genotype *ppk-Gal4,UAS-ChR2* line C;*UAS-Dicer2* were crossed to *isow* or *yw;attp[empty]*^{60100}. Knockdown of *paralytic, shadrach,* and *dTRPA1* results in decreased NEL following blue light exposure. Data are presented as a percentage ± 95% confidence interval. Fisher's exact tests with a Bonferroni correction. N=73-493. *p<0.05, **p<.001, ***p<.0001

4.4 Discussion

We screened 90% of the ion channels in the *Drosophila* genome for insensitivity to a noxious thermal stimulus. The screen revealed eighteen independent RNAi lines that target fourteen genes that are necessary for thermal nociception (Fig. 8C). Of these genes, eight function are required specifically in the nociceptors (Fig. 10). Only one of the genes, *paralytic*, was required for optogentically triggered nociception (Fig. 11). This is consistent with the well-known role of paralytic in transmitting action potentials [160, 161]**.** A wide variety of genes emerged from the screen, including potassium channels, calcium channels, and voltage gated sodium channels. Several of the genes that emerged from the screen were previously unnamed. We named three of the newly characterized genes after characters in the Old Testament. Shadrach, Meshach and Abednego were sentenced to death in a fiery furnace. Even though the furnace was heated to seven times the usual temperature, they were not harmed. Like our thermal nociception mutants, they failed to feel pain from the noxious heat. The remaining newly characterized gene was named after a fire resistant plant, coyotemint.

Recently, Neely et al completed a pan neuronal screen in adult flies that targeted the vast majority (82%) of the genes in the fly genome [13]. Their screen differed from ours in several crucial ways. First, their screen was not solely limited to ion channels. Additionally, and perhaps more importantly, they used adult flies rather than larvae.

The cellular basis of thermal nociception in adult flies in not well understood, and although the class IV neurons exist in adult flies [162], it is unknown if they continue to function as the nociceptors. Additionally, the Neely et al paradigm for screening mutants is quite different. Neely et al used a plate heated to a noxious temperature on one side, thus creating a gradient, and measured the number of flies incapacitated by the noxious heat. Therefore, the thermal nociception mutants from the Neely screen could include strains deficient in detecting a gradient rather than failure to detect a noxious thermal temperature.

Although α2δ3 did not show a thermal nociception defect in our initial screen, there were several overlapping hits between the two screens. The Neely screen used a pan-neuronal driver, which caused two of the hits from our screen to be lethal (*Abednego*, *slowpoke*). *coyotemint* was not included in the Neely screen. Of the remaining eleven genes that came out of our screen, *dTrpA1*, *nanchung*, *Ir7c*, and *meshach* were also hits in the Neely screen. The Neely screen did not identify *Task6*, *shadrach*, *paralytic*, *pyrexia*, *bruchpilot*, *nAcRα-96ab*, and *Irk3*. This could indicate that the pathways for sensing noxious heat in adults and larvae differ. The genes that came out of both screens are likely important in both larval and adult thermal nociception.

We decided to knockdown the ion channels in all the md neurons in the initial screen since *painless*, an ion channel known to be important in thermal nociception, is

expressed in all of the md neurons [16]. In our screen, five genes came out of the *md-GAL4* portion of the screen that were not necessary for nociception when knocked down in the class IV neurons. There are several potential explanations for this. First, it is possible that the class I-III neurons have an undescribed role in directly sensing noxious heat, or in modulating the output of the class IV neurons. Additionally, it is possible that *md-GAL4* is a stronger driver than *ppk*-GAL4, resulting in higher expression of the *UAS-RNAi* transgenes which may lead to a more efficient knockdown. Lastly, when these ion channels are knocked down with *md-GAL4*, they could disrupt proprioception in the class I neurons. This could lead to an apparent insensitivity through lack of coordination, but have nothing to do with perception of a noxious thermal stimulus, per se. In the discussion section, we will discuss the ion channels that emerged from the class IV specific portion of the screen, since they are most likely to be directly involved in thermal nociception.

dTrpA1 is the *Drosophila* orthologue of the human TrpA channel. It has a previously described role in *Drosophila* thermal nociception [18, 39], and represents a good internal control that the screen is adequately sensitive. Another *Drosophila TrpA* channel, *painless*, is also important for thermal nociception, but was not included in our screen since it had been fully characterized in previous studies [16, 36, 163]. *dTrpA1* has a strong thermal nociception phenotype, but the response to noxious heat is not totally

eliminated (as it is in *paralytic* mutants (Fig. 10), or animals expressing tetanus toxin light chain in the class IV neurons [8]). Since *dTrpA1* was a hit in our screen, this is a good indication that our screen can detect milder thermal nociception phenotypes.

paralytic encodes a voltage gated sodium channel. Interestingly, in mammals three voltage gated sodium channels, Nav1.7, Nav1.8, and Nav1.9 are expressed in the dorsal root ganglion neurons [32]. Mutations in NaV1.7 cause pain insensitivity disorder, as well as paroxysmal extreme pain disorder and erythermalgia [10, 30, 31, 35, 43]. In the case of pain insensitivity disorder, one of the children studied was a street performer in Pakistan known for performing feats of pain tolerance including putting knives through his arm, and walking on burning coals [10]. Children with this condition have to be monitored carefully, since they lack pain sensation. Common injuries include biting off the tongue, or infections which go untreated because the pain is undetectable [10]. Although the mammalian genome encodes many voltage gated sodium channels, flies have only *paralytic*. The paralytic gene encodes at least 59 different isoforms through alternative splicing and RNA editing [164]. Further investigation of *paralytic* could concentrate on the role of isoform specificity in governing the noxious pain transmission.

meshach (CG31065) and *shadrach* (CG13121) are DEG/ENaC channels and both are nociceptor specific regulators of thermal nociception. DEG/EnaC's are thought to be

sodium-selective trimers [165, 166]. Although DEG/ENaCs are necessary for mechanical nociception in *C. elegans*, *Drosophila* and mammals, this is the first reported evidence of DEG/ENaCs involvement in thermal nociception [17, 69, 167, 168]. Interestingly, the venom of the coral snake persistently activates mammalian ASICs, causing severe pain [27].

adednego (CG7589) is predicted to encode a glycine gated channel necessary for thermal nociception. This gene was targeted by multiple RNAi lines identified in the screen as significantly insensitive to a noxious stimulus. On first glance, it is unusual for a glycine gated channel to cause insensivitity when knocked down, since these channels are normally chloride channels. However, depending on the intracellular concentration of chloride, a chloride current can be either hyperpolarizing or depolarizing. In mammals, intracellular chloride concentration in the central nervous system changes with development, altering the direction of the current as the animal ages [169]. There is reason to believe that in mammalion nociceptors, the chloride concentration may lead to outward chloride currents. For example, a calcium activated chloride channel (CaCC) anoctamin is activated by noxious heat, and deletion of this channel causes insensitivity to a noxious thermal stimulus [29]. In *Drosophila*, perhaps *abednego* is functioning similarly to a CaCC in mammals.

Task6 is a potassium channel. The insensitive phenotype caused by knockdown of this potassium channel is surprising because knockdown of potassium channels would be predicted to cause hyperexcitability. *Task6* encodes a two pore potassium channel, thought to be important in setting the resting membrane potential [170]. *Task6* may also have a potentially important role in nociception specifically, since other members of the TASK family are activated by inhaled anesthetics [40], and local anesthetics such as lidocaine, bupivacaine, and quinidine, inhibit *Task6* and other TASK family members [37, 170]. In a heterologous system, *Task6* and *Task7* can form heteromers [171]. In our screen, the *Task6* phenotype was statistically different from the controls, however, *Task7* showed a phenotype in the initial screen but failed to show a robust phenotype with the increased sample size upon retesting. *Irk3* encodes an inward rectifying potassium channel, and knockdown of this channel caused an insensitive thermal nociception phenotype. These two channels are studied in greater depth in the following chapters, and a mechanism for their action is proposed there.

Lastly, *nAcRα-96ab* is predicted to encode a nicotinic acetylcholine receptor (nAChR). In mammals, nAChR agonists and antagonists are potent analgesics [34, 172, 173]. nAChRs are expressed in the dorsal root ganglion neurons, as well as in the dorsal horn of the spinal cord [174, 175]. Two studies have found that nAChR agonists cause analgesia through increased excitation of inhibitory neurons in the dorsal horn [176,

177]. Interestingly, the class IV neurons are cholinergic [178]. This indicates that there could be feedback on the class IV neurons through this receptor which when disrupted causes changes in sensitivity to heat. However, as with the other ligand gated channels that came out of the screen, we have not yet determined where the ligand is coming from, or what causes its secretion.

In summary, we conducted an *in vivo* RNAi screen of 90% of the ion channels in the *Drosophila* genome. We found a wide variety of channels govern sensitivity to noxious heat, some of which are involved in action potential transduction.

5. Regulation of the class IV dendritic field by ion channels

5.1 Introduction

The elaborately branched dendritic fields of the class IV nociceptor neurons have been developed as a model system to study dendritic branching. Many genes that affect the branching pattern, including transcription factors, cytoskeletal elements and cell adhesion elements, have been discovered [84, 86, 87, 92, 94, 98-100, 179-187]. However, to date no one has investigated the role of ion channels in regulating the morphological structure of the class IV dendritic field. This study aims to determine the interaction between ion channels, nociception and dendritic field structure.

Several transcription factors affect the branching patterns of the class IV multidendritic neurons, including *spineless* [180]. *spineless* is expressed in all of the multidendritic sensory neurons, and deletion of spineless causes the class IV branching to be less complex [180]. Other transcription factors important in regulating the dendritic field of the class IV neurons include *cut* and *collier* [91, 92].

The class IV neurons have a complicated dendritic field, but the branches of the field rarely overlap. Dendrites of the same neuron repel each other, a process known as self-avoidance. Additionally, the class IV neurons avoid crossing into the dendritic field of neighboring class IV neurons, a phenomenon referred to as tiling. Cell adhesion molecules, such as *Dscam* (down syndrome cell adhesion molecule), are important in self

avoidance [96-98, 184]. *Dscam* is a type I immunoglobulin protein that can be spliced in to 38,000 isoforms [188]. Expression of unique isoforms of *Dscam* allows for proper self-avoidance, while allowing overlap with the dendritic fields of other classes of md neurons [96-98]. Other molecules, such as *tricorner kinase*, a serine/threonine kinase, and *furry*, which positively regulates tricorner kinase, are important in both self-avoidance and tiling [187]. In addition to exhibiting self-avoidance and tiling, the class IV neurons also scale the dendritic field with the growth of the larva, so that the dendrites continue to cover the growing larval body wall. *bantam*, a microRNA, is important for the scaling of the class IV neurons with larval growth [84].

In order to be effective, neural circuitry has to balance the need for stability with that of the flexibility to adapt to new situations. Homeostatic regulation of neuronal function ensures that neurons maintain a certain excitability set-point. Neural homeostasis can involve changes in the molecular make-up of the neuron, changes in the size of the synapses, or changes to the structure and size of the dendritic field. In order to exhibit homeostatic regulation, neurons have to be able to detect changes in neuronal state, and then change neuronal attributes to return the state to normal. The mechanism by which neurons accomplish this is still not well understand, and could be through intrinsic recognition of changes in firing rate, detecting local changes in synaptic transmission, or detecting changes in circuit output [189-192].

One of the best characterized examples of neuronal homeostasis is synaptic scaling, which causes an overall homeostatic regulation of synapse strength [193-197]. This homeostatic regulation can also affect the morphology of the synapse. Cultures of hippocampal neurons show increased synapse size following treatment with tetrodotoxin [197]. Other studies have found that neurons alter the molecular make-up of the cell to achieve intrinsic homeostasis. This can be accomplished through the regulation of ion channel expression in the cell. For example, treatment of cells with tetrodotoxin results in the up-regulation of excitatory glutamate receptors at synapses [198, 199].

In this study, we are most concerned with the morphological homeostatic regulation of the dendritic field. Homeostatic regulation of the morphology of the dendritic field causes an enlargement of the dendritic field when pre-synaptic input is reduced, and a decrease in the size of the dendritic field when pre-synaptic input is increased. This is thought to ensure that the post-synaptic neuron maintains excitability within a certain range. Homeostatic regulation of synapses has been shown to occur in a wide range of animals, from *Drosophila* to primates [200]; however, the role of homeostatic regulation on the size of the dendritic field itself remains to be fully characterized.

In *Drosophila*, there have been several studies demonstrating homeostatic regulation of the dendritic field in the CNS [201-204]. Notably, a recent study has shown that the ventral lateral neurons, which are post-synaptic to the photoreceptors, homeostatically alter their dendritic field in response to alterations in the light/dark cycle [202]. For example, exposing flies to constant light conditions results in a diminished dendritic field [202]. By using the GAL4 UAS system to express ion channels that either increased or decreased excitability, it was demonstrated that altering the excitability of the ventral lateral neurons themselves results in intrinsic homeostatic regulation of the dendritic field through a cAMP pathway [202]. Since intrinsic alteration of neuronal excitability through ion channels results in homeostatic regulation of the dendritic field in the CNS, it is possible that these same principles may apply to the nociceptors in the PNS, which lack pre-synaptic partners. The nociceptors represent a potentially simplified system of dendritic homeostasis – since there are no pre-synaptic partners, adaptation of pre-synaptic input due to alterations in the post-synaptic electrical state can be disregarded. Additionally, since nociceptor morphology has a demonstrated role in nociception, studying ion channel regulation of nociceptor morphology is intrinsically interesting [93].

In this study, in collaboration with Kia Walcott and Richard Hwang, we screened all of the ion channels that were insensitive to a noxious thermal stimulus for dendritic

defects in the class IV neurons. We find that of the fourteen genes that result in insensitivity to noxious heat when knocked down in larvae, six have a reduced dendrite phenotype. These genes are from diverse ion channel families, and include TRP channels, an ABC transporter, potassium channels, and ligand gated channels. I have begun characterization of several of the genetic mutants. Specifically, I have generated a genetic mutant of the ABC transporter *coyotemint*. Additionally, since we are altering ion channels, which may alter the intrinsic electrical properties of the neuron, I tested the hypothesis that some of the dendritic defects may be due to homeostatic regulation of the dendritic field.

5.2 Materials and methods

5.2.1 Fly stocks and husbandry

Stocks used were *w[1118]*, *w;md-GAL4, UAS-mcd8::GFP;UAS-Dicer2/k87*, *w;ppk-GAL4, UAS-mcd8::GFP;UAS-dicer2/k87*, *w;ppk-GAL4, UAS-mcd8::GFP*, *w; UAS-mcd8::GFP*, *w;ppk-GAL4, UAS-mcd8::GFP; nan36a/k87*, *w;UAS-task6 RNAi; UAS-para RNAi/k87*, *nan36a, w[1118]; Df(3L)BSC801/TM6B, w;ppk-GAL4; UAS-mcd8::GFP*, *PBac[RB]e02146*, *P[XP]CG17646^{d05547}*, *w[*]; P{w[+mW.hs=GawB}CG17646[NP0969] / TM3, Ser[1], w[*]; P{w[+mW.hs=GawB}CG17646[NP2719] / CyO, w[*]; P{w[+mW.hs=GawB}CG17646[NP0697] / CyO, w[*]; P{w[+mW.hs=GawB}CG17646[NP3037], w[*]; P{w[+mW.hs=GawB}CG17646[NP0525] / CyO*. A list of RNAi lines can be found in

Appendix A. Six virgin females were crossed to three male flies of the relevant RNAi line and placed in standard cornmeal molasses medium vials at 25°C. Wandering third instar larvae were selected for imaging five to seven days after the crosses were performed.

5.2.2 Imaging of class IV neurons

Wandering third instar larvae were rinsed in water and then placed in a glass petri dish on a coverslip containing a drop of glycerol. Ether was applied to a cotton ball in the petri dish, and the dish was enclosed using lab tape. After 15 minutes, larvae were mounted on slides in glycerol for imaging. Larvae were imaged using an LSM 5 Live confocal microscope. Images of the medial segments (3-6) were taken using the tiling macro on the LSM 5 Live software.

5.2.3 Image analysis

A maximum intensity projection of the image was made using the LSM 5 Live software. Images were then cropped to hold a single neuron, with the boundaries of the cell determined by the length of the longest dendrite. A grid was put over the neuron, and the number of boxes containing dendrites was counted [91]. For Figure 17D, a matlab code developed by Ken Honjo was used to score the dendritic coverage. The cell body and axon were omitted from the counting. Scoring was done blind to genotype.

5.2.4 Thermal nociception assay

Larvae were tested using the thermal nociception assay as described in Chapter 4 with the exception that the probe temperature was 40°C. Briefly, 6 virgin females were crossed to 3 males, and kept on standard molasses cornmeal medium at 25°C. 5-7 days after the crosses were established, larvae were tested for sensitivity to a 40°C thermal probe.

5.2.5 Generation of *coyotemint* genetic mutants

PBac[RB]e02146 and P[XP]CG17646 ^{d05547} were used to create the *coyotemint* mutant as described in [205]. Putative mutants were initially screened by eye color for lack of the *white* gene. Next, DNA was extracted using the Qiagen DNeasy Blood and Tissue Kit. PCR was performed with Phusion polymerase using primers across the FRT site. The primers were 5'- AATGATTCGCAGTGGAAGGCT-3' and 5'-TGCATTTGCCTTTCGCCTTAT-3'.

5.3 Results

5.3.1 Screen for class IV dendritic morphology mutants

Of the fourteen genes that had an insensitive phenotype to a noxious thermal stimulus, six of them (*task6*, *nAcRα-96ab*, *coyotemint*, *nanchung*, *bruchpilot*, and *Irk3*) had dendritic defects (Fig. 12 and Fig. 13). While the controls showed approximately 75%

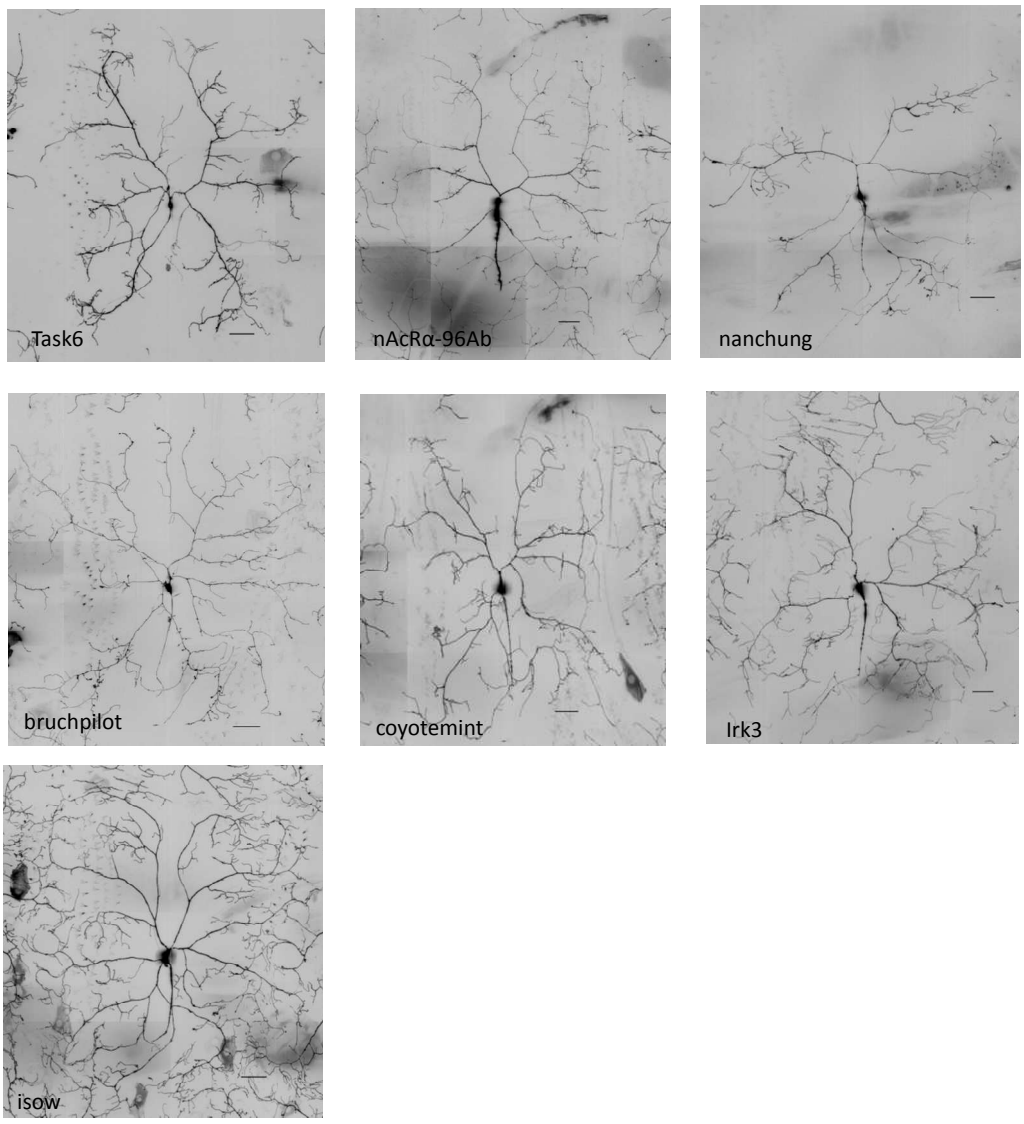

Figure 12: Knockdown of six different ion channels causes a sparse dendritic phenotype.

Figure 12: Representative photomicrographs of dendritic coverage in the 6 RNAi mutants discovered in our screen. Scale bars are 50 μm.

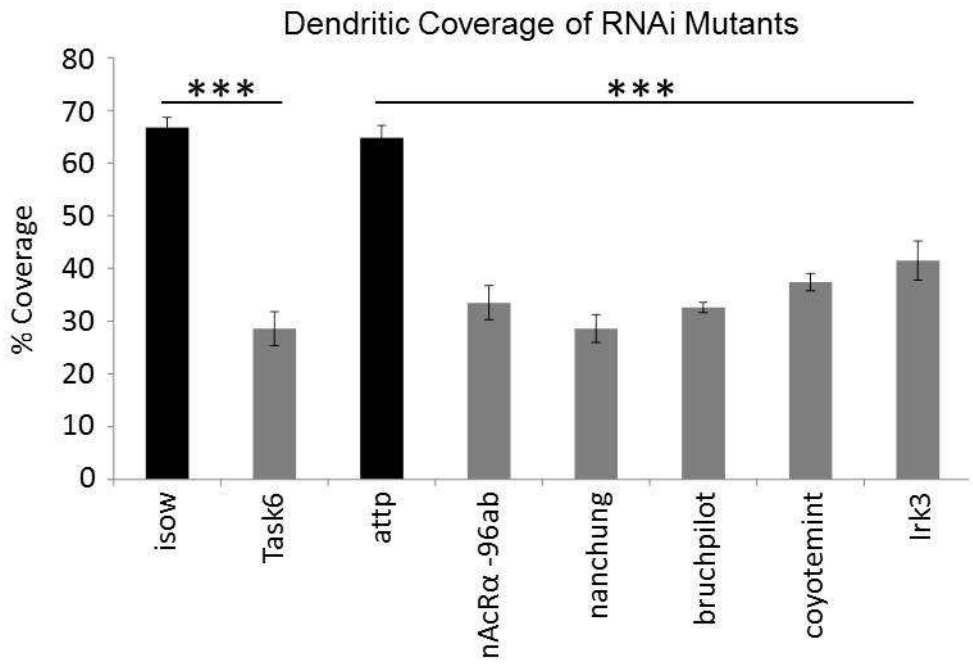

Figure 13: Knockdown of six different ion channels causes a significant reduction in dendritic coverage.

Figure 13: Knockdown of six different ion channels causes a significant reduction in dendritic coverage. The percent dendrite coverage by class IV md neurons (ddaC) in the RNAi mutant backgrounds of *Task6*, *nAcRα-96ab*, *nanchung*, *bruchpilot*, *coyote mint*, and *IrK3*. The *Task6 UAS-IR* line is in the *isow* background. The remaining *UAS-IR* lines are in the *yw;attp[empty]*^{60100} background. Data are presented as the mean ± SEM. One way ANOVA followed by Dunnett's test was performed. N=5-6. ***$p<0.001$

dendritic coverage, dendritic coverage in many of the mutants was reduced by half (Fig. 13). None of the lines appeared to have a hyper-branching phenotype.

5.3.2 Genetic verification of the RNAi mutants

Next, I attempted to verify the RNAi mutants using genetic tools. I began with *nanchung*. *nanchung* (*nan*) is a TRPV channel that has a role in hearing and hygrosensation in *Drosophila* [52, 54]. TRPV channels have previously been identified as thermosensors in mammals [206], but the role of TRPV channels in *Drosophila* nociception has not been reported. First, I tested whether *nanchung* genetic mutants phenocopy the RNAi mutant. RNAi can have off-target effects, and it is thus important to test genetic mutants for the phenotype seen with RNAi. RNAi lines targeting two different regions of *nanchung* caused two distinct phenotypes (Fig. 14A) (Chapter 4, [207]). When knocked down with a first generation RNAi line targeting the 5′ region of the gene, *nanchung* showed a hypersensitive phenotype to a noxious thermal stimulus. However, when using a second generation RNAi line targeting the middle of the gene, *nanchung* showed an insensitive phenotype. The *nan36a* genetic mutant has a deletion in the first 150 codons of *nanchung* resulting in deafness, as well as defects in proprioception and hygrosensation in adult flies [52, 54]. The *nan36a* genetic mutant shows a hypersensitive response to a thermal probe when compared to the controls, and

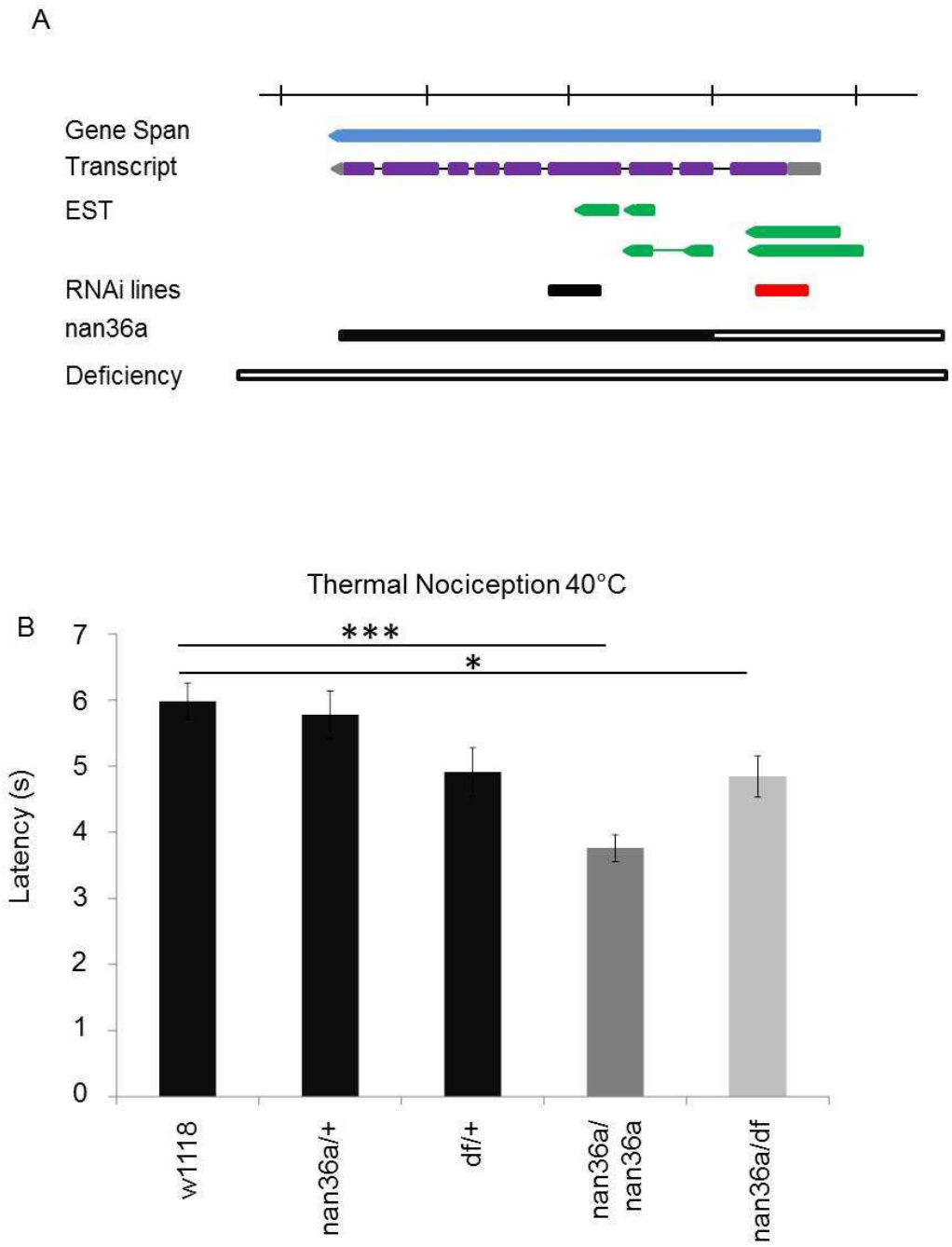

Figure 14: *nanchung* genetic mutants show a hypersensitive thermal nociception phenotype.

Figure 14: *nanchung* genetic mutants show a hypersensitive thermal nociception phenotype. A. Genetic structure of *nanchung*. An RNAi line targeting the 5′ region of *nanchung* (red) causes a hypersensitive phenotype when knocked down in all the md neurons and no dendritic phenotype. An RNAi line targeting the middle of the gene (black) causes an insensitive nociception phenotype when knocked down in all of the md neurons and a severe dendritic defect. Tick marks indicate 1 Kb. **B.** The *nan36a* mutant exhibits a hypersensitive response to a 40°C thermal probe. N=72-141. Tukey's Test, *p<.05, ***p<.001. Genotypes are w[1118], *w;nan36a/+*, *w; Df(3L)BSC801/+*, *nan36a/nan36a*, and *nan36a/Df(3L)BSC801*.

when placed over a deficiency (Fig. 14B). However, the deficiency alone is slightly hypersensitive and neither homozygous *nan36a* larvae nor larvae with *nan36a* over the deficiency show a significant difference in the latency to respond to a noxious thermal stimulus from the deficiency alone (Fig. 14B). This indicates that there could be a second site mutation in the *nan36a* background which causes the hypersensitive thermal nociception phenotype.

Next, I wanted to determine the expression pattern of *nanchung* in larvae. Using the *nanchung-GAL4*, I found that in accordance with the expression pattern in adults and embryos, *nanchung-GAL4* did not drive expression of GFP in the class IV neurons, but did drive GFP expression in the chordotonal neurons (Fig. 15A)[208, 209]. Although this could indicate that *nanchung* is not being expressed in the class IV neurons, the GAL4 was made by fusing GAL4 to a small, cloned region of the promoter, so important regulatory elements could be missing [208].

The RNAi line targeting the 5′ region of the gene, which caused a hypersensitive phenotype, showed no dendritic defects. However, the RNAi line targeting the middle of the gene caused a severe decrease in dendritic coverage (Fig. 12, Fig. 13). I observed the dendritic phenotype of the class IV neurons in *nan36a* mutants. While the *nan36a* mutants show a slight reduction in dendritic coverage compared to controls (Fig. 15B and 15C), this reduction is eliminated when the mutant is placed over a deficiency (Fig.

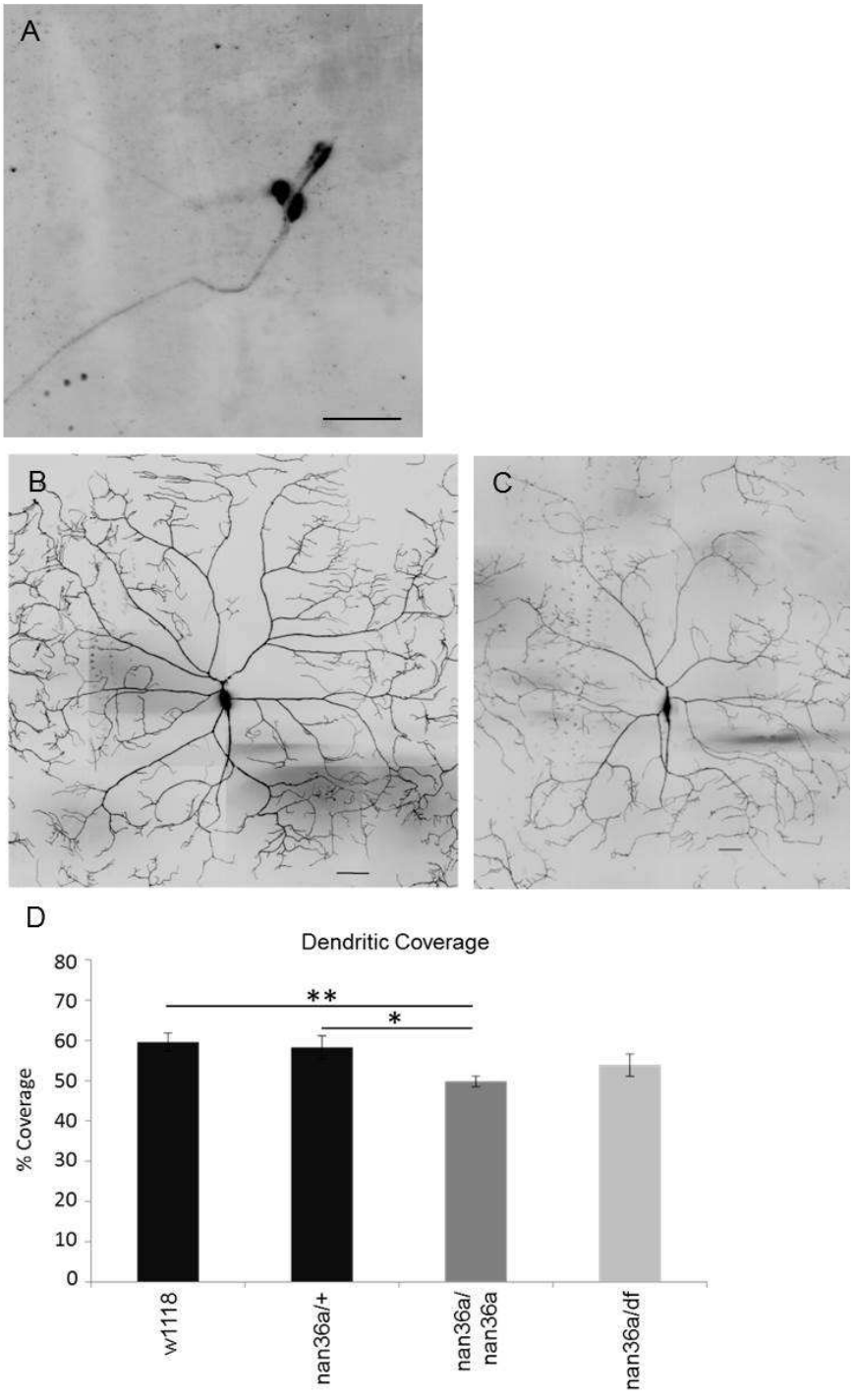

Figure 15: A *nanchung* genetic mutant shows a reduction in dendritic coverage.

Figure 15: A *nanchung* genetic mutant shows a reduction in dendritic coverage. A. *nan-GAL4* is expressed in the chordotonal neurons. **B and C.** Representative photomicrographs of control (B) and *nan36a* mutant (C) class IV neurons. **D.** The *nan36a* mutant shows a significant reduction in dendritic coverage. Data are mean ± SEM. Tukey's Test. N=6-13. *p<.05, **P<.01 Genotypes are *w;ppk-GAL4, UAS-mcd8::GFP/+, w;ppk-GAL4, UAS-mcd8::GFP/+;nan36a/+, w;ppk-GAL4, UAS-mcd8::GFP/+;nan36a/nan36a, w;ppk-GAL4, UAS-mcd8::GFP/+;nan36a/Df(3L)BSC801*.

15D). Additionally, the reduction seen in dendritic coverage in the *nanchung* genetic mutants is not as great as that seen in the RNAi mutant (Fig. 13, Fig. 14D). This indicates that the long isoform of *nanchung* is not likely involved in dendrite morphogenesis.

5.3.3 Generation of *coyotemint* mutant

In order to verify the dendritic phenotype of *coyotemint*, I have generated a genetic mutant using FRT-mediated deletion (Fig. 16A) [205]. I am currently testing this mutant for dendritic defects. Additionally, I have observed the expression pattern of 5 enhancer trap lines close to the gene. Enhancer traps are genetic elements that have been randomly inserted in the genome, and contain a GAL4. By observing enhancer trap lines that have inserted close to the gene of interest, it is possible to observe the expression pattern of the gene. None of these five enhancer trap lines caused the expression of GFP in the class IV neurons (Table 1). However, there is expression of the enhancer traps in the periphery, with some of the lines showing expression in the oenocytes and the epidermal cells (Fig. 16B). There are two isoforms of *coyotemint*, and the enhancer trap lines were only located in the 5'UTR of one of the isoforms (Fig. 16A).

5.3.4 Evaluation of the homeostatic hypothesis

Task6 had an insensitive phenotype to a noxious thermal stimulus. This is surprising, since knockdown of potassium channels would be expected to cause hypersensitivity. In addition to being insensitive to a noxious thermal stimulus,

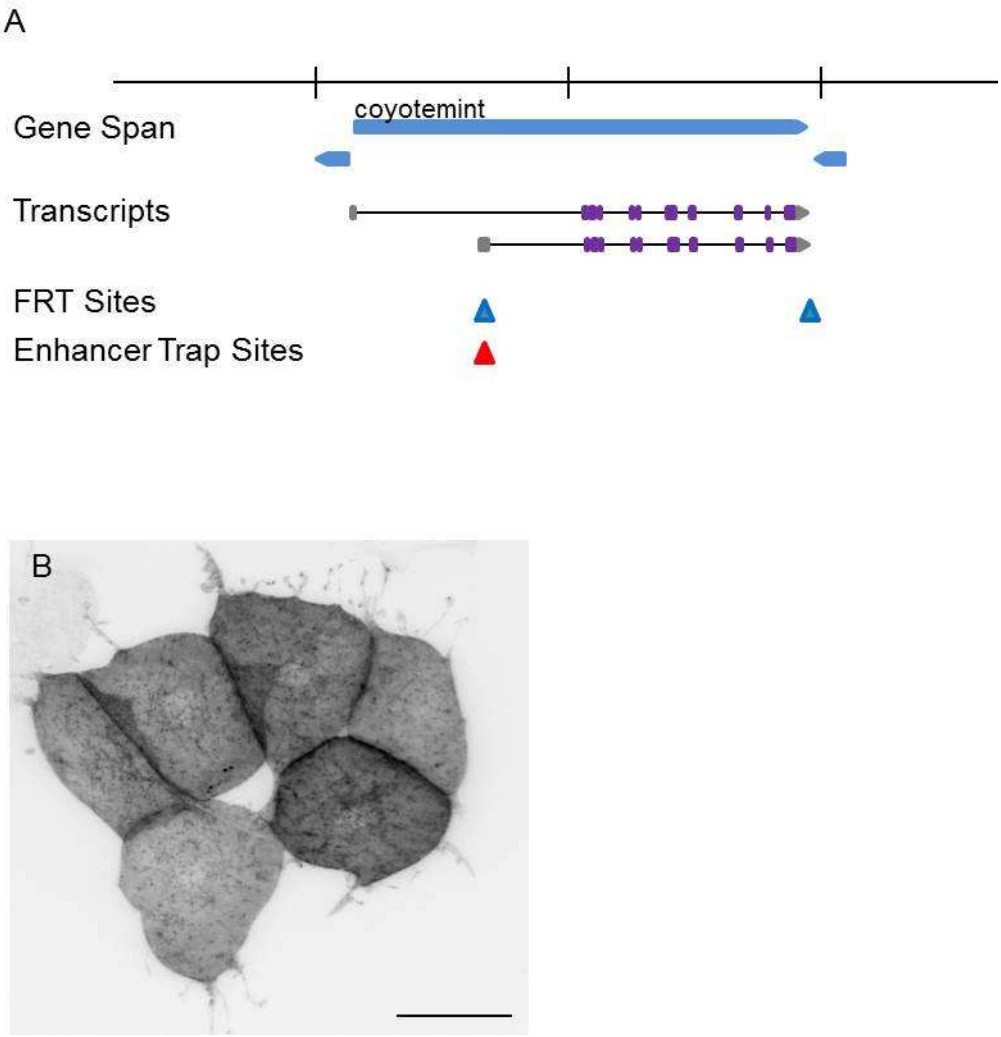

Figure 16: Generation of *coyotemint* mutant and *coyotemint* expression pattern.

Figure 16: Generation of *coyotemint* mutant and *coyotemint* expression pattern A. Genetic tools used to characterize *coyotemint*. The sites of the genetic elements used to create the deletion are indicated by the blue triangles. The red triangle indicates the site of the enhancer trap lines. Hash marks indicate 10 KB. **B.** An enhancer trap line drives GFP expression in the oenocytes. Scale bar is 50 μm.

Table 1: Expression pattern of *coyotemint* enhancer trap lines.

DGRC Number	Insertion point	Orientation	Expression Pattern
112-424	2L:1,737,425..1,737,425 [+]	Correct	Oenocytes, Epithelial cells, Fat body
112-292	2L:1,737,425..1,737,524 [+]	Correct	Oenocytes, Epithelial cells
113-073	2L:1,737,406..1,737,406 [+]	Correct	Oenocytes
113-024	2L:1,737,414..1,737,414 [-]	Opposite	Oenocytes, Epithelial cells
112-198	2L:1,737,433..1,737,433 [-]	Opposite	Trachae, Epithelial cells, Fat body, Malphigean tubules

Table 1: Expression pattern of *coyotemint* enhancer trap lines. This table shows the expression pattern of the enhancer trap lines that have inserted closely to the CG17646 gene. Only the periphery was examined.

knockdown of *Task6* caused a sparse dendritic phenotype (Fig. 12). We hypothesize that the sparse dendrite phenotype that is seen in some of our RNAi knockdown lines is caused by neuronal hyper-excitability induced by knockdown of the ion channels, which subsequently causes a homeostatic regulation of the dendritic field. If this is so, we should be able to suppress the dendritic defects caused by ion channel knockdown through alteration of the electrical properties of the neuron.

If the dendritic field is being reduced due to a homeostatic mechanism, the signaling mechanism for homeostatic regulation could be electrical changes in the dendrites themselves, electrical changes in the axon, or circuit level feedback on the neuron. If the sparse dendritic phenotype seen in *Task6* RNAi mutants is caused by over-excitation in the axon, silencing action potentials may rescue the phenotype. The voltage-gated sodium channel *paralytic* is known to function in action potential propagation [210]. We have an RNAi line directed against *paralytic* that effectively eliminates NEL responses [17]. We made flies that expressed RNAi against both *paralytic* and *Task6* (Fig. 17A-C). However, we were not able to suppress the *Task6* phenotype by knocking down *paralytic*. This indicates that if homeostatic regulation is present, it likely is not signaled through axonal excitability.

If the homeostatic hypothesis is true, increasing the excitability of the neuron should cause a homeostatic decrease in the size of the dendritic field. To test this

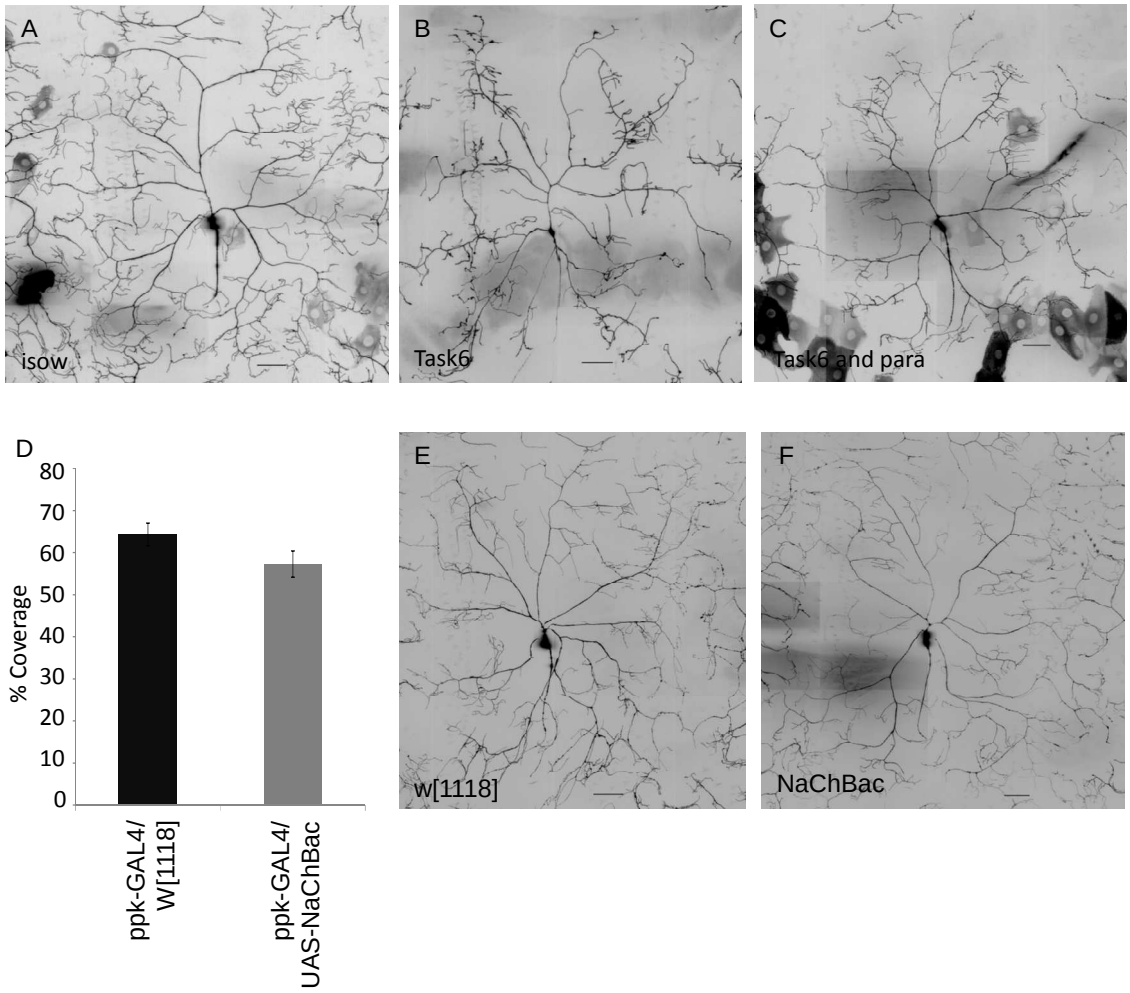

Figure 17: Evaluation of the homeostatic hypothesis.

Figure 17: Evaluation of the homeostatic hypothesis. A-C. Representative photomicrograph of isow control, *Task6* RNAi and a double knockdown of *Task6* and *paralytic*, a voltage gated sodium channel known to silence the class IV neurons. Silencing the class IV neurons by knocking down *paralytic* does not rescue the *Task6* dendritic phenotype. Genotypes are *ppk-GAL4, UAS-mcd8::GFP; UAS-dicer2/+*, *ppk-GAL4, UAS-mcd8::GFP/UAS-Task6Rnai; UAS-dicer2/+*, *ppk-GAL4, UAS-mcd8::GFP/UAS-Task6RNAi; UAS-dicer2/UAS-ParaRNAi.* **D-F.** Expression of the *NaChBac* in the class IV neurons does not cause a homeostatic regulation in the dendritic field. Genotypes are *ppk-GAL4,UAS-mcd8::GFP* (N=7), and *ppk-GAL4, UAS-mcd8::GFP; UAS-NaChBac* (N=6). Scale bars are 50 μm.

hypothesis, I expressed the bacterial sodium channel *NaChBac* in the class IV neurons. *NaChBac* is a bacterial voltage-gated sodium channel that, when over-expressed in *Drosophila* neurons, causes hyperexcitability [211]. *NaChBac* has a lower threshold of activation, and remains open for longer than voltage gated sodium channels encoded within the *Drosophila* genome [211]. When expressing *NaChBac*, neurons that are normally quiescent may have spontaneous action potentials [202]. Expression of *NaChBac* in the class IV neurons caused a slight, non-significant decrease in the coverage of the dendritic field (Fig. 17D-F).

5.4 Discussion

In this study, we found a wide variety of channels important in governing the dendritic phenotype of the class IV neurons. These channels included potassium channels, ligand gated channels, calcium channels and an ABC transporter. We also observed the thermal nociception and dendritic phenotypes for the genetic mutants of *nanchung*, as well as generated a genetic mutant for *coyotemint*.

nanchung is a TRPV channel that had both an insensitive and hypersensitive response to a noxious thermal stimulus and had a severely reduced dendritic phenotype when knocked down by RNAi. Although the phenotype of the *nan36a* genetic mutants did not match the severe dendritic defects seen in the *nanchung* RNAi mutant, there are explanations for this. First, this mutant only takes out the 5′ region of the gene. TRP

channels are often alternatively spliced [18], so the isoform important for causing the dendritic defect may not be deleted. Indeed, preliminary PCR analysis of the mutant has indicated that there may be a second transcript present (data not shown), and EST sites denoted on FlyBase indicate that there could be other transcripts downstream of the deleted region in the *nan36a* mutants (Fig. 14A). Further analysis of *nanchung* should concentrate on mutants where the entire gene is deleted, eliminating all potential transcripts.

nAcRα-96ab also emerged from the dendritic screen. Although it was not further characterized as a genetic mutant due to lack of genetic tools, it is a very interesting hit. *nAcRα-96ab* is a nicotinic acetycholine receptor. Acetycholine has been implicated in Alzheimer's disease [212], a neurodegenerative disorder. Although it remains to be seen if the neurons are actually degenerating, it would be interesting to evaluate the class IV neurons as potential model for neural degeneration. Future studies could concentrate on the development of the dendritic defect in *nAcRα-96ab* RNAi mutants.

coyotemint is an ABC transporter, and has a severe Class IV dendritic defect. A *Drosophila* screen for genes involved in obesity found that two EP elements located just upstream of *coyotemint* caused increased triglyceride storage [213]. Further characterization of ABCG1, the mammalian homologue of *coyotemint*, has found that it is important in the intracellular regulation of cholesterol (reviewed in [214]). Based on

enhancer trap lines in one isoform of *coyotemint*, *coyotemint* is expressed in the oenocytes, which are the primary site of lipid metabolism in the fly [215]. This could indicate that there is a general disruption in lipid export, leading to dendritic defects in the class IV neurons. However, if the enhancer trap results are accurate and *coyotemint* is not expressed in the class IV neurons, it is difficult to understand how the dendritic phenotype persists when RNAi knockdown is only in the class IV neurons. Alternatively, the enhancer trap is inserted into the 5′ UTR of one of the transcripts, but there is a second transcript that has a different 5′ UTR (Fig. 15B). This could indicate that the second transcript is expressed in the class IV neurons.

Task6 emerged as insensitive to a noxious thermal stimulus, and also had severe dendritic defects in the class IV neurons. This led us to hypothesize that the sparse dendritic phenotype could be due to a homeostatic regulation of the dendritic field. We tested this hypothesis by knocking down *paralytic*, a voltage gated sodium channel, in the class IV neurons in *Task6* RNAi mutants. This did not rescue the *Task6* sparse dendritic phenotype, indicating that action potentials are not necessary for causing the sparse dendritic phenotype (Fig. 17A-C). We also were not able to cause homeostatic regulation of the dendritic field by hyperactivating the cells through the expression of *NaChBac* (Fig. 17 D-F).

Additionally, contradictory to the homeostatic hypothesis, three RNAi lines targeting potassium channels had a hypersensitive thermal phenotype, but no dendritic defect. The RNAi lines targeted voltage gated potassium channels (*Seizure* and *CG10440*) and a calcium-activated potassium channel (*SK*) (covered in the next chapter, [207]). This could indicate that these potassium channels are involved in detecting hyperexcitability and communicating this activity to the homeostatic machinery. Thus, lack of these channels causes hypersensitivity to a noxious stimulus but no dendritic phenotype. It is also possible that the homeostasis hypothesis is incorrect, and that the reduced dendrite phenotype seen in the *Task6* mutants is due to downstream effectors particular to those ion channels. *Seizure*, CG10440 and *SK* may be interesting to investigate as gates to the homeostatic machinery.

Our screen revealed several novel ion channel regulators of dendritic morphology. However, it is unclear whether the cause of the sparse dendritic phenotype is alterations of neuronal electrical properties through the ion channels, or through downstream effectors specific to the ion channel itself. Further research should concentrate on understanding how the sparse dendritic phenotypes develop.

6. Characterization of the potassium channel *SK* in thermal nociception

6.1 Introduction

In addition to identifying novel ion channels that cause an insensitive phenotype to a noxious thermal stimulus when knocked down in the sensory neurons, Kia Walcott conducted an additional screen to identify ion channels that cause a hypersensitive phenotype to a noxious thermal stimulus when knocked down. Several genes emerged from this screen, including *NmdaR1* and potassium channels. One of the potassium channels to come out of the screen was *SK*, a calcium-activated potassium channel.

Nociceptor neurons show little spontaneous activity in the absence of a noxious stimulus, and are normally silent [216, 217]. Potassium channels are important for setting the membrane potential and regulating the electrical properties of the cell. There are four main classes of potassium channels: voltage-gated potassium channels, two-pore potassium channels, calcium-activated potassium channels and inward-rectifying potassium channels. With some exceptions, under physiological conditions in neurons these channels largely pass potassium current in the outward direction, causing hyperpolarization of the cell. Disruption of these outward potassium currents can lead to hyperexcitability of the neuron. For example, mutations in the calcium-activated potassium channel *BK* have been associated with epilepsy in humans [218]. Therefore, changes in potassium channel activity in the nociceptors could cause the highly

regulated electrical properties of the nociceptors to change, leading to hyperexcitability and pain.

Potassium channels play an important role in the regulation of pain in mammals. In mammals, the dorsal root ganglion (DRG) cells, a subset of which are the nociceptors, show decreased potassium currents following nerve injury [41, 219] . This decrease causes hyperexcitability of the neurons. Additionally, a recent study has found that autoimmuninty against a voltage gated potassium channel is associated with chronic pain in humans [38].

Apamin, a component of bee venom, specifically blocks the *SK* channel in mammals [220, 221], allowing for precise manipulation of the current during electrophysiology. When a neuron becomes depolarized and calcium enters, the *SK* channel opens [222]. The resultant potassium current can lead to the afterhyperpolarization (AHP), during which the membrane potential drops below the resting membrane potential. There are three types of AHP currents. The fast AHP begins during the depolarization of the cell in the action potential, and lasts for only a few milliseconds. These currents are thought to be mediated primarily by *BK* channels [223]. In contrast, the medium AHP lasts longer, in the hundreds of milliseconds [222]. These currents are often apamin sensitive, meaning that the current is likely being caused by *SK* [224-227]. The slow afterhyperpolarization can persist for several seconds

and is not blocked by apamin, indicating that an unknown channel is mediating the slow AHP.

There are three *SK* channels encoded in the mammalian genome, and one *SK* channel encoded in the *Drosophila* genome. In mammals, *SK* channels can form heteromeric or homomeric assemblies [228-230]. Additionally, in both mammals and *Drosophila*, *SK* is differentially spliced producing distinct isoforms of *SK*. In *Drosophila*, while there is only one *SK* gene, it can be spliced into 10 different isoforms. Thus far, the role of different *SK* isoforms in modulating neuronal excitability is not well understood.

In a previous study, Kia Walcott developed an *SK* genetic mutant that eliminates all isoforms of *SK* [207](Fig. 18A). This mutant shows a hypersensitive phenotype to noxious thermal and mechanical stimulus, but has normal gentle touch responses (Fig. 18B-D). The hypersensitive thermal and mechanical phenotypes could be rescued by genomic DNA encoding the deleted region (Fig. 18). However, since the genomic DNA could ostensibly be expressed throughout the larvae, the location of action for *SK* was unknown. In these studies, I have performed a tissue specific rescue of *SK*, investigated the role of *SK* isoforms in thermal nociception, and developed a tool to aid in the understanding of the physiological properties of the class IV neurons. My results show that *SK* is important for thermal nociception in the class IV neurons.

6.2 Materials and methods

6.2.1 Fly strains and husbandry

Flies of the genotype *SK* mutant [207], e. isow, *UAS-SK-M, UAS-SK-N, ppk-GAL4, ppk-GAL4; UAS-mcd8::GFP*, and *ppk-GAL4;UAS-gCAMP3.0* were used. The *SK* mutant was created using FRT-mediated deletion. The fly strains p[XP]^{d01963} and pBac[WH]^{f01403} were used to create the mutant. Flies were maintained on standard molasses cornmeal medium at 25° C.

6.2.2 Immunohistochemistry

Larvae were fileted in cold PBS, and then fixed for 30 minutes with 4% paraformalydehyde. Larvae were then washed with PBS-T, and placed in to a blocking buffer with 2% BSA and 10% normal goat serum at 4°C overnight. The next day, the filets were incubated at room temperature with the primary antibody for four hours, washed with PBS-T, and then incubated overnight at 4°C with the secondary antibody. Larvae were washed with PBS-T and then mounted in VectaShield mounting medium. Images were taken on a LSM 5 Live confocal microscope using a 40X objective. The primary *SK* antibody was kindly provided by the Dolph lab [231]. The SK antibody was used at a concentration of 1:2000, the GFP antibody was used at a concentration of 1:250, the 22C10 antibody was used at a concentration of 1:100. All secondary antibodies were used at a concentration of 1:600.

6.2.3 Thermal nociception assays

Thermal nociception assays were performed as described in Chapter 4. Crosses were set up with six to ten virgin females and three males on standard cornmeal molasses medium at 25°C. Five to seven days later, wandering third instar larvae were tested for sensitivity to a 42°C thermal probe. The trials were video recorded and the precise latency to respond was determined following the experiment with a stopwatch. I was blind to the genotype of the larvae during testing and quantification.

6.2.4 Thermal imaging assay

Further details on making the thermal imaging apparatus are described in detail in the Results section. Larvae were immobilized with a thread of hair tied around the anterior region, severing the brain from the rest of the body. Larvae were then placed on the apparatus and imaged for calcium activity in the class IV neurons using gCAMP3, a calcium sensitive indicator on a Zeiss LSM 5 Live confocal microscope with a 20X objective. By using a fast piezo drive, we were able to capture 30 optical sections every second.

The Zeiss software system was used to analyze the data. First a region of interest (ROI) was designated around the cell body, allowing the software to measure changes in fluorescence, a readout of calcium, inside this area. The ROI was moved as necessary to compensate for larval movement during the experiment. The plot of fluorescence

intensity over time was evaluated, and changes in fluorescence were noted. To calculate the change in fluorescence, a peak in fluorescence was normalized to the fluorescence 15 frames earlier. If no peaks in fluorescence were observed, the maximum fluorescence over the entire trial was used. To ensure that the class IV neurons were functioning properly, a UV light was shown on the class IV neurons following the trial. Larvae that showed no response to the UV light and no fluorescence peaks were excluded from the analysis.

6.2.5 Dendrite imaging and quantification

Imaging was carried out as described in Chapter 5. Wandering third instar larvae were rinsed in water and then placed in a glass petri dish on a coverslip containing a drop of glycerol. Ether was applied to a cotton ball in the petri dish, and the dish was enclosed using lab tape. After 15 minutes, larvae were mounted on slides in glycerol for imaging. Larvae were imaged using an LSM 5 Live confocal. Images of the medial segments (4-6) were taken using the tiling MACRO on the LSM 5 Live software. A maximum intensity projection of the image was made using the LSM 5 Live software. Images were then cropped to hold a single neuron, with the boundaries of the cell determined by the length of the longest dendrite. A grid was put over the neuron, and the number of boxes containing dendrites was calculated [91]. The cell body and axon were omitted from the counting. Scoring was done blind to genotype.

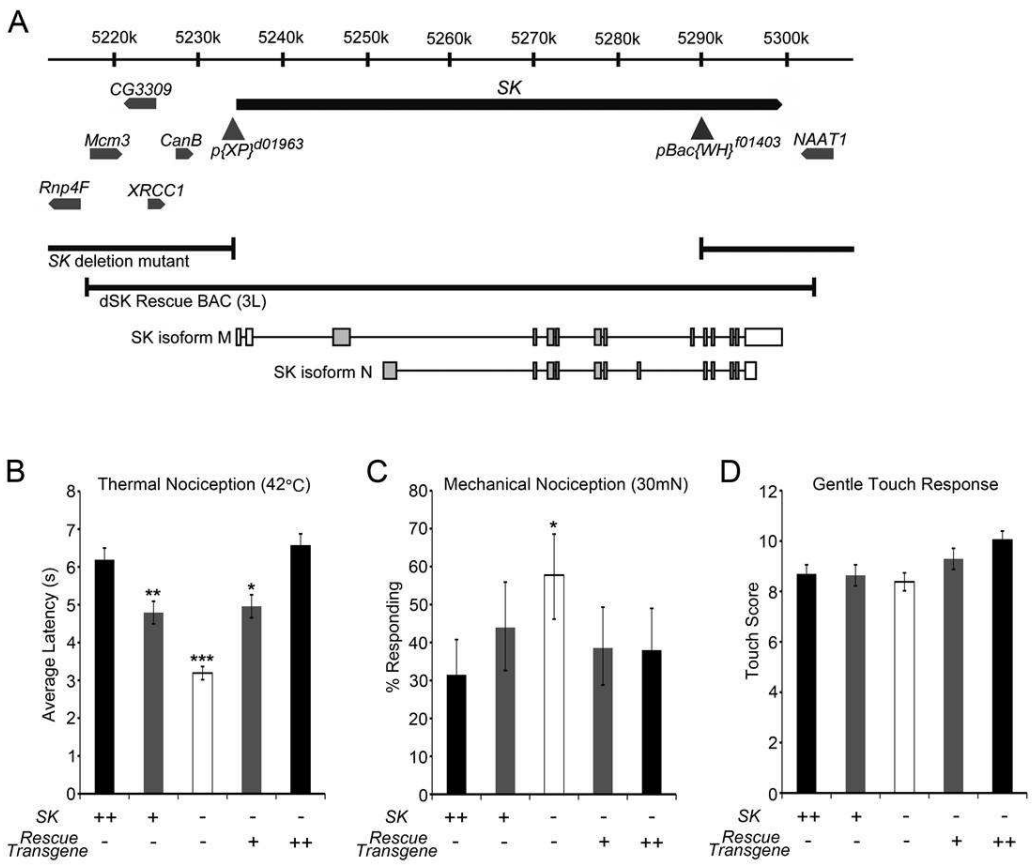

Figure 18: *SK* genetic nulls show a hypersensitive phenotype to a noxious thermal and mechanical stimulus.

Figure 18. ***SK* genetic nulls show a hypersensitive phenotype to a noxious thermal and mechanical stimulus. A.** Genetic elements used to create *SK* transgenic animals. The FRT elements insertion sites are indicated by the triangles. Both the *SK-M* and *SK-N* transcripts are denoted. **B.** *SK* mutant larvae show a hypersensitive phenotype to a 42°C probe. Compared to wildtype larvae (E. isow) larvae null for *SK* show significantly faster latency to respond to a noxious thermal stimulus. One copy of the BAC element covering the *SK* gene results in a partial rescue, while two copies of the BAC element rescue the *SK* phenotype to wildtype levels. N=66-72 One way ANOVA with Dunnett's Test. P<.05*, p<.01**, p<.001*** **C.** *SK* mutant larvae show a hypersensitive phenotype to a noxious mechanical stimulus. Using a 30 mN mechanical probe, *SK* null mutants are significantly hypersensitive compared to controls. Genomic rescue of *SK* eliminates the hypersensitive phenotype. N=66-83. Fisher's Exact Test with Bonferroni Correction. P<.05*, p<.01**, p<.001*** **D.** *SK* null larvae show a normal response to gentle touch. *SK* null larvae show no significant difference from controls in the gentle touch assay, where an eyelash is used to gently stroke the larvae. P<.05*, p<.01**, p<.001***. Kia Walcott, Asako Tsubouchi.

6.3 Results

6.3.1 *SK-M*, but not *SK-N*, rescues thermal nociception when expressed in the class IV neurons

Dr. Walcott's previous work had shown that *SK* has a hypersensitive thermal nociception phenotype, which can be rescued through the insertion of genomic DNA containing the *SK* gene into flies mutant for *SK* (Fig. 218B). Additionally, RNAi knockdown of *SK* in the class IV neurons results in a hypersensitive thermal nociception phenotype, pointing to a role for *SK* in the class IV neurons specifically. In this experiment, I expressed the longest isoform of *SK*, *SK-M* in the class IV neurons, as well as a shorter isoform of *SK*, *SK-N* (Fig. 18A). While *SK-M* rescued the hypersensitive nociception phenotype to wildtype levels, *SK-N* failed to rescue (Fig. 19). This indicates that specific *SK* isoforms are required to rescue the nociception phenotype in the class IV neurons.

6.3.2 *SK-M* is not expressed in the class IV neurons

Next, I wanted to determine the expression pattern of *SK-M*. To do this, we used an antibody developed by the Dolph lab [231]. This antibody targets the M isoform of *SK*. In wildtype larvae, we saw expression of *SK* in neurons close to the class IV neuron, and also in axons close to the class IV axons (Fig. 20A-C). There is no detectable antibody staining in *SK* null larvae (Fig. 20D-E). To determine if the antibody was accurately detecting the *SK-M* isoform, we overexpressed *SK-M* in the class IV

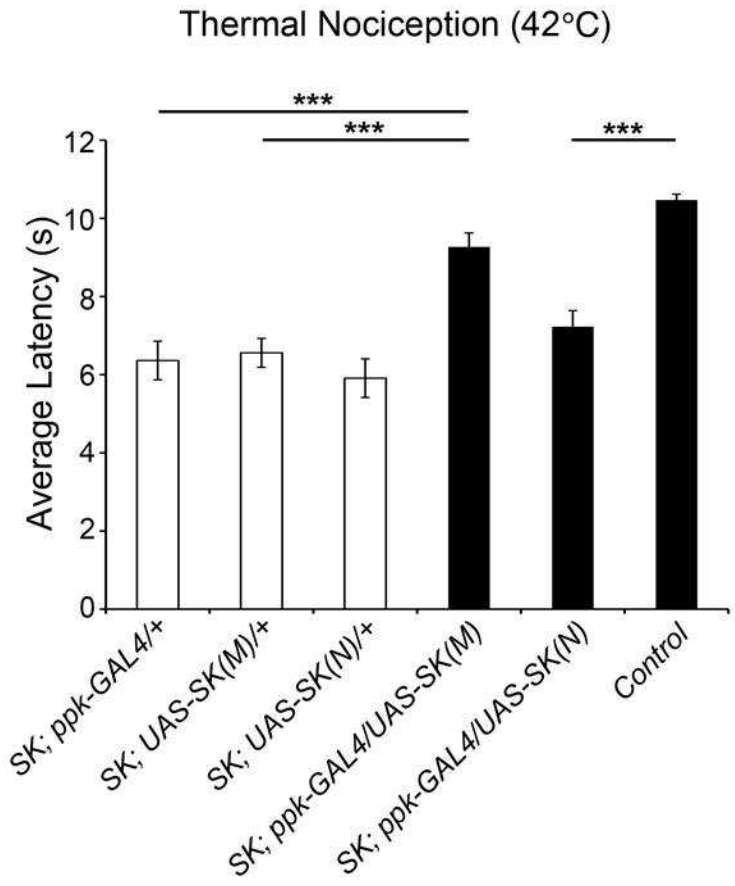

Figure 19: The hypersensitive thermal phenotype in *SK* mutant larvae is rescued by Class IV specific expression of *SK-M*, but not *SK-N*.

Figure 19: The hypersensitive thermal phenotype in *SK* mutant larvae is rescued by Class IV specific expression of *SK-M*, but not *SK-N*. A. Latency to respond to a 42°C probe in larvae null for *SK*, but expressing *SK-M* in the class IV neurons is not significantly different from wildtype controls. Data are presented as mean ± SEM. N=45-118. One way ANOVA followed by Tukey's test. P<.05*, p<.01**, p<.001***.

neurons. The antibody detected *SK-M* strongly in the cell body and axon of the class IV neurons, with slight expression in the dendrites (Fig. 20F-I). This indicates that the antibody can detect the *SK-M* isoform.

To determine if the *SK* staining seen near the axons of the class IV neurons overlapped with that of the class IV neurons, I stained the brains of wildtype larvae expressing GFP in the class IV neurons using the *SK* antibody. However, the axonal staining *SK* and the class IV staining do not overlap (Fig. 21A-C), indicating that *SK-M* is not detectable by the antibody in the class IV neurons.

SK is expressed in the periphery, in a cell body close to the class IV neurons. To determine the identity of this neuron, I performed double labeling with the 22C10 antibody and the *SK* antibody. This staining revealed that *SK-M* is endogenously expressed in the external sensory (es) cells (Fig. 32A-C). The es neurons are ciliated sensory neurons. It is unclear what role *SK* is playing in these neurons.

6.3.3 Physiology of *SK* in the class IV neurons

In order to fully understand hyper- or insensitivity to a thermal stimulus *in vivo*, it is necessary to have a method for determining the physiological response of the neurons to a heat stimulus. To achieve this, I built an apparatus to heat and cool larvae in a controlled manner while optically recording genetically encoded calcium

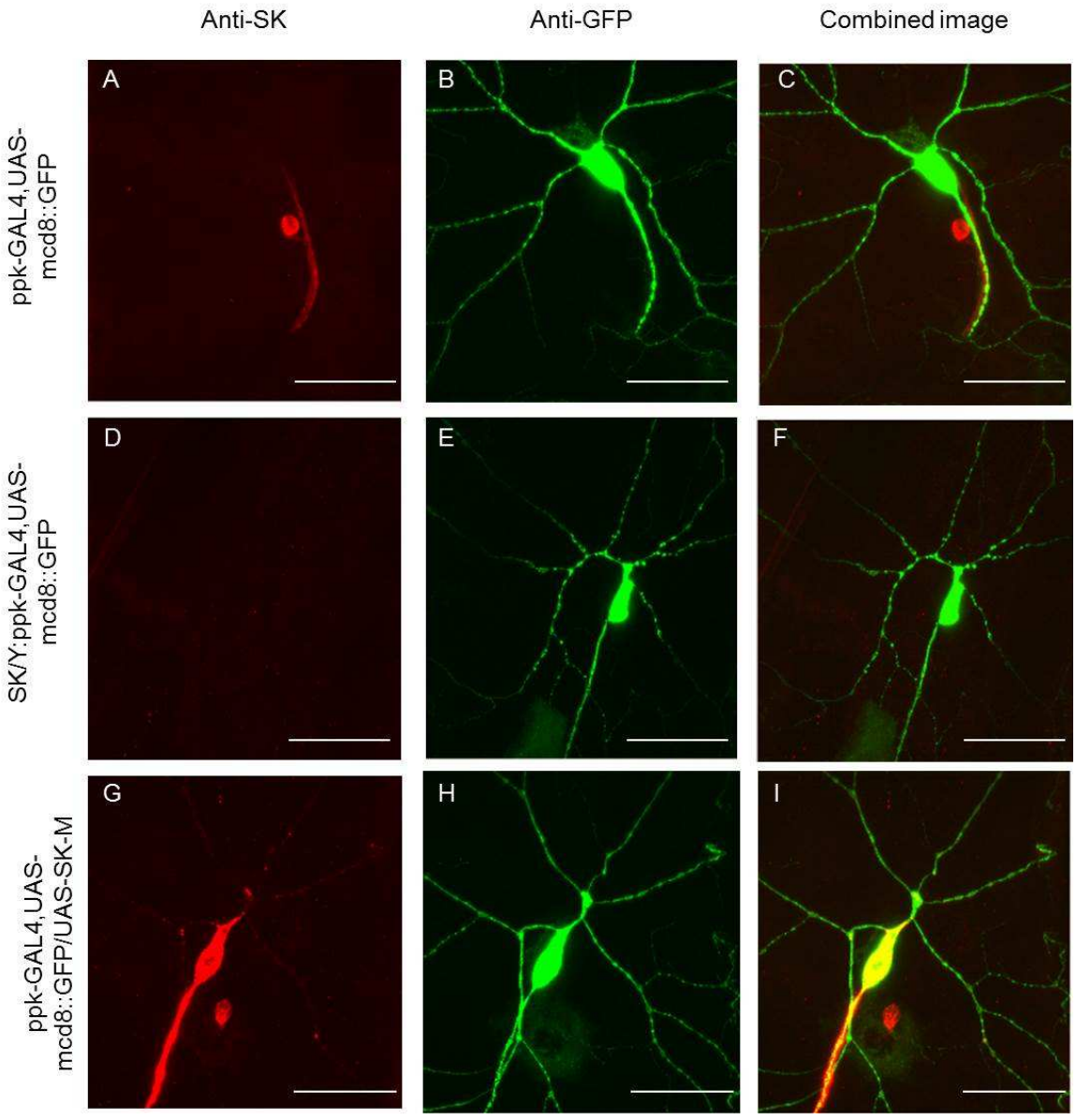

Figure 20: *SK-M* is not detectable in the class IV neurons.

Figure 20. *SK-M* is not detectable in the class IV neurons. In all figures, the class IV neurons are illuminated using *ppk-GAL4, UAS-mcd::GFP*. **A-C.** In wildtype larvae, *SK* is expressed in cells in the periphery, but not in the class IV neurons cells. **D-F.** There is no detectable *SK* antibody staining in *SK* null animals. **G-I.** *SK-M* is detected by the *SK* antibody when overexpressed in the class IV neurons. Genotype is ppk-GAL4, UAS-mcd8::GFP; UAS-SK-M.

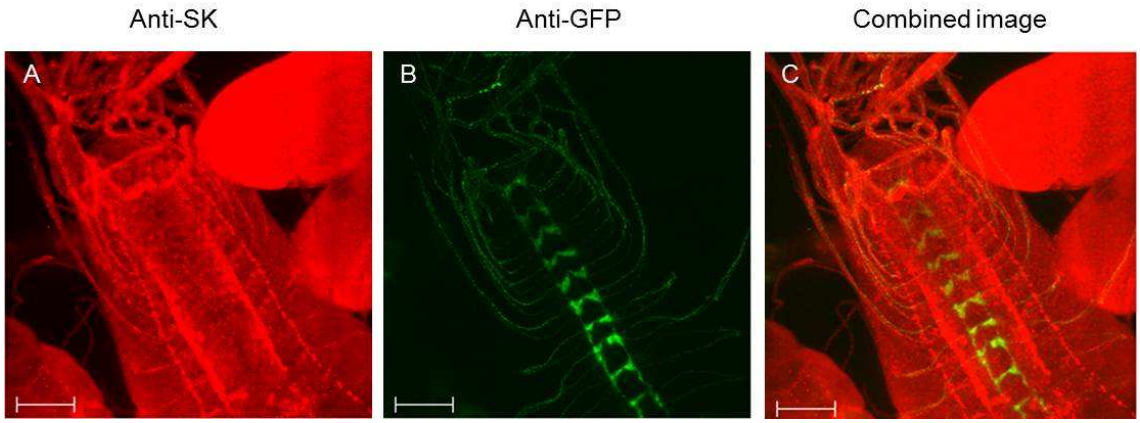

Figure 21: The *SK* antibody does not label the class IV axons.

Figure 21. The *SK* antibody does not label the class IV axons. **A-C.** Staining of *SK* is present in axonal projections to the ventral nerve cord, but did not overlap with the axonal projections of the class IV neurons. The class IV neurons are illuminated using ppk-GAL4, UAS-mcd::GFP.

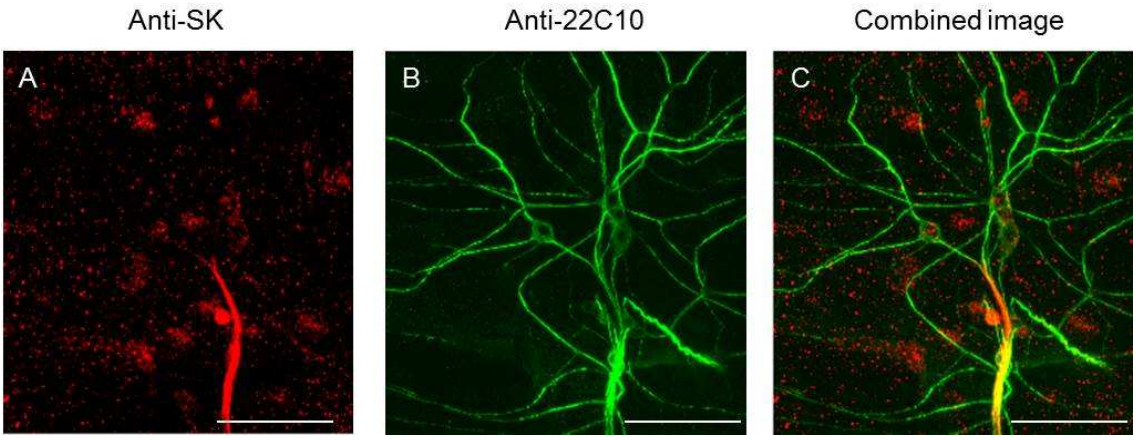

Figure 22: *SK* is present in the ES neurons.

Figure 22. *SK* is present in the ES neurons. A-C. The 22C10 antibody was used to label all of the peripheral neurons. The *SK* antibody overlapped with the ES neurons.

indicators expressed in the nociceptor neurons (Fig. 23A, B).

This system was originally designed for optical recordings in *C. elegans* [232], but I have modified it to allow for imaging of larvae, as well as for imaging on an inverted microscope. In order to heat and cool the larvae while imaging, the apparatus uses a peltier device mounted to a brass plate. The peltier device is operated by a thermal control unit equipped with a feedback mechanism. To paralyze the larvae for the purpose of imaging they are ligated below the brain with a fine hair (the ligation presumably severs the motor neuron connections to the muscles). The larvae are then placed between two coverslips and attached to the brass plate. We use a genetically encoded calcium indicator, UAS-*gCAMP3.0*, to detect calcium activity in a tissue specific manner. Our LSM 5 live system with a fast piezo motor allows for rapid imaging of calcium responses. The heating device is capable of producing highly controlled and replicable heat ramps (Fig. 23C-D). I have also designed the apparatus so that it can be used to visualize calcium responses to temperature changes in the antennae of adult flies.

Utilizing this assay, we found that larvae null for *SK* show a greater increase in fluorescence during a temperature ramp than wildtype larvae or larvae with the *SK* gene rescued (Fig. 24). This indicates that there is a greater influx of calcium into the class IV

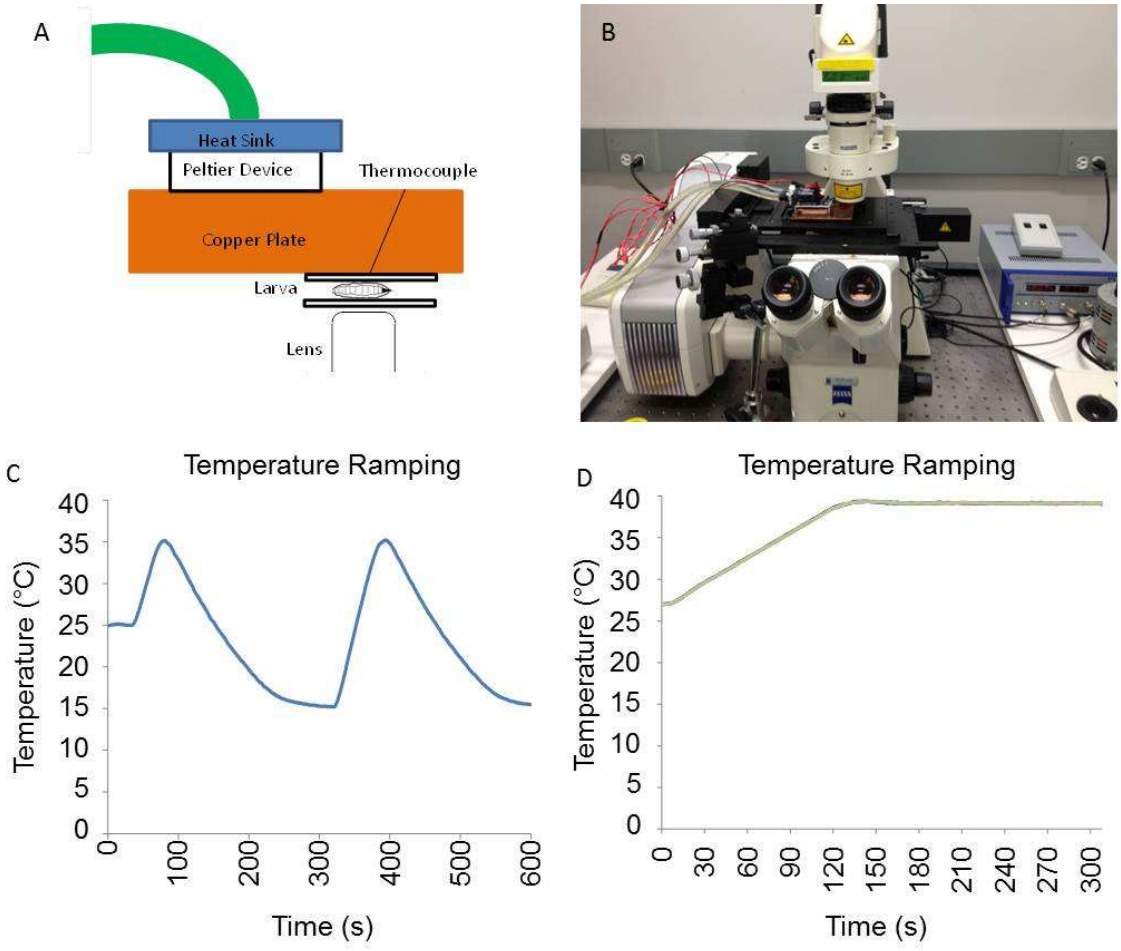

Figure 23: A device for imaging genetically encoded calcium indicators during changes in temperature.

Figure 23. A device for imaging genetically encoded calcium indicators during changes in temperature. A. Schematic of thermal ramping device. Larvae are placed between two coverslips under the copper plate, and the temperature is controlled by a peltier device. **B.** Photograph of apparatus on confocal microscope. **C.** The thermal ramping device can increase and decrease the temperature. **D.** The thermal ramping device can perform consistent temperature ramps. Nine different ramping trials are represented.

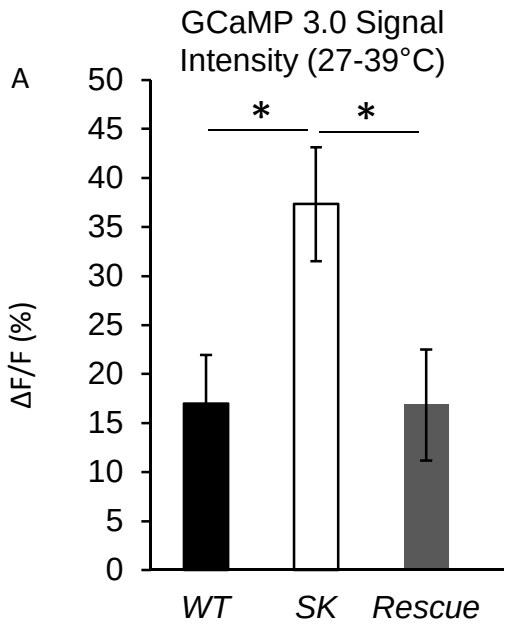

Figure 24: Calcium transients in *SK* null larvae.

Figure 24. Calcium transients in *SK* null larvae. Thermal ramping from 27 - 39°C was performed using the apparatus presented in Figure 23. *SK* null larvae expressing gCAMP show significantly higher changes in fluorescence compared to controls and the BAC rescue. N=18. Data presented are mean ± SEM. One Way ANOVA. Kia Walcott, Asako Tsubouchi

neurons of *SK* null larvae. However, there are difficulties in interpreting these data. For example, the changes in fluorescence we saw in the *SK* mutants did not seem to be related to a temperature threshold. Additionally, we rarely saw these spontaneous changes in fluorescence in the wild type larvae, even when the temperature threshold for nociceptive behavior was overcome.

6.3.4 Larvae null for *SK* show no dendritic defects

In the previous chapter, I found that some ion channels caused changes to the dendritic morphology of the class IV neuron. To determine if *SK* plays a role in dendrite morphogenesis, I imaged the class IV neurons in *SK* null larvae. We found no significant differences in dendritic coverage in the *SK* null larvae (Fig. 25).

6.4 Discussion

In this chapter, I show that the hypersensitive phenotype seen in *SK* null larvae can be rescued by the expression of the *SK-M* isoform in the class IV neurons, but not by *SK-N* (Fig. 19). However, *SK-M* is not detectable by antibody staining in the class IV neurons (Fig. 20). There are several possible explanations for this phenotype. For example, it is possible that by using the GAL4 UAS system to express *SK-M*, I am overexpressing the channel relative to wildtype levels. *SK* is a calcium activated

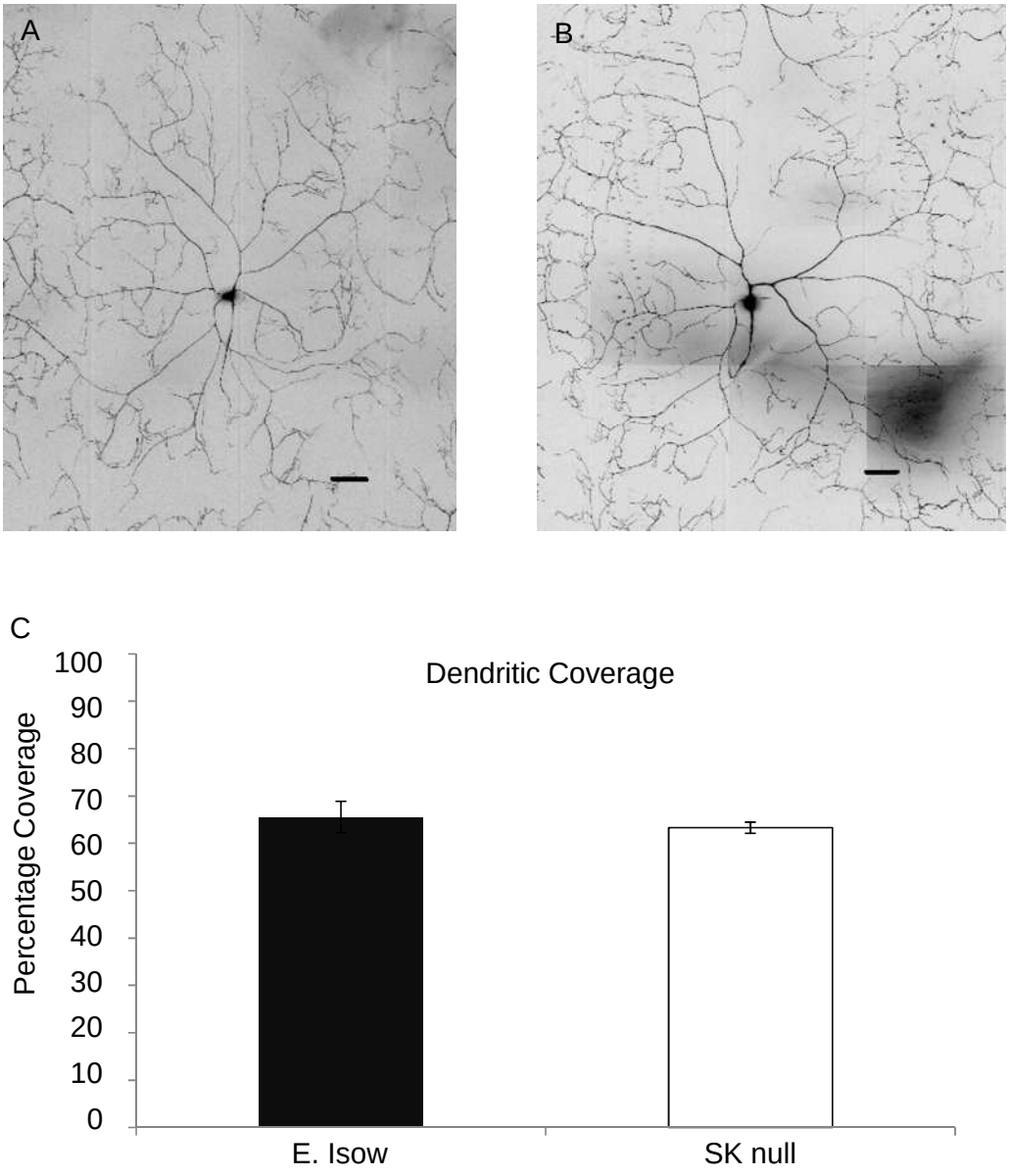

Figure 25: *SK* null larvae show no defects in dendritic coverage.

Figure 25. *SK* null larvae show no defects in dendritic coverage. **A, B.** Representative photomicrographs of the class IV neurons in a control (A) and SK null (B) larvae. **C.** Quantification of the dendritic coverage in *SK* null larvae shows no significant difference than controls. T-test. N=6. P value=.54

potassium channel, so increasing the expression of the channel could increase the length of time of the AHP, causing a general insensitivity in the class IV neurons. Since *SK* does not have a gentle touch phenotype (Fig. 18D), overexpressing *SK-M* in the class III neurons, which are responsible for detection of gentle touch, and testing for insensitivity to gentle touch would test this hypothesis. It is also possible that a different isoform of *SK* that is not detected by the antibody functions in the class IV neurons.

SK-M, but not *SK-N*, was able to rescue the hypersensitive phenotype when expressed in the class IV neurons of *SK* null larvae. This indicates that these two *SK* isoforms are functionally distinct. In mammals the three genes encoding *SK* have different sensitivities to apamin, and are expressed differentially through the nervous system [228, 233, 234]. The *Drosophila* genome only encodes one *SK* channel, so regulation of the functional properties of the channel could be regulated through differential splicing. Isoform specific GAL4s and isoform specific antibodies should be developed so that the specific isoform of *SK* which is endogenously expressed in the class IV neurons can be identified. Once the isoform is known, it would be interesting to investigate how the electrophysiological properties of the isoforms vary.

In this chapter, I developed a machine to monitor the physiology of the class IV neurons as they undergo a thermal ramp. In this preparation, the larvae remain whole, and are ligated to ensure that they are still during imaging. Surprisingly, we saw little

activation of genetic encoded calcium indicators during a thermal ramp, even though we ramped up to 39°C, which is thought to be the threshold of the class IV neurons in *Drosophila* [16, 217]. When 39°C was exceeded, the larvae began to seize, causing a motion artifact in the imaging. Thus, it was difficult to test the larvae at higher temperatures. When we did see calcium influx, it seemed to be random, occurring at various points during the thermal ramp, seemingly unrelated to a temperature threshold. One possibility is that the temperature ramping is too slow, and that to ensure activation of the class IV neurons the ramping speed needs to be faster.

It is possible that the calcium influx we see during temperature ramping in the class IV neurons are back propagating action potentials, perhaps due to injury to the axons during the ligation preparation. It would be interesting to try different preparations, for instance using genetic tools that paralyze larvae at higher temperatures. Additionally, another laboratory member is developing a preparation where a hot probe is applied directly to a larva while performing calcium imaging on the confocal microscope. This paradigm eliminates the potential for a slow ramping speed to interfere with signaling, and also delivers a localized stimulus.

Lastly, the dendritic phenotype of *SK* does not appear to be showing homeostatic regulation. *SK* produces a robust hypersensitive thermal nociception phenotype, and yet maintains a normal dendritic structure. Assuming that the homeostatic hypothesis is

correct, this could indicate that *SK* is a potential gate to the homeostatic machinery, and elimination serves to stop the homeostatic machinery from working. This hypothesis could be investigated by observing *Task6 SK* double mutants. If *SK* is an integral part of the homeostatic machinery, these mutants should exhibit no dendritic phenotype.

Potassium channels are being investigated as interesting new targets for drug discovery in mammals. Further characterization of *SK*, including the isoform specific properties of the neuron and structure function analysis, could lead to interesting new targets in the fight against chronic pain.

7. Discussion

In my dissertation, I utilized a wide range of nociception paradigms, from parasitoid wasps to thermal nociception. I have developed a new, ethologically relevant nociception paradigm in which larvae are attacked by parasitoid wasps. Additionally, I implicated a putative mechanosensory ion channel that is involved in detecting wasp attacks, as well as fourteen ion channels that are important in detecting a noxious thermal stimulus. Lastly, I have described six ion channels that are important in regulating the development of the nociceptor neurons. I have also made a genetic mutant for the ABC transporter gene *coyotemint*. In the next few pages, I will discuss the future directions that might build upon this body of work.

7.1 Natural variation in mechanosensitive genes

I found that *pickpocket*, a DEG/ENaC channel, is necessary for showing NEL (NEL) in response to parasitoid wasp attacks. However, we utilized animals that are null for the *pickpocket* gene, which is unlikely to exist in nature. An interesting way to discover natural variation in mechanosensing genes would be to use the fly collection made by Trudy Mackay at North Carolina State University [235]. She has made 129 isogenized lines of flies collected from around the Raleigh, NC area, and sequenced their genome [235]. It would be interesting to observe if the different fly lines have different susceptibilities to attack by parasitoid wasps. If certain fly lines came out as being

extremely sensitive or insensitive to surviving wasp attacks, the genome could be evaluated for variant genes of interest. Additionally, the fly lines could be tested in our other behavioral paradigms for sensitivity to a gentle touch and sensitivity to a noxious mechanical stimulus.

Since we found that *pickpocket* is important for NEL in response to wasp attacks, it would be interesting to determine the genetic variation in the *pickpocket* locus in the Mackay lines *in silico*. Lines that had significant variation from wildtype could be tested for responses to a noxious mechanical stimulus or to the wasp, to see how the behavioral responses vary. Using this technique, we could determine interesting structure function relationships that are present in the wild.

7.2 Using parasitoid wasps to probe the function of the class IV dendritic field

The elaborately branched dendritic field of the class IV neurons is predicted to be important in detecting noxious thermal stimulus. However, our screen found several genes, such as *coyotemint* and *nanchung*, that showed severe defects in class IV dendritic coverage, but no thermal nociception defect when knocked down specifically in the class IV neurons. One potential reason for this seeming disparity could be that the thermal nociception probe is very large, and covers several segments. Therefore, the class IV neurons could still receive input from the probe, even if the class IV dendritic field size is much smaller. To address this possibility, we could use the wasps to attack the RNAi

mutants that showed a severe dendritic phenotype but no thermal nociception phenotype. If direct contact with the dendrites is important for detecting a wasp attack, larvae with reduced dendritic coverage should show altered rates of nocifensive behavior in response to wasp attacks. These experiments would further our knowledge of the role of dendrites in detecting noxious stimuli.

7.3 Coyotemint

coyotemint is an ABC transporter that when knocked down in the multidendritic neurons causes an insensitive thermal nociception phenotype and severely reduced dendritic coverage. I generated a *coyotemint* genetic mutant, which needs further characterization. The mammalian homologue of *coyotemint*, ABCG1, is important in intracellular regulation of cholesterol [214]. It would be interesting to first determine how lipid concentrations are affected in *coyotemint* mutant larvae. Lipids are known to modulate TRPV channels, which are important for thermosensation [236]. Additionally, there is evidence for a role of cholesterol in modulating mechanotransduction (For review see [237]). Given this, it would be interesting to test the *coyotemint* mutants for defects in mechanotransduction. Using the wealth of fly genetic tools, we could potentially develop a model for lipid interactions in nociception in flies, and manipulate important molecules in the signaling pathway.

7.4 Ion channel regulation of class IV dendritic morphology

nacrα-96ab encodes a putative nicotinic acetycholine receptor that, when knocked down in the class IV neurons, had severe dendritic defects. Namely, the coverage was less than half of that of wildtype controls. Nicotinic acetycholine receptors have a known role in the etiology of Alzheimer's disease, with Alzheimer's patients showing deficits in nicotinic acetycholine receptor production [238]. It would be interesting to see if the *nacrα-96ab* knockdown neurons degenerate over time. To do this, I would look at RNAi knockdown in first instar larvae compared to the effect in third instar larvae. This would allow us to determine if the dendritic defect developed over time and through development, or if the dendritic field never formed properly in the first place. Since the class IV neurons are a well-established model of dendritic development, it would be interesting to try and push the model forward to determine if the model could be extended to include Alzheimer's.

Task6 is a two pore potassium channel with a severe dendritic defect. Other members of the two pore potassium family are important in detecting stretch [239], indicating that the defects we see could be due to a failure to detect the growing size of the larval body. It would be interesting to look at the development of the defects in the RNAi mutants. If *Task6* is important in detecting the stretch of the membrane, I would predict that the dendritic coverage would be normal in younger instars, and deteriorate

as the larva grew older. Further analysis in to how the class IV dendritic defects is crucial for our understanding of how the ion channels govern dendritic development.

Lastly, it would be advantageous to develop genetic nulls for all of the RNAi lines. The genetic nulls would provide important verification of the RNAi phenotype.

7.5 Homeostatic hypothesis

We found that *Task6*, a two pore potassium channel, shows an insensitive phenotype to a noxious thermal stimulus, and a reduced dendritic field. Since knockdown of a two pore potassium channel would be predicted to cause hyperexcitability, we hypothesized that there was homeostatic regulation of the dendrititic field. If the dendritic field is being reduced due to a homeostatic mechanism, the signaling mechanism for homeostatic regulation could be electrical changes in the dendrites themselves, electrical changes in the axon, or circuit level feedback on the neuron. I have already eliminated the possibility that electrical changes in the axon are important for modulating the dendritic morphology.

If the homeostatic pruning is due to electrical changes in the dendrite, it might be possible to suppress the defect caused by *Task6* knockdown by over-expressing the human inwardly rectifying potassium channel *Kir2.1* specifically in the class IV neurons. I have generated *ppk*-GAL4;UAS-*dicer2*, UAS-*Task6* RNAi, UAS-*Kir2.1* animals, which I will test for rescue of the *Task6* phenotype. Endogenously, *Kir2.1* localizes to the

dendrites in rats [240], and overexpression of *Kir2.1* has been used to silence neurons in *Drosophila* [241]. In the central nervous system, over-expression of *Kir2.1* alone has been shown to homeostatically alter the dendritic field [202], indicating that this may be a promising way to suppress the dendritic defects in the *Task6* knockdown mutants.

When *Drosophila* larvae pupate, the class IV neurons undergo dendritic pruning, and are reformed during pupariation. A recent paper by Kanamori and colleagues has found that local calcium transients through voltage gated calcium channels are necessary for the dendritic pruning [242]. If knockdown of *Task6* increases neuronal excitability, it is possible that calcium transients through the voltage gated calcium channels are activated, causing premature pruning of the dendritic field. This hypothesis could be tested by knocking down voltage gated calcium channels in a *Task6* mutant, to see if the *Task6* dendritic phenotype is rescued.

7.6 Tool development

To increase the rapidity of the thermal nociception testing and screening, I would like to develop a probe with a feedback loop, so that the probe temperature would remain constant. The time taken to test large groups of larvae would decrease, since there would be no waiting for the probe to heat up or cool down to the appropriate temperature. This would make our thermal nociception paradigm more accurate and faster.

In my dissertation, I fabricated an instrument that allows for imaging genetically encoded calcium sensors during heat ramps. While using this device, we found that wildtype larvae rarely show calcium responses to the increase in temperature in the class IV neurons, even when the nociceptive threshold is crossed. One potential reason for this is that the ramping speed is relatively slow. To address this problem, I would decrease the size of the copper plate to be only slightly larger than the peltier device to allow for more rapid heating and cooling. Therefore, if a fast temperature ramp is necessary to produce a calcium response in the class IV neurons we would be able to look at the physiology more accurately.

7.7 Conclusion

My dissertation has set the groundwork for the characterization of several novel genes involved in thermal nociception. In addition to the thermal nociception screen, I have also developed a novel paradigm for testing behavioral responses to an ethologically relevant noxious stimulus, the parasitoid wasp. The tools, behavioral paradigms, and genes that I have discovered and developed during my thesis work are an excellent base for future studies in *Drosophila* nociception.

Appendix A

FBGN	VDRC Stock Number	CG Number	Gene
FBgn0026255	w[1118]; P{GD413}v1479	CG8681	clumsy
FBgn0259242	w[1118]; P{GD1165}v3292	CG42340	-
FBgn0032706	w[1118]; P{GD1764}v3886/TM3	CG10369	Irk3
FBgn0039081	w[1118]; P{GD203}v4341	CG4370	Irk2
FBgn0033755	w[1118]; P{GD1958}v4642/TM3	CG8594	ClC-b
FBgn0040238	w[1118]; P{GD2894}v5963/TM3	CG6264	Best1
FBgn0037950	w[1118]; P{GD2925}v6065	CG14723	HisCl1
FBgn0036566	w[1118]; P{GD1663}v6465	CG5284	ClC-c
FBgn0036566	w[1118]; P{GD1663}v6466	CG5284	-
FBgn0085425	w[1118]; P{GD2120}v6585/CyO	CG34396	-
FBgn0085425	w[1118]; P{GD2120}v6586	CG34396	-
FBgn0003429	w[1118]; P{GD244}v6723	CG10693	slo
FBgn0260971	w[1118]; P{GD3229}v7042	CG42594	-
FBgn0029761	w[1118]; P{GD3233}v7054/TM3	CG10706	SK
FBgn0039916	w[1118]; P{GD536}v7559	CG9935	-
FBgn0031634	w[1118]; P{GD891}v7842	CG15627	Ir25a
FBgn0020429	w1118; P{GD917}v7878	CG7234	GluRIIB
FBgn0038621	w[1118]; P{GD3048}v8302	CG10864	-
FBgn0037690	w[1118]; P{GD3628}v8564	CG9361	Task7
FBgn0037690	w[1118]; P{GD3628}v8565	CG9361	Task7
FBgn0038165	w[1118]; P{GD3931}v9073	CG9637	Task6
FBgn0000535	w[1118]; P{GD3363}v9126/TM3	CG10952	eag
FBgn0000535	w[1118]; P{GD3363}v9127	CG10952	eag
FBgn0085392	w[1118]; P{GD3495}v10268	CG34363	-
FBgn0259145	w[1118]; P{GD2159}v11817	CG42260	-
FBgn0039927	w1118; P{GD4652}v11963	CG11155	-
FBgn0035107	w[1118]; P{GD7508}v17043	CG1216	mri
FBgn0025394	w[1118]; P{GD7621}v18226	CG32810	inc
FBgn0037244	w[1118]; P{GD8390}v18297	CG14647	-
FBgn0039840	w[1118]; P{GD12622}v22854/TM3	CG11340	-
FBgn0003380	w[1118]; P{GD13718}v23671	CG12348	Sh
FBgn0003380	w[1118]; P{GD13718}v23673	CG12348	Sh
FBgn0029761	w[1118]; P{GD12601}v28155	CG10706	SK

FBgn0030529	w[1118]; P{GD12617}v28302/CyO	CG10997	clic
FBgn0030529	w[1118]; P{GD12617}v28303	CG10997	clic
FBgn0014462	w[1118]; P{GD13196}v28625	CG7779	Cng
FBgn0052704	w[1118]; P{GD15330}v29918/CyO	CG32704	Ir8a
FBgn0027589	w[1118]; P{GD3490}v30270/CyO	CG1688	-
FBgn0038839	w[1118]; P{GD7102}v31362	CG10830	-
FBgn0033558	w[1118]; P{GD1921}v37165/CyO	CG12344	-
FBgn0010399	w[1118]; P{GD2808}v37333	CG2902	Nmdar1
FBgn0010399	w[1118]; P{GD2808}v37334	CG2902	Nmdar1
FBgn0030303	w[1118]; P{GD4013}v37516	CG1756	-
FBgn0033494	w[1118]; P{GD7865}v38738	CG33135	KCNQ
FBgn0028422	w[1118]; P{GD3089}v40929	CG18039	KaiRIA
FBgn0017561	w[1118]; P{GD3306}v40953	CG1615	Ork1
FBgn0029090	w[1118]; P{GD3370}v40964	CG9176	cngl
FBgn0038837	w[1118] P{GD3677}v40985	CG3822	-
FBgn0085395	w[1118]; P{GD1033}v42770/TM3	CG34366	Shawl
FBgn0028431	w[1118]; P{GD3584}v42890	CG4481	Glu-RIB
FBgn0004619	w[1118]; P{GD3582}v44438	CG8442	Glu-RI
FBgn0004619	w[1118]; P{GD3582}v44439/CyO	CG8442	Glu-RI
FBgn0011589	w[1118]; P{GD3555}v45198/TM3	CG5076	elk
FBgn0037758	w[1118] P{GD14223}v45806	CG9467	-
FBgn0045073	w[1118]; P{GD16187}v47073	CG9126	Stim
FBgn0038840	w[1118]; P{GD3092}v47550	CG5621	-
FBgn0001203	w[1118]; P{GD15937}v47805	CG32688	Hk
FBgn0033257	w[1118]; P{GD1866}v47977	CG8713	-
FBgn0051201	w[1118]; P{GD16345}v49547	CG31201	GluRIIE
FBgn0051792	w[1118]; P{GD16483}v50152	CG31792	-
FBgn0052704	w[1118]; P{GD3293}v51067	CG32704	Ir8a
FBgn0046113	w[1118] P{GD796}v51438	CG4226	GluRIIC
FBgn0000039	w[1118]; P{GD236}v1194	CG6844	nAcRα-96Ab
FBgn0004118	w[1118]; P{GD237}v1199/TM3	CG6798	nAcRβ-96A
FBgn0004118	w[1118]; P{GD237}v1200	CG6798	nAcRβ-96A
FBgn0051065	w[1118]; P{GD317}v1268	CG31065	-
FBgn0039675	w[1118]; P{GD361}v1345/TM3	CG12048	ppk21
FBgn0039675	w[1118]; P{GD361}v1346	CG12048	ppk21
FBgn0039677	w[1118]; P{GD363}v1349/TM3	CG18110	-
FBgn0039677	w[1118]; P{GD363}v1351/TM3	CG18110	-

FBgn0029147	w[1118]; P{GD2144}v3479	CG6698	NtR
FBgn0028863	w[1118]; P{GD1734}v3839	CG4587	-
FBgn0028859	w[1118]; P{GD1738}v3849	CG12455	-
FBgn0085434	w[1118]; P{GD2219}v4061/TM3	CG9071	NaCP60E
FBgn0040697	w[1118]; P{GD2292}v4480	CG18676	Teh3
FBgn0261401	w[1118]; P{GD2701}v5327/CyO	CG42643	Ir75b/c
FBgn0001134	w[1118]; P{GD2702}v5329	CG7446	Grd
FBgn0037630	w[1118]; P{GD2868}v5820	CG11775	Ir85a
FBgn0260993	w[1118]; P{GD3392}v6132/TM3	CG9907	para
FBgn0010051	w[1118]; P{GD1676}v6486	CG1063	tp-r83A
FBgn0041195	w[1118]; P{GD1101}v6941	CG6504	Pkd2
FBgn0030989	w[1118]; P{GD1177}v6950	CG7537	inx5
FBgn0086693	w[1118]; P{GD3260}v7128	CG4536	iav
FBgn0031802	w[1118]; P{GD946}v7900	CG9499	ppk7
FBgn0031803	w[1118]; P{GD947}v7903	CG9501	ppk14
FBgn0036874	w[1118]; P{GD2731}v8424	CG9472	brv1
FBgn0022981	w[1118]; P{GD3621}v8549	CG1058	rpk
FBgn0027107	w[1118]; P{GD3692}v8638	CG17063	inx6
FBgn0027107	w[1118]; P{GD3692}v8639	CG17063	inx6
FBgn0039941	w[1118]; P{GD3721}v8677	CG17167	-
FBgn0040031	w[1118]; P{GD3722}v8681/TM3	CG12061	-
FBgn0036150	w[1118]; P{GD1661}v8957/TM3	CG6185	Ir68a
FBgn0032151	w[1118]; P{GD1045}v8889	CG4128	nAcRα-30D
FBgn0032151	w[1118]; P{GD1045}v8890	CG4128	nAcRα-30D
FBgn0034489	w[1118]; P{GD2102}v9004	CG11209	ppk6
FBgn0035604	w[1118]; P{GD2314}v9011	CG10633	Ir64a
FBgn0086350	w[1118]; P{GD3383}v9138	CG8961	tef
FBgn0053508	w[1118]; P{GD412}v9494	CG33508	ppk13
FBgn0028875	w[1118]; P{GD1138}v10330	CG32975	nAcRα-34E
FBgn0016041	w[1118]; P{GD5210}v13177	CG12157	Tom40
FBgn0016041	w[1118]; P{GD5210}v13178/TM3	CG12157	Tom40
FBgn0027106	w[1118]; P{GD12738}v22948	CG2977	inx7
FBgn0085387	w[1118]; P{GD12666}v26801	CG34358	shakB
FBgn0085387	w[1118]; P{GD12666}v26802/CyO	CG34358	shakB
FBgn0039839	w[1118]; P{GD3140}v30196	CG15555	-
FBgn0041233	w[1118]; P{GD2180}v31111	CG33151	Gr59E
FBgn0029846	w[1118]; P{GD7754}v31963	CG12544	Ca-α1T

FBgn0024177	w[1118]; P{GD2338}v33277	CG10125	zpg
FBgn0039679	w[1118]; P{GD14969}v36660/TM3	CG18287	ppk19
FBgn0035934	w[1118]; P{GD2375}v37249	CG5751	TrpA1
FBgn0069354	w[1118]; P{GD15043}v39107	CG17137	Porin2
FBgn0069354	w[1118]; P{GD15043}v39108	CG17137	Porin2
FBgn0040030	w[1118]; P{GD3723}v40987	CG2893	-
FBgn0036727	w[1118]; P{GD2692}v42582	CG7589	-
FBgn0260005	w[1118]; P{GD2850}v42620	CG31284	wtrw
FBgn0031220	w[1118]; P{GD776}v42730	CG4822	-
FBgn0031261	w[1118] P{GD787}v42740	CG11822	nAcRβ-21C
FBgn0028373	w[1118]; P{GD14965}v44767	CG1448	inx3
FBgn0024319	w[1118]; P{GD2039}v45920	CG8178	Nach
FBgn0036904	w[1118]; P{GD555}v45989	CG8743	trpml
FBgn0260453	w[1118]; P{GD17181}v46869/TM3	CG17140	-
FBgn0034885	w[1118]; P{GD17187}v46880	CG4019	-
FBgn0052792	w[1118]; P{GD15955}v47047	CG32792	-
FBgn0051105	w[1118]; P{GD15282}v47946/TM3	CG31105	-
FBgn0085387	w[1118]; P{GD15830}v48101	CG34358	shakB
FBgn0000036	w[1118]; P{GD16733}v48159	CG5610	nAcRα-96Aa
FBgn0053289	w[1118]; P{GD16046}v48289	CG33289	-
FBgn0003861	w[1118]; P{GD372}v1366	CG7875	trp
FBgn0031209	w[1118]; P{GD773}v2472	CG2657	Ir21a
FBgn0020445	w[1118]; P{GD866}v2620/CyO	CG3327	E23
FBgn0032166	w[1118]; P{GD1048}v2756/CyO	CG5853	-
FBgn0032145	w[1118]; P{GD1043}v2850/TM3	CG13121	-
FBgn0053513	w[1118]; P{GD1621}v3196/TM3	CG14793	Nmdar2
FBgn0002917	w[1118]; P{GD1172}v3306	CG1517	na
FBgn0002917	w[1118]; P{GD1172}v3307	CG1517	na
FBgn0085434	w[1118]; P{GD2219}v4062	CG9071	NaCP60E
FBgn0003710	w[1118]; P{GD2293}v4482	CG1232	tipE
FBgn0035785	w[1118]; P{GD2350}v5109/TM3	CG8546	-
FBgn0035785	w[1118]; P{GD2350}v5110	CG8546	-
FBgn0036414	w[1118]; P{GD2456}v5261	CG5842	nan
FBgn0005563	w[1118]; P{GD3326}v5551/CyO	CG1522	cac
FBgn0260993	w[1118]; P{GD3392}v6131	CG9907	para
FBgn0010051	w[1118]; P{GD1676}v6484	CG1063	Itp-r83A
FBgn0041195	w[1118]; P{GD1101}v6940	CG6504	Pkd2

FBgn0004646	w[1118]; P{GD3264}v7136	CG3039	ogre
FBgn0053349	w[1118]; P{GD1837}v7343	CG33349	ppk25
FBgn0035458	w[1118] P{GD2281}v7470	CG10858	-
FBgn0036829	w[1118]; P{GD2714}v7500	CG14076	Ir75d
FBgn0259188	w[1118]; P{GD3538}v8169	CG15327	Ir7d/e/f
FBgn0036937	w[1118]; P{GD2741}v8433/CyO	CG7385	Ir76b
FBgn0032593	w[1118]; P{GD539}v9337	CG5996	trpγ
FBgn0037212	w[1118]; P{GD3904}v11392	CG12414	nAcRα-80B
FBgn0032142	w[1118]; P{GD5237}v13211/TM3	CG13120	-
FBgn0051856	w[1118]; P{GD13169}v23114/CyO	CG31856	-
FBgn0085398	w[1118]; P{GD13468}v23391	CG34369	-
FBgn0033074	w[1118]; P{GD13779}v23764/TM3	CG8330	tomboy40
FBgn0260453	w[1118]; P{GD8697}v25052/CyO	CG17140	-
FBgn0037238	w[1118]; P{GD12612}v26783	CG1090	-
FBgn0259822	w[1118]; P{GD11888}v27581	CG42403	Ca-β
FBgn0003996	w[1118]; P{GD14981}v30033	CG2759	w
FBgn0083959	w[1118]; P{GD4541}v30610	CG34123	TrpM
FBgn0000037	w[1118]; P{GD630}v33123	CG4356	mAcR-60C
FBgn0034882	w[1118]; P{GD2183}v33257	CG5398	-
FBgn0083959	w[1118]; P{GD9986}v33669/CyO	CG34123	TrpM
FBgn0000038	w[1118]; P{GD15409}v33824	CG11348	nAcRβ-64B
FBgn0039676	w[1118]; P{GD14968}v36659	CG7577	ppk20
FBgn0035934	w[1118]; P{GD2375}v37250/TM3	CG5751	TrpA1
FBgn0010240	w[1118]; P{GD3384}v37408	CG17336	Lcch3
FBgn0028373	w[1118]; P{GD14965}v39095	CG1448	inx3
FBgn0028875	w[1118]; P{GD15691}v39411	CG32975	nAcRα-34E
FBgn0030385	w[1118]; P{GD3331}v39576	CG15732	Ir11a
FBgn0040030	w[1118]; P{GD3723}v40988	CG2893	-
FBgn0004244	w[1118]; P{GD4609}v41101/CyO	CG10537	Rdl
FBgn0039424	w[1118]; P{GD569}v42521/TM3	CG14239	-
FBgn0010240	w[1118]; P{GD3384}v42546	CG17336	Lcch3
FBgn0036727	w[1118]; P{GD2692}v42580/TM3	CG7589	-
FBgn0260005	w[1118]; P{GD2850}v42617	CG31284	wtrw
FBgn0031220	w[1118]; P{GD776}v42729	CG4822	-
FBgn0020762	w[1118]; P{GD883}v42750	CG2969	Atet
FBgn0029079	w[1118]; P{GD11473}v43788	CG4924	icln
FBgn0030795	w[1118]; P{GD3398}v44412	CG4805	ppk28

FBgn0037501	w[1118]; P{GD2844}v44548	CG10101	Ir84a
FBgn0040842	w[1118]; P{GD3848}v44953/TM3	CG15212	-
FBgn0030031	w[1118]; P{GD15293}v45062/TM3	CG2156	-
FBgn0024319	w[1118]; P{GD2039}v45921	CG8178	Nach
FBgn0036904	w[1118]; P{GD555}v45988/CyO	CG8743	trpml
FBgn0027107	w[1118]; P{GD16939}v46398	CG17063	inx6
FBgn0260453	w[1118]; P{GD17181}v46870	CG17140	-
FBgn0034885	w[1118]; P{GD17187}v46879	CG4019	-
FBgn0029846	w[1118]; P{GD3252}v48009	CG15899	Ca-α1T
FBgn0000036	w[1118]; P{GD16733}v48162	CG5610	nAcRα-96Aa
FBgn0034883	w[1118]; P{GD16877}v49978	CG17664	-
FBgn0029079	w[1118]; P{GD16277}v50123	CG4924	icln
FBgn0053348	w[1118]; P{GD16072}v51193	CG33348	CheB42a
FBgn0053348	w[1118] P{GD16072}v51194	CG33348	CheB42a
FBgn0028704	w[1118] P{GD1040}v51459	CG18660	Nckx30C
FBgn0001991	w[1118]; P{GD1737}v51491	CG4894	Ca-α1D
FBgn0028704	w[1118]; P{GD1040}v51877	CG18660	Nckx30C
FBgn0015872	w[1118]; P{GD1936}v51936/TM3	CG9023	Drip
FBgn0001991	w[1118]; P{GD1737}v52644/TM3	CG4894	Ca-α1D
FBgn0029761	w[1118]; P{KK107699}v103985	CG10706	SK
FBgn0033755	w[1118]; P{KK100840}v103420	CG8594	-
FBgn0005614	w[1118]; P{KK106424}v104450	CG18345	trpl
FBgn0051792	w[1118]; P{KK104760}v107237	CG31792	-
FBgn0034730	w[1118]; P{KK101805}v105131	CG10972	ppk12
FBgn0034884	w[1118]; P{KK112650}v104067	CG17662	-
FBgn0031362	w[1118]; P{KK106103}v100378	CG17646	-
FBgn0028875	w[1118]; P{KK109791}v101820	CG32975	nAcRα-34E
FBgn0032593	w[1118]; P{KK107656}v105280	CG5996	trpγ
FBgn0003011	w[1118]; P{KK106461}v107363	CG7411	ort
FBgn0029966	w[1118]; P{GD3524}v8152/CyO	CG15324	Ir7c
FBgn0014462	w[1118]; P{KK108314}v101745	CG7779	Cng
FBgn0005614	w[1118]; P{GD12722}v35571	CG18345	trpl
FBgn0005563	w[1118]; P{KK101478}v104168	CG1522	cac
FBgn0005564	w[1118]; P{KK100264}v103363	CG9262	Shal
FBgn0031261	w[1118]; P{KK110036}v101868	CG11822	nAcRβ-21C
FBgn0020429	w[1118]; P{KK105825}v105581	CG7234	GluRIIB
FBgn0037950	w[1118]; P{KK112578}v104966	CG14723	HisCl1

FBgn0004244	w[1118]; P{KK104293}v100429	CG10537	Rdl
FBgn0036566	w[1118]; P{KK109221}v106844	CG5284	-
FBgn0016920	w[1118]; P{KK105819}v105579	CG11020	nompC
FBgn0024319	w[1118]; P{KK108198}v106647	CG8178	Nach
FBgn0085398	w[1118]; P{KK112456}v104952	CG34369	-
FBgn0259215	w[1118]; P{KK103661}v100837	CG42315	Ir93a
FBgn0040333	w[1118]; P{KK106574}v101019	CG13762	brv3
FBgn0067311	w[1118]; P{KK111534}v104635	CG33321	CheB38b
FBgn0037501	w[1118]; P{KK103985}v101238	CG10101	Ir84a
FBgn0036829	w[1118]; P{KK105293}v106286	CG14076	Ir75d
FBgn0039679	w[1118]; P{KK105267}v107638/CyO	CG18287	ppk19
FBgn0046113	w[1118]; P{KK107050}v101180/CyO	CG4226	GluRIIC
FBgn0027106	w[1118]; P{KK112684}v103256/CyO	CG2977	inx7
FBgn0053289	w[1118]; P{KK105372}v101664	CG33289	-
FBgn0001203	w[1118]; P{KK109058}v101402	CG32688	Hk
FBgn0051065	w[1118]; P{KK110745}v106385	CG31065	-
FBgn0030303	w[1118]; P{KK109309}v101483	CG1756	-
FBgn0039927	w[1118]; P{KK105030}v100883	CG11155	-
FBgn0020445	w[1118]; P{KK113210}v105055	CG3327	E23
FBgn0027108	w[1118]; P{KK111067}v102194	CG4590	inx2
FBgn0024963	w[1118]; P{KK109167}v105754	CG7535	GluClα
FBgn0085395	w[1118]; P{KK106451}v100980	CG34366	-
FBgn0030529	w[1118]; P{KK101604}v105975	CG10997	Clic
FBgn0085425	w[1118]; P{KK104335}v100436	CG34396	-
FBgn0036727	w[1118]; P{KK112026}v102570	CG7589	-
FBgn0051201	w[1118]; P{KK112790}v103530	CG31201	GluRIIE
FBgn0032167	w[1118]; P{KK108593}v100782	CG5853	-
FBgn0033494	w[1118]; P{KK109039}v106655	CG33135	KCNQ
FBgn0033074	w[1118]; P{KK104751}v105557	CG8330	tomboy40
FBgn0003353	w[1118]; P{GD2196}v3606/TM3	CG3182	sei
FBgn0010399	w[1118]; P{KK107519}v104773	CG2902	Nmdar1
FBgn0029079	w[1118]; P{KK105587}v101268	CG4924	icln
FBgn0000037	w[1118]; P{KK109077}v101407	CG4356	mAcR-60C
FBgn0035107	w[1118]; P{KK108441}v101345	CG1216	mri
FBgn0086693	w[1118]; P{KK107960}v100701	CG4536	iav

FBgn0004620	w[1118]; P{KK105437}v101686	CG6992	GluRIIA
FBgn0032151	w[1118]; P{KK103877}v101571	CG4128	nAcRα-30D
FBgn0086778	w[1118]; P{KK108471}v100756	CG32538	gfA
FBgn0259242	w[1118]; P{KK109734}v104521	CG42340	-
FBgn0039916	w[1118]; P{KK111536}v102351	CG9935	-
FBgn0031634	w[1118]; P{KK106802}v106731	CG15627	Ir25a
FBgn0030385	w[1118]; P{KK104276}v100422	CG15732	Ir11a
FBgn0260874	w[1118]; P{KK104048}v101590	CG42584	Ir76a
FBgn0004363	w[1118]; P{KK107645}v101336	CG6647	porin
FBgn0031802	w[1118]; P{KK104094}v100643	CG9499	ppk7
FBgn0033017	w[1118]; P{KK105756}v107131	CG10465	-
FBgn0053348	w[1118]; P{KK112784}v106020	CG33348	CheB42a
FBgn0032706	w[1118]; P{KK107031}v101174	CG10369	Irk3
FBgn0020762	w[1118]; P{KK104214}v100404	CG2969	Atet
FBgn0034885	w[1118]; P{KK113252}v107980	CG4019	-
FBgn0030707	w[1118]; P{KK105273}v101633	CG8916	-
FBgn0037690	w[1118]; P{KK102756}v106135	CG9361	Task7
FBgn0045073	w[1118]; P{KK102366}v106256	CG9126	Stim
FBgn0261401	w[1118]; P{KK105422}v101682	CG42643	Ir75b/c
FBgn0260005	w[1118]; P{KK103625}v107423	CG31284	wtrw
FBgn0034489	w[1118]; P{KK106876}v101091	CG11209	ppk6
FBgn0003353	w[1118]; P{KK105733}v104698	CG3182	sei
FBgn0259822	w[1118]; P{KK108900}v105748	CG42403	Ca-β
FBgn0017561	w[1118]; P{KK107843}v104883	CG1615	Ork1
FBgn0035785	w[1118]; P{KK103619}v100834	CG8546	-
FBgn0030844	w[1118]; P{KK110717}v106873	CG8527	ppk23
FBgn0051105	w[1118]; P{KK110744}v106384	CG31105	-
FBgn0015872	w[1118]; P{KK107343}v106911/CyO	CG9023	Drip
FBgn0028431	w[1118]; P{KK104241}v106269	CG4481	Glu-RIB
FBgn0041233	w[1118]; P{KK103101}v103954	CG33151	Gr59e
FBgn0032145	w[1118]; P{KK113051}v105199	CG13121	-
FBgn0039675	w[1118]; P{KK104787}v107892	CG12048	ppk21
FBgn0038621	w[1118]; P{KK104447}v107858	CG10864	-
FBgn0035113	w[1118]; P{KK104597}v107870/CyO	CG17142	pyx
FBgn0003380	w[1118]; P{KK109112}v104474	CG12348	Sh

FBgn0066292	w[1118]; P{GD13381}v23314	CG33350	CheB42c
FBgn0034656	w[1118]; P{KK105029}v100882	CG17922	-
FBgn0039061	w[1118]; P{KK102249}v107389	CG6747	Ir
FBgn0003429	w[1118]; P{KK108671}v104421	CG10693	slo
FBgn0053349	w[1118]; P{KK109736}v101808	CG33349	ppk25
FBgn0065109	w[1118]; P{KK106798}v107741	CG34058	ppk11
FBgn0022981	w[1118]; P{KK104901}v105463	CG1058	rpk
FBgn0039839	w[1118]; P{KK113354}v102923	CG15555	-
FBgn0066292	w[1118]; P{KK112212}v105947	CG33350	CheB42c
FBgn0260993	w[1118]; P{KK108534}v104775	CG9907	para
FBgn0259246	w[1118]; P{KK109701}v107748	CG42344	brp
FBgn0000535	w[1118]; P{KK107309}v100260	CG10952	eag
FBgn0031220	w[1118]; P{KK106446}v105922/CyO	CG4822	-
FBgn0036542	w[1118]; P{KK112646}v103247	CG33989	pHCl
FBgn0000039	w[1118]; P{KK109442}v101760	CG6844	nAcRα-96Ab
FBgn0034883	w[1118]; P{KK109956}v101847	CG17664	-
FBgn0036414	w[1118]; P{KK103594}v100090	CG5842	nan
FBgn0029733	w[1118]; P{KK104726}v104345	CG6927	-
FBgn0039677	w[1118]; P{KK104053}v105896	CG18110	-
FBgn0015519	w[1118]; P{KK109718}v101806	CG2302	nAcRα-7E
FBgn0033558	w[1118]; P{KK112723}v103271	CG12344	-
FBgn0030989	w[1118]; P{KK103391}v102814	CG7537	inx5
FBgn0085434	w[1118]; P{KK105476}v101695	CG9071	NaCP60E
FBgn0026255	w[1118]; P{KK104645}v105870	CG8681	clumsy
FBgn0004646	w[1118]; P{KK104770}v103816	CG3039	ogre
FBgn0066293	w[1118]; P{KK112377}v103796	CG33351	CheB42b
FBgn0000180	w[1118]; P{KK112898}v103327	CG4722	bib
FBgn0065108	w[1118]; P{GD12781}v22989	CG34059	ppk16
FBgn0002917	w[1118]; P{KK102435}v103754	CG1517	na
FBgn0034636	y[1] v[1]; P{TRiP.JF01867}attP2	CG10440	-
FBgn0035192	y[1] v[1]; P{TRiP.JF01941}attP2	CG9194	-
FBgn0065110	y[1] v[1]; P{TRiP.JF02565}attP2	CG34042	ppk10
FBgn0011286	y[1] v[1]; P{TRiP.JF03381}attP2	CG10844	Rya-r44F
FBgn0003383	y[1] v[1]; P{TRiP.JF01823}attP2	CG1066	Shab
FBgn0003386	y[1] v[1]; P{TRiP.JF02982}attP2	CG2822	Shaw
FBgn0261041	y[1] v[1]; P{TRiP.JF01825}attP2	CG12295	stj

Appendix B

Gene Name	Predicted Function	Nociceptor Specific?	Downstream of transduction?	Dendrite defect?
abednego	glycine-gated channel	Yes	No	No
nAcRα-96Ab	nicotinic acetycholine receptor	Yes	No	Yes
Ir7c	glutamate-gated channel	No	N/A	No
meshach	DEG/ENaC	Yes	No	No
shadrach	DEG/ENaC	Yes	Mild	No
paralytic	voltage-gated sodium channel	Yes	Yes	No
dTRPA1	TRPA	Yes	Mild	No
pyrexia	TRPA	No	N/A	No
nanchung	TRPV	No	N/A	Yes
Task6	two-pore potassium channel	Yes	No	Yes
Irk3	inward rectifying potassium channel	Yes	No	Yes
slowpoke	calcium-activated potassium channel	No	N/A	No
coyotemint	ABC transporter	No	N/A	Yes
bruchpilot	coiled coil protein	No	N/A	Yes

Appendix C

Abbreviation	Full Name
LH	Leptopilina heterotoma
LB	Leptopilina boulardi
GWAS	Genome-wide association study
SNP	single nucleotide polymorphism
RNAi	RNA interference
siRNA	small interfering RNA
NEL	nocifensive escape locomotion
FEPS	familial episodic pain syndrome
TRP	transient receptor potential
DEG/ENaC	Degenerin epithelial channel
AITC	allyl isothiocyanate
BITC	benzy isothiocyanate
ppk	pickpocket
ASIC	acid-sensing ion channel
DRG	dorsal root ganglion
md	multidendritic
Kat60-L1	Katanin p60-Like1
TNT	tetanus toxin light chain
Bc	Black cells
VLP	virus-like particles
UAS	upstream activating sequence
TRiP	Transgenic RNAi Project
VDRC	Vienna Drosophila Research Center
dsRNA	double stranded RNA
nan	nanchung
AHP	after hyperpolarization
ROI	region of interest
es	external sensory
nAChR	nicotinic acetycholine receptor

References

1. *Relieving pain in America: A blueprint for transforming prevention, care, education and research.*, in *National Academies Press*, N.R. Council, Editor 2011.

2. Katon, W., K. Egan, and D. Miller, *CHRONIC PAIN - LIFETIME PSYCHIATRIC DIAGNOSES AND FAMILY HISTORY.* American Journal of Psychiatry, 1985. **142**(10): p. 1156-1160.

3. Cheatle, M.D., *Depression, Chronic Pain, and Suicide by Overdose: On the Edge.* Pain Medicine, 2011. **12**: p. S43-S48.

4. Stewart, W.F., et al., *Lost Productive Time and Cost Due to Common Pain Conditions in the US Workforce.* JAMA: The Journal of the American Medical Association, 2003. **290**(18): p. 2443-2454.

5. Kavaliers, M., *Evolutionary and comparative aspects of nociception.* Brain Research Bulletin, 1988. **21**(6): p. 923-931.

6. Malafoglia, V., et al., *The zebrafish as a model for nociception studies.* Journal of cellular physiology, 2013. **228**(10): p. 1956-66.

7. Adwanikar, H., F. Karim, and R.W. Gereau, *Inflammation persistently enhances nocifensive behaviors mediated spinal group I mGluRs through sustained ERK activation.* Pain, 2004. **111**(1-2): p. 125-135.

8. Hwang, R.Y., et al., *Nociceptive neurons protect Drosophila larvae from parasitoid wasps.* Current Biology, 2007. **17**(24): p. 2105-2116.

9. Kremeyer, B., et al., *A gain-of-function mutation in TRPA1 causes familial episodic pain syndrome.* Neuron, 2010. **66**(5): p. 671-80.

10. Cox, J.J., et al., *An SCN9A channelopathy causes congenital inability to experience pain.* Nature, 2006. **444**(7121): p. 894-898.

11. Kim, H., et al., *Genome-wide association study of acute post-surgical pain in humans.* Pharmacogenomics, 2009. **10**(2): p. 171-179.

12. Peters, M.J., et al., *Genome-wide association study meta-analysis of chronic widespread pain: evidence for involvement of the 5p15.2 region.* Annals of the Rheumatic Diseases, 2013. **72**(3): p. 427-436.

13. Neely, G.G., et al., *A Genome-wide Drosophila Screen for Heat Nociception Identifies ±2´3 as an Evolutionarily Conserved Pain Gene.* Cell, 2010. **143**(4): p. 628-638.

14. Mogil, J.S., et al., *Heritability of nociception I: Responses of 11 inbred mouse strains on 12 measures of nociception.* Pain, 1999. **80**(1–2): p. 67-82.

15. Mogil, J.S., et al., *Heritability of nociception II. 'Types' of nociception revealed by genetic correlation analysis.* Pain, 1999. **80**(1-2): p. 83-93.

16. Tracey, W.D., et al., *painless, a Drosophila gene essential for nociception.* Cell, 2003. **113**(2): p. 261-273.

17. Zhong, L., R.Y. Hwang, and W.D. Tracey, *Pickpocket Is a DEG/ENaC Protein Required for Mechanical Nociception in Drosophila Larvae.* Current Biology, 2010. **20**(5): p. 429-434.

18. Zhong, L., et al., *Thermosensory and Nonthermosensory Isoforms of Drosophila melanogaster TRPA1 Reveal Heat-Sensor Domains of a ThermoTRP Channel.* Cell Reports, 2012. **1**(1): p. 43-55.

19. Dietzl, G., et al., *A genome-wide transgenic RNAi library for conditional gene inactivation in Drosophila.* Nature, 2007. **448**(7150): p. 151-6.

20. Hannon, G.J., *RNA interference.* Nature, 2002. **418**(6894): p. 244-251.

21. Aldrich, B.T., et al., *The amnesiac gene is involved in the regulation of thermal nociception in Drosophila melanogaster.* J Neurogenet, 2010. **24**(1): p. 33-41.

22. Xu, S.Y., et al., *Thermal nociception in adult Drosophila: behavioral characterization and the role of the painless gene.* Genes, Brain and Behavior, 2006. **5**(8): p. 602-613.

23. Im, S.H. and M.J. Galko, *Pokes, sunburn, and hot sauce: Drosophila as an emerging model for the biology of nociception.* Developmental Dynamics, 2011: p. n/a-n/a.

24. Lee, M.J., et al., *Virulence Factors and Strategies of Leptopilina spp.: Selective Responses in Drosophila Hosts*, in *Advances in Parasitology, Vol 70*. 2009, Elsevier Academic Press Inc: San Diego. p. 123-+.

25. Schlenke, T.A., et al., *Contrasting Infection Strategies in Generalist and Specialist Wasp Parasitoids of Drosophila melanogaster.* PLoS Pathog, 2007. **3**(10): p. e158.

26. Milan, Neil F., Balint Z. Kacsoh, and Todd A. Schlenke, *Alcohol Consumption as Self-Medication against Blood-Borne Parasites in the Fruit Fly.* Current Biology, 2012. **22**(6): p. 488-493.

27. Bohlen, C.J., et al., *A heteromeric Texas coral snake toxin targets acid-sensing ion channels to produce pain.* Nature, 2011. **479**(7373): p. 410-414.

28. Caterina, M.J., et al., *The capsaicin receptor: a heat-activated ion channel in the pain pathway.* Nature, 1997. **389**(6653): p. 816-24.

29. Cho, H., et al., *The calcium-activated chloride channel anoctamin 1 acts as a heat sensor in nociceptive neurons.* Nat Neurosci, 2012. **15**(7): p. 1015-21.

30. Cox, J.J., et al., *Congenital insensitivity to pain: novel SCN9A missense and in-frame deletion mutations.* Hum Mutat, 2010. **31**(9): p. E1670-86.

31. Cummins, T.R., S.D. Dib-Hajj, and S.G. Waxman, *Electrophysiological properties of mutant Nav1.7 sodium channels in a painful inherited neuropathy.* J Neurosci, 2004. **24**(38): p. 8232-6.

32. Cummins, T.R., P.L. Sheets, and S.G. Waxman, *The roles of sodium channels in nociception: Implications for mechanisms of pain.* Pain, 2007. **131**(3): p. 243-57.

33. Davis, J.B., et al., *Vanilloid receptor-1 is essential for inflammatory thermal hyperalgesia.* Nature, 2000. **405**(6783): p. 183-7.

34. Decker, M.W. and M.D. Meyer, *Therapeutic potential of neuronal nicotinic acetylcholine receptor agonists as novel analgesics.* Biochemical Pharmacology, 1999. **58**(6): p. 917-923.

35. Fertleman, C.R., et al., *SCN9A mutations in paroxysmal extreme pain disorder: allelic variants underlie distinct channel defects and phenotypes.* Neuron, 2006. **52**(5): p. 767-74.

36. Hwang, R.Y., N.A. Stearns, and W.D. Tracey, *The ankyrin repeat domain of the TRPA protein painless is important for thermal nociception but not mechanical nociception.* PLoS One, 2012. **7**(1): p. e30090.

37. Kindler, C.H. and C.S. Yost, *Two-pore domain potassium channels: New sites of local anesthetic action and toxicity.* Regional Anesthesia and Pain Medicine, 2005. **30**(3): p. 260-274.

38. Klein, C.J., et al., *Chronic pain as a manifestation of potassium channel-complex autoimmunity.* Neurology, 2012. **79**(11): p. 1136-1144.

39. Neely, G.G., et al., *<italic>TrpA1</italic> Regulates Thermal Nociception in <italic>Drosophila</italic>.* PLoS ONE, 2011. **6**(8): p. e24343.

40. Patel, A.J., et al., *Inhalational anesthetics activate two-pore-domain background K+ channels.* Nature Neuroscience, 1999. **2**(5): p. 422-426.

41. Rasband, M.N., et al., *Distinct potassium channels on pain-sensing neurons.* Proceedings of the National Academy of Sciences, 2001. **98**(23): p. 13373-13378.

42. Xu, H., et al., *TRPV3 is a calcium-permeable temperature-sensitive cation channel.* Nature, 2002. **418**(6894): p. 181-186.

43. Yang, Y., et al., *Mutations in SCN9A, encoding a sodium channel alpha subunit, in patients with primary erythermalgia.* Journal of Medical Genetics, 2004. **41**(3): p. 171-174.

44. Milkman, R., *An Escherichia coli homologue of eukaryotic potassium channel proteins.* Proc Natl Acad Sci U S A, 1994. **91**(9): p. 3510-4.

45. Martinac, B., Y. Saimi, and C. Kung, *Ion Channels in Microbes.* Physiological Reviews, 2008. **88**(4): p. 1449-1490.

46. Kang, K., et al., *Analysis of Drosophila TRPA1 reveals an ancient origin for human chemical nociception.* Nature, 2010. **464**(7288): p. 597-600.

47. Waxman, S.G., *Channelopathic Pain: A Growing but Still Small List of Model Disorders.* Neuron, 2010. **66**(5): p. 622-624.

48. Kremeyer, B., et al., *A Gain-of-Function Mutation in TRPA1 Causes Familial Episodic Pain Syndrome.* Neuron, 2010. **66**(5): p. 671-680.

49. Neely, G.G., et al., *A Genome-wide Drosophila Screen for Heat Nociception Identifies Î±2Î´3 as an Evolutionarily Conserved Pain Gene.* Cell, 2010. **143**(4): p. 628-638.

50. Zhong, L., et al., *Thermosensory and Nonthermosensory Isoforms of Drosophila melanogaster TRPA1 Reveal Heat-Sensor Domains of a ThermoTRP Channel.* 2012.

51. Gallio, M., et al., *The Coding of Temperature in the Drosophila Brain.* Cell, 2011. **144**(4): p. 614-624.

52. Kim, J., et al., *A TRPV family ion channel required for hearing in Drosophila.* Nature, 2003. **424**(6944): p. 81-84.

53. Liedtke, W., et al., *Mammalian TRPV4 (VR-OAC) directs behavioral responses to osmotic and mechanical stimuli in Caenorhabditis elegans.* Proceedings of the National Academy of Sciences of the United States of America, 2003. **100**(Suppl 2): p. 14531-14536.

54. Liu, L., et al., *Drosophila hygrosensation requires the TRP channels water witch and nanchung.* Nature, 2007. **450**(7167): p. 294-298.

55. McKemy, D.D., W.M. Neuhausser, and D. Julius, *Identification of a cold receptor reveals a general role for TRP channels in thermosensation.* Nature, 2002. **416**(6876): p. 52-58.

56. Montell, C. and G.M. Rubin, *Molecular characterization of the drosophila trp locus: A putative integral membrane protein required for phototransduction.* Neuron, 1989. **2**(4): p. 1313-1323.

57. Niemeyer, B.A., et al., *The Drosophila Light-Activated Conductance Is Composed of the Two Channels TRP and TRPL.* Cell, 1996. **85**(5): p. 651-659.

58. Peier, A.M., et al., *A TRP Channel that Senses Cold Stimuli and Menthol.* Cell, 2002. **108**(5): p. 705-715.

59. Sidi, S., R.W. Friedrich, and T. Nicolson, *NompC TRP Channel Required for Vertebrate Sensory Hair Cell Mechanotransduction.* Science, 2003. **301**(5629): p. 96-99.

60. Smith, G.D., et al., *TRPV3 is a temperature-sensitive vanilloid receptor-like protein.* Nature, 2002. **418**(6894): p. 186-190.

61. Story, G.M., et al., *ANKTM1, a TRP-like Channel Expressed in Nociceptive Neurons, Is Activated by Cold Temperatures.* Cell, 2003. **112**(6): p. 819-829.

62. Walker, R.G., A.T. Willingham, and C.S. Zuker, *A Drosophila Mechanosensory Transduction Channel.* Science, 2000. **287**(5461): p. 2229-2234.

63. Hoenderop, J.G.J., et al., *Homo- and heterotetrameric architecture of the epithelial Ca2+ channels TRPV5 and TRPV6.* EMBO J, 2003. **22**(4): p. 776-785.

64. Al-Anzi, B., W.D. Tracey Jr, and S. Benzer, *Response of Drosophila to Wasabi Is Mediated by painless, the Fly Homolog of Mammalian TRPA1/ANKTM1.* Current Biology, 2006. **16**(10): p. 1034-1040.

65. Firsov, D., et al., *The heterotetrameric architecture of the epithelial sodium channel (ENaC).* EMBO J, 1998. **17**(2): p. 344-352.

66. Kosari, F., et al., *Subunit Stoichiometry of the Epithelial Sodium Channel.* Journal of Biological Chemistry, 1998. **273**(22): p. 13469-13474.

67. Mano, I. and M. Driscoll, *DEG/ENaC channels: A touchy superfamily that watches its salt.* Bioessays, 1999. **21**(7): p. 568-578.

68. Gessmann, R., et al., *Molecular Modeling of Mechanosensory Ion Channel Structural and Functional Features.* Plos One, 2010. **5**(9): p. e12814.

69. Price, M.P., et al., *The DRASIC cation channel contributes to the detection of cutaneous touch and acid stimuli in mice.* Neuron, 2001. **32**(6): p. 1071-83.

70. Chen, C.-C., et al., *A role for ASIC3 in the modulation of high-intensity pain stimuli.* Proceedings of the National Academy of Sciences, 2002. **99**(13): p. 8992-8997.

71. Kang, S., et al., *Simultaneous Disruption of Mouse <italic>ASIC1a, ASIC2</italic> and <italic>ASIC3</italic> Genes Enhances Cutaneous Mechanosensitivity.* PLoS ONE, 2012. **7**(4): p. e35225.

72. Kim, S.E., et al., *The role of Drosophila Piezo in mechanical nociception.* Nature, 2012. **483**(7388): p. 209-212.

73. Coste, B., et al., *Piezo1 and Piezo2 Are Essential Components of Distinct Mechanically Activated Cation Channels.* Science, 2010. **330**(6000): p. 55-60.

74. Coste, B., et al., *Piezo proteins are pore-forming subunits of mechanically activated channels.* Nature, 2012. **483**(7388): p. 176-U72.

75. *Principles of Neural Science*, ed. Eric Kandel, et al. 2000: McGraw Hill Medical Publishing Division

76. Tobin, D.M. and C.I. Bargmann, *Invertebrate nociception: Behaviors, neurons and molecules.* Journal of Neurobiology, 2004. **61**(1): p. 161-174.

77. Grueber, W.B., L.Y. Jan, and Y.N. Jan, *Tiling of the Drosophila epidermis by multidendritic sensory neurons.* Development, 2002. **129**(12): p. 2867-2878.

78. Grueber, W.B., et al., *Projections of Drosophila multidendritic neurons in the central nervous system: links with peripheral dendrite morphology.* Development, 2007. **134**(1): p. 55-64.

79. Hughes, C.L. and J.B. Thomas, *A sensory feedback circuit coordinates muscle activity in Drosophila.* Molecular and Cellular Neuroscience, 2007. **35**(2): p. 383-396.

80. Song, W., et al., *Peripheral multidendritic sensory neurons are necessary for rhythmic locomotion behavior in Drosophila larvae.* Proceedings of the National Academy of Sciences of the United States of America, 2007. **104**(12): p. 5199-5204.

81. Nagel, G., et al., *Channelrhodopsin-2, a directly light-gated cation-selective membrane channel.* Proceedings of the National Academy of Sciences, 2003. **100**(24): p. 13940-13945.

82. Boyden, E.S., et al., *Millisecond-timescale, genetically targeted optical control of neural activity.* Nature Neuroscience, 2005. **8**(9): p. 1263-1268.

83. Williams, D.W. and J.W. Truman, *Cellular mechanisms of dendrite pruning in Drosophila: insights from in vivo time-lapse of remodeling dendritic arborizing sensory neurons.* Development, 2005. **132**(16): p. 3631-3642.

84. Parrish, J.Z., et al., *The microRNA bantam Functions in Epithelial Cells to Regulate Scaling Growth of Dendrite Arbors in Drosophila Sensory Neurons.* Neuron, 2009. **63**(6): p. 788-802.

85. Andersen, R., et al., *Calcium/Calmodulin-Dependent Protein Kinase II Alters Structural Plasticity and Cytoskeletal Dynamics in Drosophila.* The Journal of Neuroscience, 2005. **25**(39): p. 8878-8888.

86. Jan, Y.-N. and L.Y. Jan, *Branching out: mechanisms of dendritic arborization.* Nat Rev Neurosci, 2010. **11**(5): p. 316-328.

87. Moore, A.W., L.Y. Jan, and Y.N. Jan, *hamlet, a Binary Genetic Switch Between Single- and Multiple- Dendrite Neuron Morphology.* Science, 2002. **297**(5585): p. 1355-1358.

88. Shima, Y., et al., *Opposing roles in neurite growth control by two seven-pass transmembrane cadherins.* Nat Neurosci, 2007. **10**(8): p. 963-969.

89. Williams, D.W. and D. Shepherd, *Persistent larval sensory neurons in adult Drosophila melanogaster.* Journal of Neurobiology, 1999. **39**(2): p. 275-286.

90. Bodmer, R. and Y.N. Jan, *Morphological differentiation of the embryonic peripheral neurons in Drosophila.* Development Genes and Evolution, 1987. **196**(2): p. 69-77.

91. Jinushi-Nakao, S., et al., *Knot/Collier and cut control different aspects of dendrite cytoskeleton and synergize to define final arbor shape.* Neuron, 2007. **56**(6): p. 963-78.

92. Grueber, W.B., L.Y. Jan, and Y.N. Jan, *Different levels of the homeodomain protein cut regulate distinct dendrite branching patterns of Drosophila multidendritic neurons.* Cell, 2003. **112**(6): p. 805-818.

93. Stewart, A., et al., *Katanin p60-like1 Promotes Microtubule Growth and Terminal Dendrite Stability in the Larval Class IV Sensory Neurons of Drosophila.* Journal of Neuroscience, 2012. **32**(34): p. 11631-11642.

94. Zheng, Y., et al., *Dynein is required for polarized dendritic transport and uniform microtubule orientation in axons.* Nature Cell Biology, 2008. **10**(10): p. 1172-1180.

95. Satoh, D., et al., *Spatial control of branching within dendritic arbors by dynein-dependent transport of Rab5-endosomes.* Nature Cell Biology, 2008. **10**(10): p. 1164-1171.

96. Hughes, M.E., et al., *Homophilic Dscam Interactions Control Complex Dendrite Morphogenesis.* Neuron, 2007. **54**(3): p. 417-427.

97. Matthews, B.J., et al., *Dendrite self-avoidance is controlled by Dscam.* Cell, 2007. **129**(3): p. 593-604.

98. Soba, P., et al., *Drosophila sensory neurons require Dscam for dendritic self-avoidance and proper dendritic field organization.* Neuron, 2007. **54**(3): p. 403-416.

99. Emoto, K., et al., *Control of dendritic branching and tiling by the Tricornered-kinase/Furry signaling pathway in Drosophila sensory neurons.* Cell, 2004. **119**(2): p. 245-56.

100. Iyer, S.C., et al., *The RhoGEF trio functions in sculpting class specific dendrite morphogenesis in Drosophila sensory neurons.* PLoS One, 2012. **7**(3): p. e33634.

101. Bonhoeffer, T. and R. Yuste, *Spine motility. Phenomenology, mechanisms, and function.* Neuron, 2002. **35**(6): p. 1019-27.

102. Jancso, G., E. Kiraly, and A. Jancso-Gabor, *Pharmacologically induced selective degeneration of chemosensitive primary sensory neurones.* Nature, 1977. **270**(5639): p. 741-743.

103. Nagy, J.I. and D. Vanderkooy, *EFFECTS OF NEONATAL CAPSAICIN TREATMENT ON NOCICEPTIVE THRESHOLDS IN THE RAT.* Journal of Neuroscience, 1983. **3**(6): p. 1145-1150.

104. Nagy, J.I., et al., *DOSE-DEPENDENT EFFECTS OF CAPSAICIN ON PRIMARY SENSORY NEURONS IN THE NEONATAL RAT.* Journal of Neuroscience, 1983. **3**(2): p. 399-406.

105. Simone, D.A., et al., *Intradermal Injection of Capsaicin in Humans Produces Degeneration and Subsequent Reinnervation of Epidermal Nerve Fibers: Correlation with Sensory Function.* The Journal of Neuroscience, 1998. **18**(21): p. 8947-8959.

106. RagÃ©, M., et al., *The time course of CO2 laser-evoked responses and of skin nerve fibre markers after topical capsaicin in human volunteers.* Clinical Neurophysiology, 2010. **121**(8): p. 1256-1266.

107. Nolano, M., et al., *Topical capsaicin in humans: parallel loss of epidermal nerve fibers and pain sensation.* Pain, 1999. **81**(1â€“2): p. 135-145.

108. Chard, P.S., et al., *Capsaicin-induced neurotoxicity in cultured dorsal root ganglion neurons: Involvement of calcium-activated proteases.* Neuroscience, 1995. **65**(4): p. 1099-1108.

109. Fleury, F., et al., *Ecological and genetic interactions in Drosophila-parasitoids communities: a case study with D-melanogaster, D-simulans and their common Leptopilina parasitoids in south-eastern France.* Genetica, 2004. **120**(1-3): p. 181-194.

110. Carton, Y., Bouletreau, M., van Alphen, J.J.M., and van Lenteren, J.C., *The Drosophila parasitic waps*, in *The Genetics and Biology of Drosophila*, M. Ashburner, Carson, H.L., Thompson Jr., J.N., Editor. 1986, Academic Press: London. p. 347-394.

111. Silvers, M.J. and A.J. Nappi, *In vitro Study of Physiological Suppression of Supernumerary Parasites by the Endoparasitic Wasp Leptopilina heterotoma.* The Journal of Parasitology, 1986. **72**(3): p. 405-409.

112. Lee, M.J., et al., *Virulence Factors and Strategies of Leptopilina spp.: Selective Responses in Drosophila Hosts*, in *Advances in Parasitology, Vol 70: Parasitoids of Drosophila*, G. Prevost, Editor. 2009, Elsevier Academic Press Inc: San Diego. p. 123-+.

113. Kaiser, L., A. Couty, and R. Perez-Maluf, *Dynamic Use of Fruit Odours to Locate Host Larvae: Individual Learning, Physiological State and Genetic Variability as Adaptive Mechanisms*, in *Advances in Parasitology, Vol 70*. 2009, Elsevier Academic Press Inc: San Diego. p. 67-95.

114. Perez-Maluf, R., et al., *Differentiation of innate but not learnt responses to host-habitat odours contributes to rapid host finding in a parasitoid genotype.* Physiological Entomology, 2008. **33**(3): p. 226-232.

115. Wajnberg, É., *Time allocation strategies in insect parasitoids: from ultimate predictions to proximate behavioral mechanisms.* Behavioral Ecology and Sociobiology, 2006. **60**(5): p. 589-611.

116. Sokolowski, M.B. and T.C.J. Turlings, *Drosophila parasitoid–host interactions: vibrotaxis and ovipositor searching from the host's perspective.* Canadian Journal of Zoology, 1987. **65**(3): p. 461-464.

117. Haccou, P., et al., *Information Processing by Foragers: Effects of Intra-Patch Experience on the Leaving Tendency of Leptopilina heterotoma.* Journal of Animal Ecology, 1991. **60**(1): p. 93-106.

118. Belshaw, R., A. Grafen, and D.L.J. Quicke, *Inferring life history from ovipositor morphology in parasitoid wasps using phylogenetic regression and discriminant analysis.* Zoological Journal of the Linnean Society, 2003. **139**(2): p. 213-228.

119. Buffington, M.L., *The occurrence and phylogenetic implications of the ovipositor clip within the Figitidae (Insecta: Hymenoptera: Cynipoidea).* Journal of Natural History, 2007. **41**(33-36): p. 2267-2282.

120. Dupas, S., et al., *Immune suppressive virus-like particles in a Drosophila parasitoid: significance of their intraspecific morphological variations.* Parasitology, 1996. **113**(03): p. 207-212.

121. Whitfield, J.B. and S. Asgari, *Virus or not? Phylogenetics of polydnaviruses and their wasp carriers.* Journal of Insect Physiology, 2003. **49**(5): p. 397-405.

122. van Lenteren, J.C., N. Isidoro, and F. Bin, *Functional anatomy of the ovipositor clip in the parasitoid Leptopilina heterotoma (Thompson) (Hymenoptera : Eucoilidae), a structure to grip escaping host larvae.* International Journal of Insect Morphology & Embryology, 1998. **27**(3): p. 263-268.

123. Oswald, M., et al., *A novel thermosensitive escape behavior in Drosophila larvae.* Fly, 2011. **5**(4): p. 0--1.

124. Babcock, D.T., C. Landry, and M.J. Galko, *Cytokine Signaling Mediates UV-Induced Nociceptive Sensitization in Drosophila Larvae.* Current Biology, 2009. **19**(10): p. 799-806.

125. Kim, Michelle E., et al., *Integrins Establish Dendrite-Substrate Relationships that Promote Dendritic Self-Avoidance and Patterning in Drosophila Sensory Neurons.* Neuron, 2012. **73**(1): p. 79-91.

126. Han, C., et al., *Integrins Regulate Repulsion-Mediated Dendritic Patterning of Drosophila Sensory Neurons by Restricting Dendrites in a 2D Space.* Neuron, 2012. **73**(1): p. 64-78.

127. Wegman, L.J., J.A. Ainsley, and W.A. Johnson, *Developmental timing of a sensory-mediated larval surfacing behavior correlates with cessation of feeding and determination of final adult size.* Developmental Biology, 2010. **345**(2): p. 170-179.

128. Kernan, M., D. Cowan, and C. Zuker, *Genetic Dissection of Mechanosensory Transduction - Mechanoreception-Defective Mutations of Drosophila.* Neuron, 1994. **12**(6): p. 1195-1206.

129. Tsubouchi, A., Jason C. Caldwell, and W.D. Tracey, *Dendritic Filopodia, Ripped Pocket, NOMPC, and NMDARs Contribute to the Sense of Touch in Drosophila Larvae.* Current biology : CB, 2012. **22**(22): p. 2124-2134.

130. Galko, M.J. and M.A. Krasnow, *Cellular and Genetic Analysis of Wound Healing in Drosophila Larvae.* PLoS Biol, 2004. **2**(8): p. e239.

131. Gordon, M.D. and K. Scott, *Motor Control in a Drosophila Taste Circuit.* Neuron, 2009. **61**(3): p. 373-384.

132. Pulver, S.R., et al., *Temporal Dynamics of Neuronal Activation by Channelrhodopsin-2 and TRPA1 Determine Behavioral Output in Drosophila Larvae.* Journal of Neurophysiology, 2009. **101**(6): p. 3075-3088.

133. Hamada, F.N., et al., *An internal thermal sensor controlling temperature preference in Drosophila.* Nature, 2008. **454**(7201): p. 217-220.

134. Rosenzweig, M., et al., *The Drosophila ortholog of vertebrate TRPA1 regulates thermotaxis.* Genes & Development, 2005. **19**(4): p. 419-424.

135. Rosenzweig, M., K. Kang, and P.A. Garrity, *Distinct TRP channels are required for warm and cool avoidance in Drosophila melanogaster.* Proceedings of the National Academy of Sciences, 2008. **105**(38): p. 14668-14673.

136. Sweeney, S.T., et al., *Targeted expression of tetanus toxin light chain in Drosophila specifically eliminates synaptic transmission and causes behavioral defects.* Neuron, 1995. **14**(2): p. 341-351.

137. Ainsley, J.A., et al., *Enhanced Locomotion Caused by Loss of the Drosophila DEG/ENaC Protein Pickpocket1.* Current Biology, 2003. **13**(17): p. 1557-1563.

138. Ruangvoravat, C.P. and C.W. Lo, *Restrictions in gap junctional communication in the Drosophila larval epidermis.* Developmental Dynamics, 1992. **193**(1): p. 70-82.

139. Gal, R. and F. Libersat, *A Wasp Manipulates Neuronal Activity in the Sub-Esophageal Ganglion to Decrease the Drive for Walking in Its Cockroach Prey.* PLoS ONE, 2010. **5**(4): p. e10019.

140. Allemand, R., et al., *Phylogeny of six African Leptopilina species (Hymenoptera : Cynipoidea, Figitidae), parasitoids of Drosophila, with description of three new species.* Annales De La Societe Entomologique De France, 2002. **38**(4): p. 319-332.

141. Schlenke, T.A., et al., *Contrasting infection strategies in Generalist and specialist wasp parasitoids of Drosophila melanogaster.* Plos Pathogens, 2007. **3**(10): p. 1486-1501.

142. Carton, Y. and H. Kitano, *EVOLUTIONARY RELATIONSHIPS TO PARASITISM BY 7 SPECIES OF THE DROSOPHILA-MELANOGASTER SUBGROUP.* Biological Journal of the Linnean Society, 1981. **16**(3): p. 227-241.

143. Carton, Y., Bouletreau, M., van Alphen, J.J.M., and van Lenteren, J.C., *The Drosophila parasitic waps.* , in *The Genetics and Biology of Drosophila*, M. Ashburner, Carson, H.L., Thompson Jr., J.N., Editor. 1986, Academic Press: London. p. 347-394.

144. Rizki, T.M. and R.M. Rizki, *Parasitoid-Induced Cellular Immune Deficiency in Drosophilaa.* Annals of the New York Academy of Sciences, 1994. **712**(1): p. 178-194.

145. Chiu, H. and S. Govind, *Natural infection of D-metanogaster by virulent parasitic wasps induces apoptotic depletion of hematopoietic precursors.* Cell Death and Differentiation, 2002. **9**(12): p. 1379-1381.

146. Gueguen, G., et al., *VLPs of Leptopilina boulardi share biogenesis and overall stellate morphology with VLPs of the heterotoma clade.* Virus Research, 2011. **160**(1–2): p. 159-165.

147. Rizki, R.M. and T.M. Rizki, *Selective destruction of a host blood cell type by a parasitoid wasp.* Proceedings of the National Academy of Sciences, 1984. **81**(19): p. 6154-6158.

148. Rizki, R.M. and T.M. Rizki, *Parasitoid virus-like particles destroy Drosophila cellular immunity.* Proceedings of the National Academy of Sciences, 1990. **87**(21): p. 8388-8392.

149. Rizki, T.M., R.M. Rizki, and Y. Carton, *LEPTOPILINA-HETEROTOMA AND L-BOULARDI - STRATEGIES TO AVOID CELLULAR DEFENSE RESPONSES OF DROSOPHILA-MELANOGASTER.* Experimental Parasitology, 1990. **70**(4): p. 466-475.

150. Russo, J., M. Brehelin, and Y. Carton, *Haemocyte changes in resistant and susceptible strains of D-melanogaster caused by virulent and avirulent strains of the parasitic wasp Leptopilina boulardi.* Journal of Insect Physiology, 2001. **47**(2): p. 167-172.

151. Labrosse, C., et al., *Haemocyte changes in D. Melanogaster in response to long gland components of the parasitoid wasp Leptopilina boulardi: a Rho-GAP protein as an important factor.* Journal of Insect Physiology, 2005. **51**(2): p. 161-170.

152. Sorrentino, R.P., Y. Carton, and S. Govind, *Cellular Immune Response to Parasite Infection in the Drosophila Lymph Gland Is Developmentally Regulated.* Developmental Biology, 2002. **243**(1): p. 65-80.

153. Sulkowski, M.J., M.S. Kurosawa, and D.N. Cox, *Growing Pains: Development of the Larval Nocifensive Response in Drosophila.* The Biological Bulletin, 2011. **221**(3): p. 300-306.

154. Reiter, L.T., et al., *A systematic analysis of human disease-associated gene sequences in Drosophila melanogaster.* Genome Research, 2001. **11**(6): p. 1114-1125.

155. Tillman, D.B., et al., *RESPONSE OF C-FIBER NOCICEPTORS IN THE ANESTHETIZED MONKEY TO HEAT STIMULI - CORRELATION WITH PAIN THRESHOLD IN HUMANS.* Journal of Physiology-London, 1995. **485**(3): p. 767-774.

156. Xiang, Y., et al., *Light-avoidance-mediating photoreceptors tile the Drosophila larval body wall.* Nature, 2010. **468**(7326): p. 921-U312.

157. Giniger, E., S.M. Varnum, and M. Ptashne, *Specific DNA binding of GAL4, a positive regulatory protein of yeast.* Cell, 1985. **40**(4): p. 767-774.

158. Duffy, J.B., *GAL4 system in Drosophila: A fly geneticist's Swiss army knife.* Genesis, 2002. **34**(1-2): p. 1-15.

159. Kittel, R.J., et al., *Bruchpilot promotes active zone assembly, Ca2+ channel clustering, and vesicle release.* Science, 2006. **312**(5776): p. 1051-1054.

160. Siddiqi, O. and S. Benzer, *Neurophysiological defects in temperature-sensitive paralytic mutants of Drosophila melanogaster.* Proc Natl Acad Sci U S A, 1976. **73**(9): p. 3253-7.

161. Wu, C.F. and B. Ganetzky, *Genetic alteration of nerve membrane excitability in temperature-sensitive paralytic mutants of Drosophila melanogaster.* Nature, 1980. **286**(5775): p. 814-6.

162. Shimono, K., et al., *Multidendritic sensory neurons in the adult Drosophila abdomen: origins, dendritic morphology, and segment- and age-dependent programmed cell death.* Neural Dev, 2009. **4**: p. 37.

163. Al-Anzi, B., W.D. Tracey, Jr., and S. Benzer, *Response of Drosophila to wasabi is mediated by painless, the fly homolog of mammalian TRPA1/ANKTM1.* Curr Biol, 2006. **16**(10): p. 1034-40.

164. Lin, W.-H., et al., *Alternative Splicing in the Voltage-Gated Sodium Channel DmNav Regulates Activation, Inactivation, and Persistent Current.* Journal of Neurophysiology, 2009. **102**(3): p. 1994-2006.

165. Gonzales, E.B., T. Kawate, and E. Gouaux, *Pore architecture and ion sites in acid-sensing ion channels and P2X receptors.* Nature, 2009. **460**(7255): p. 599-604.

166. Jasti, J., et al., *Structure of acid-sensing ion channel 1 at 1.9 A resolution and low pH.* Nature, 2007. **449**(7160): p. 316-23.

167. O'Hagan, R., M. Chalfie, and M.B. Goodman, *The MEC-4 DEG/ENaC channel of Caenorhabditis elegans touch receptor neurons transduces mechanical signals.* Nat Neurosci, 2005. **8**(1): p. 43-50.

168. Suzuki, H., et al., *In vivo imaging of C. elegans mechanosensory neurons demonstrates a specific role for the MEC-4 channel in the process of gentle touch sensation.* Neuron, 2003. **39**(6): p. 1005-17.

169. Ben-Ari, Y., *Excitatory actions of gaba during development: the nature of the nurture.* Nat Rev Neurosci, 2002. **3**(9): p. 728-739.

170. Döring, F., et al., *Novel Drosophila two-pore domain K+ channels: rescue of channel function by heteromeric assembly.* European Journal of Neuroscience, 2006. **24**(8): p. 2264-2274.

171. Doring, F., et al., *Novel Drosophila two-pore domain K channels: rescue of channel function by heteromeric assembly.* Eur J Neurosci, 2006. **24**(8): p. 2264-74.

172. Bannon, A.W., et al., *Broad-spectrum, non-opioid analgesic activity by selective modulation of neuronal nicotinic acetylcholine receptors.* Science, 1998. **279**(5347): p. 77-81.

173. Hama, A. and F. Menzaghi, *Antagonist of nicotinic acetylcholine receptors (nAChR) enhances formalin-induced nociception in rats: tonic role of nAChRs in the control of pain following injury.* Brain Research, 2001. **888**(1): p. 102-106.

174. Hone, A.J., et al., *Nicotinic acetylcholine receptors in dorsal root ganglion neurons include the α6β4* subtype.* The FASEB Journal, 2012. **26**(2): p. 917-926.

175. Cordero-Erausquin, M., et al., *Nicotine differentially activates inhibitory and excitatory neurons in the dorsal spinal cord.* Pain, 2004. **109**(3): p. 308-18.

176. Takeda, D., et al., *The activation of nicotinic acetylcholine receptors enhances the inhibitory synaptic transmission in the deep dorsal horn neurons of the adult rat spinal cord.* Molecular Pain, 2007. **3**(1): p. 26.

177. Cheng, L.Z., et al., *Enhanced inhibitory synaptic transmission in the spinal dorsal horn mediates antinociceptive effects of TC-2559.* Mol Pain, 2011. **7**: p. 56.

178. Hwang, R.Y., *Circuitry and genes of Drosophila larval nociception*, in *Neuroscience*2009, Duke University: Durham, NC.

179. Emoto, K., et al., *The tumour suppressor Hippo acts with the NDR kinases in dendritic tiling and maintenance.* Nature, 2006. **443**(7108): p. 210-213.

180. Kim, M.D., L.Y. Jan, and Y.N. Jan, *The bHLH-PAS protein Spineless is necessary for the diversification of dendrite morphology of Drosophila dendritic arborization neurons.* Genes & Development, 2006. **20**(20): p. 2806-2819.

181. Kuo, C.T., et al., *Identification of E2/E3 ubiquitinating enzymes and caspase activity regulating Drosophila sensory neuron dendrite pruning.* Neuron, 2006. **51**(3): p. 283-290.

182. Parrish, J.Z., et al., *Polycomb genes interact with the tumor suppressor genes hippo and warts in the maintenance of Drosophila sensory neuron dendrites.* Genes & Development, 2007. **21**(8): p. 956-972.

183. Ye, B., et al., *Differential Regulation of Dendritic and Axonal Development by the Novel Kruppel-Like Factor Dar1.* Journal of Neuroscience, 2011. **31**(9): p. 3309-3319.

184. Matthews, Benjamin J. and Wesley B. Grueber, *Dscam1-Mediated Self-Avoidance Counters Netrin-Dependent Targeting of Dendrites in Drosophila.* Current biology : CB, 2011. **21**(17): p. 1480-1487.

185. Ultanir, S.K., et al., *Chemical genetic identification of NDR1/2 kinase substrates AAK1 and Rabin8 Uncovers their roles in dendrite arborization and spine development.* Neuron, 2012. **73**(6): p. 1127-42.

186. Loncle, N. and D.W. Williams, *An interaction screen identifies headcase as a regulator of large-scale pruning.* J Neurosci, 2012. **32**(48): p. 17086-96.

187. Matsubara, D., et al., *The seven-pass transmembrane cadherin Flamingo controls dendritic self-avoidance via its binding to a LIM domain protein, Espinas, in Drosophila sensory neurons.* Genes Dev, 2011. **25**(18): p. 1982-96.

188. Schmucker, D., et al., *Drosophila Dscam is an axon guidance receptor exhibiting extraordinary molecular diversity.* Cell, 2000. **101**(6): p. 671-84.

189. Turrigiano, G.G., *The Self-Tuning Neuron: Synaptic Scaling of Excitatory Synapses.* Cell, 2008. **135**(3): p. 422-435.

190. Turrigiano, G.G. and S.B. Nelson, *Homeostatic plasticity in the developing nervous system.* Nat Rev Neurosci, 2004. **5**(2): p. 97-107.

191. Hou, Q., et al., *Homeostatic regulation of AMPA receptor expression at single hippocampal synapses.* Proc Natl Acad Sci U S A, 2008. **105**(2): p. 775-80.

192. Rutherford, L.C., S.B. Nelson, and G.G. Turrigiano, *BDNF has opposite effects on the quantal amplitude of pyramidal neuron and interneuron excitatory synapses.* Neuron, 1998. **21**(3): p. 521-30.

193. Thiagarajan, T.C., M. Lindskog, and R.W. Tsien, *Adaptation to Synaptic Inactivity in Hippocampal Neurons.* Neuron, 2005. **47**(5): p. 725-737.

194. Maffei, A. and A. Fontanini, *Network homeostasis: a matter of coordination.* Current Opinion in Neurobiology, 2009. **19**(2): p. 168-173.

195. Turrigiano, G.G., et al., *Activity-dependent scaling of quantal amplitude in neocortical neurons.* Nature, 1998. **391**(6670): p. 892-896.

196. Tyler, W.J., et al., *Experience-dependent modification of primary sensory synapses in the mammalian olfactory bulb.* Journal of Neuroscience, 2007. **27**(35): p. 9427-9438.

197. Murthy, V.N., et al., *Inactivity Produces Increases in Neurotransmitter Release and Synapse Size.* Neuron, 2001. **32**(4): p. 673-682.

198. Ibata, K., Q. Sun, and G.G. Turrigiano, *Rapid synaptic scaling induced by changes in postsynaptic firing.* Neuron, 2008. **57**(6): p. 819-26.

199. Wierenga, C.J., K. Ibata, and G.G. Turrigiano, *Postsynaptic expression of homeostatic plasticity at neocortical synapses.* J Neurosci, 2005. **25**(11): p. 2895-905.

200. Turrigiano, G., *Too Many Cooks? Intrinsic and Synaptic Homeostatic Mechanisms in Cortical Circuit Refinement.* Annual Review of Neuroscience, 2011. **34**(1): p. 89-103.

201. Tripodi, M., et al., *Structural Homeostasis: Compensatory Adjustments of Dendritic Arbor Geometry in Response to Variations of Synaptic Input.* PLoS Biol, 2008. **6**(10): p. e260.

202. Yuan, Q., et al., *Light-Induced Structural and Functional Plasticity in Drosophila Larval Visual System.* Science, 2011. **333**(6048): p. 1458-1462.

203. Singh, A.P., K. VijayRaghavan, and V. Rodrigues, *Dendritic refinement of an identified neuron in the Drosophila CNS is regulated by neuronal activity and Wnt signaling.* Development, 2010. **137**(8): p. 1351-1360.

204. Kazama, H. and R.I. Wilson, *Homeostatic Matching and Nonlinear Amplification at Identified Central Synapses.* Neuron, 2008. **58**(3): p. 401-413.

205. Parks, A.L., et al., *Systematic generation of high-resolution deletion coverage of the Drosophila melanogaster genome.* Nat Genet, 2004. **36**(3): p. 288-292.

206. Benham, C.D., M.J. Gunthorpe, and J.B. Davis, *TRPV channels as temperature sensors.* Cell Calcium, 2003. **33**(5-6): p. 479-487.

207. Walcott, K., *Genetic analysis of the contribution of ion channels to Drosophila nociception*, in *Pharmacology and Cancer Biology*2012, Duke University: Durham, NC.

208. Kim, J., et al., *A TRPV family ion channel required for hearing in Drosophila.* Nature, 2003. **424**(6944): p. 81-4.

209. Gong, Z., et al., *Two interdependent TRPV channel subunits, inactive and Nanchung, mediate hearing in Drosophila.* J Neurosci, 2004. **24**(41): p. 9059-66.

210. Wu, C.-F. and B. Ganetzky, *Genetic alteration of nerve membrane excitability in temperature-sensitive paralytic mutants of Drosophila melanogaster.* Nature, 1980. **286**(5775): p. 814-816.

211. Nitabach, M.N., et al., *Electrical Hyperexcitation of Lateral Ventral Pacemaker Neurons Desynchronizes Downstream Circadian Oscillators in the Fly Circadian Circuit and Induces Multiple Behavioral Periods.* The Journal of Neuroscience, 2006. **26**(2): p. 479-489.

212. Oddo, S. and F.M. LaFerla, *The role of nicotinic acetylcholine receptors in Alzheimer's disease.* Journal of Physiology-Paris, 2006. **99**(2–3): p. 172-179.

213. Buchmann, J., et al., *Ablation of the cholesterol transporter adenosine triphosphate-binding cassette transporter G1 reduces adipose cell size and protects against diet-induced obesity.* Endocrinology, 2007. **148**(4): p. 1561-73.

214. Tarling, E.J., *Expanding roles of ABCG1 and sterol transport.* Current Opinion in Lipidology, 2013. **24**(2): p. 138-146.

215. Gutierrez, E., et al., *Specialized hepatocyte-like cells regulate Drosophila lipid metabolism.* Nature, 2007. **445**(7125): p. 275-280.

216. Ritter, A.M. and L.M. Mendell, *Somal membrane properties of physiologically identified sensory neurons in the rat: effects of nerve growth factor.* Journal of Neurophysiology, 1992. **68**(6): p. 2033-2041.

217. Xiang, Y., et al., *Light-avoidance-mediating photoreceptors tile the Drosophila larval body wall.* Nature, 2010. **468**(7326): p. 921-926.

218. Du, W., et al., *Calcium-sensitive potassium channelopathy in human epilepsy and paroxysmal movement disorder.* Nat Genet, 2005. **37**(7): p. 733-738.

219. Everill, B. and J.D. Kocsis, *Nerve growth factor maintains potassium conductance after nerve injury in adult cutaneous afferent dorsal root ganglion neurons.* Neuroscience, 2000. **100**(2): p. 417-22.

220. Hugues, M., H. Schmid, and M. Lazdunski, *IDENTIFICATION OF A PROTEIN-COMPONENT OF THE CA2+-DEPENDENT K+ CHANNEL BY AFFINITY LABELING WITH APAMIN.* Biochemical and Biophysical Research Communications, 1982. **107**(4): p. 1577-1582.

221. Blatz, A.L. and K.L. Magleby, *SINGLE APAMIN-BLOCKED CA-ACTIVATED K+ CHANNELS OF SMALL CONDUCTANCE IN CULTURED RAT SKELETAL-MUSCLE.* Nature, 1986. **323**(6090): p. 718-720.

222. Adelman, J.P., J. Maylie, and P. Sah, *Small-conductance Ca2+-activated K+ channels: form and function.* Annu Rev Physiol, 2012. **74**: p. 245-69.

223. Storm, J.F., *ACTION-POTENTIAL REPOLARIZATION AND A FAST AFTER-HYPERPOLARIZATION IN RAT HIPPOCAMPAL PYRAMIDAL CELLS.* Journal of Physiology-London, 1987. **385**: p. 733-759.

224. Zhang, L. and K. Krnjevic, *APAMIN DEPRESSES SELECTIVELY THE AFTER-HYPERPOLARIZATION OF CAT SPINAL MOTONEURONS.* Neuroscience Letters, 1987. **74**(1): p. 58-62.

225. Bourque, C.W. and D.A. Brown, *APAMIN AND D-TUBOCURARINE BLOCK THE AFTER-HYPERPOLARIZATION OF RAT SUPRAOPTIC NEUROSECRETORY NEURONS.* Neuroscience Letters, 1987. **82**(2): p. 185-190.

226. Sah, P.A.J. and E.M. McLachlan, *POTASSIUM CURRENTS CONTRIBUTING TO ACTION-POTENTIAL REPOLARIZATION AND THE*

AFTERHYPERPOLARIZATION IN RAT VAGAL MOTONEURONS. Journal of Neurophysiology, 1992. **68**(5): p. 1834-1841.

227. Goldberg, J.A. and C.J. Wilson, *Control of spontaneous firing patterns by the selective coupling of calcium currents to calcium-activated potassium currents in striatal cholinergic interneurons.* Journal of Neuroscience, 2005. **25**(44): p. 10230-10238.

228. Kohler, M., et al., *Small-conductance, calcium-activated potassium channels from mammalian brain.* Science, 1996. **273**(5282): p. 1709-1714.

229. Monaghan, A.S., et al., *The SK3 subunit of small conductance Ca(2+)-activated K(+) channels interacts with both SK1 and SK2 subunits in a heterologous expression system.* Journal of Biological Chemistry, 2004. **279**(2): p. 1003-1009.

230. Strassmaier, T., et al., *A novel isoform of SK2 assembles with other SK subunits in mouse brain.* Journal of Biological Chemistry, 2005. **280**(22): p. 21231-21236.

231. Abou Tayoun, A.N., et al., *The Drosophila SK channel (dSK) contributes to photoreceptor performance by mediating sensitivity control at the first visual network.* J Neurosci, 2011. **31**(39): p. 13897-910.

232. Clark, D.A., et al., *The AFD Sensory Neurons Encode Multiple Functions Underlying Thermotactic Behavior in Caenorhabditis elegans.* The Journal of Neuroscience, 2006. **26**(28): p. 7444-7451.

233. Ishii, T.M., J. Maylie, and J.P. Adelman, *Determinants of apamin and d-tubocurarine block in SK potassium channels.* Journal of Biological Chemistry, 1997. **272**(37): p. 23195-23200.

234. Stocker, M. and P. Pedarzani, *Differential Distribution of Three Ca2+-Activated K+ Channel Subunits, SK1, SK2, and SK3, in the Adult Rat Central Nervous System.* Molecular and Cellular Neuroscience, 2000. **15**(5): p. 476-493.

235. Mackay, T.F.C., et al., *The Drosophila melanogaster Genetic Reference Panel.* Nature, 2012. **482**(7384): p. 173-178.

236. Cao, E., et al., *TRPV1 Channels Are Intrinsically Heat Sensitive and Negatively Regulated by Phosphoinositide Lipids.* Neuron, 2013. **77**(4): p. 667-679.

237. Kung, C., *A possible unifying principle for mechanosensation.* Nature, 2005. **436**(7051): p. 647-654.

238. Buckingham, S.D., et al., *Nicotinic Acetylcholine Receptor Signalling: Roles in Alzheimer's Disease and Amyloid Neuroprotection.* Pharmacological Reviews, 2009. **61**(1): p. 39-61.

239. Kim, D., *Fatty acid-sensitive two-pore domain K+ channels.* Trends in pharmacological sciences, 2003. **24**(12): p. 648-654.

240. Howe, M.W., et al., *Cellular and subcellular localization of Kir2.1 subunits in neurons and glia in piriform cortex with implications for K+ spatial buffering.* The Journal of Comparative Neurology, 2008. **506**(5): p. 877-893.

241. Baines, R.A., et al., *Altered Electrical Properties in DrosophilaNeurons Developing without Synaptic Transmission.* The Journal of Neuroscience, 2001. **21**(5): p. 1523-1531.

242. Kanamori, T., et al., *Compartmentalized Calcium Transients Trigger Dendrite Pruning in Drosophila Sensory Neurons.* Science, 2013. **340**(6139): p. 1475-1478.

Biography

Jessica Robertson grew up in Huntingtown, Maryland. She attended the College of William and Mary in Williamsburg, VA and graduated *magna cum laude* in 2007. Her research resulted in a second author publication in the Journal of Mammalogy. After graduation, she attended the University of Washington where she received a Master's Degree in Biology in 2009. While there, she received the National Science Foundation's Graduate Research Fellowship, and published a first author paper in Endocrinology. Jessica continued to Duke University in 2009, where she was a James B. Duke scholar. While at Duke she has published in Cell Reports, and was a second author on a book chapter to be published in the Handbook of behavioral genetics of *Drosophila melanogaster*: Behavioral phenotypes and models of neurobehavioral disorders.